Research and study of an innovative solution for the optimization of the conversion into biomethane of the gaseous effluents of the non-hazardous waste storage facility (Landfill Site)

Mohammad Samim Ghafoori

THESE DE DOCTORAT DE

L'ÉCOLE NATIONALE SUPERIEURE MINES-TELECOM ATLANTIQUE
BRETAGNE PAYS DE LA LOIRE - IMT ATLANTIQUE

ECOLE DOCTORALE N° 602
Sciences pour l'Ingénieur
Spécialité : *énergétique, thermique, combustion*

Par

Mohammad Samim GHAFOORI

Recherche et étude d'une solution innovante pour l'optimisation de la conversion en bioGNV des effluents gazeux de l'Installation de stockage de déchets non dangereux (ISDND)

Thèse présentée et soutenue à IMT Atlantique, le 09/12/2021

Unité de recherche : GEPEA

Thèse N° : 2021IMTA0274

Rapporteurs avant soutenance :

Abdelkrim LIAZID Professeur, Université Abou-Bekr Belkaid de Tlemcen (Algérie)
Said ABBOUDI Professeur, Université de Technologie de Belfort-Montbéliard (France)

Composition du Jury :

Président : Abdelkrim LIAZID Professeur, Université Abou-Bekr Belkaid de Tlemcen (Algérie)

Examinateurs : Karim ALLAF Professeur, Université de La Rochelle (France)
Tudor PRISECARU Professeur, Université polytechnique de Bucarest (Roumanie)

Dir. de thèse : Mohand TAZEROUT Professeur IMT Atlantique Nantes (France)

Co-dir. de thèse : Khaled LOUBAR Maitre-assistant HDR IMT Atlantique Nantes (France)

Co-encadrant : Mylène MARIN GALLEGO Maître de Conférences ENSIACET Toulouse (France)

Invité(s)
BRANGEON Victor Directeur général Groupe Brangeon

Published Articles

- **GHAFOORI M.S**, Loubar, K., Marin Gallego, M, Tazerout, M**. Techno-economic and sensitivity analysis of biomethane production via landfill biogas upgrading and power-to-gas technology**, Energy The International Journal (2021).
- **GHAFOORI M.S**, Loubar, K., Marin Gallego, M, Tazerout, M. **Pre-feasibility study of synthetic methane production via power-to-gas integration into landfill biogas**, Sardinia 2021. 18th international symposium on waste management and sustainable landfilling.
- **GHAFOORI M.S**, Loubar, K., Marin Gallego, M, Tazerout, M**. Mathematical modeling of landfill biogas production**, (Under Submission)

Acknowledgement

Three years of dedication, commitment and hard work to successfully complete my thesis was a true discovery and an excellent research experience. I would like to express my deepest gratitude and thank the following people who helped me throughout the entire thesis project.

I would like to firstly thank my thesis director Mohand TAZEROUT, co-director and supervisor Khaled LOUBAR and co-supervisor Mylène MARIN GALLEGO for their technical and academic support, time, guidance and immense efforts throughout this thesis.

Secondly, my deepest gratitude goes for the company tutors from Groupe Brangeon side, I would like to kindly thank Victor BRANGEON, Wilfried FASSINOU and Valérie MÜLHAUPT for their constant help and support all over the thesis journey. Their tireless efforts and kind attention in successfully completing this project was contributive.

I express my sincere thanks to ABBOUDI Said professor in the Technology University of Belfort-montbéliard (UTBM) and Abdelkrim LIAZID professor in University of Abou-Bekr Belkaid Tlemcen for agreeing to be the reviewers of this PhD thesis.

I felt in depth that the knowledge and skills I gained during my two years master journey in IMT Atlantique was undeniably supportive during my thesis, I would like to extend my sincere gratitude to all the academic professors. I additionally thank all the examiners of this thesis, ALLAF Karim professor in the University of La Rochelle and PRISECARU Tudor professor in the polytechnic university of Bucharest.

Thank you very much my dearest parents M. Naim and Karima GHAFOORI, my beloved wife Moharram HAKIMY, my brothers M. Shafiq, Dr. Shekib, Wasim GHAFOORI and my dearest sisters, Mahrangiz and Ayper GHAFOORI. Your amazing care, attention, courage and support were a true strength during my thesis; it pushed me through and succeed during my thesis during the difficult times I have been through especially during the COVID-19 pandemic. There is no exact words to express how much grateful I am to have you all and your constant help.

Moreover, I am grateful to all of my colleagues in IMT-Atlantique, especially Emmanuel, Siavoche, Walid, Christelle, Sara, Rita, Nouha, Loubna, Shawki, Gaetan, Morgane, Hasbi, and Wasim for their cheerful time-shared, encouragement, admiration and friendship.

Finally, this tireless achievement and doctorate is dedicated for my dearest parents and beloved wife. Who did not hesitate to support me constantly from beginning until the end of my PhD life.

Table of Contents

List of Tables

List of Figures

Nomenclature

Variables

α_t	Landfill gas production at a given time	(m^3 LFG. y^{-1})
ϑ	Dissimilation factor	(-)
A	Amount of waste in place	(ton)
C_0	Amount of organic carbon in waste	(KgC. ton $waste^{-1}$)
k	Degradation rate constant	(y^{-1})
t	Time elapsed since depositing	(y)
i	Waste fraction with degradation rate $k_{1,i}$	($kg_i.kg^{-1}$waste)
c	Conversion factor	(m^3 LFG. kgC^{-1}degraded)
Q_{CH4}	Flow rate of methane generation	(m^3/year)
n	(year of the calculation) – (initial year of waste acceptance)	(-)
j	0.1-year time increment	(-)
L_0	Potential methane generation capacity	(m^3/ton)
Mi	Mass of waste accepted in the i^{th} year	(m^3/ton)
G_t	Total LFG production at a given time	(ton)
C_{org}	Organic carbon in waste	(kg OC/ton waste)
M_t	Waste in place in a given time	(ton/year)
C_m	Methane generation	(m^3 CH_4/dry-ton)
A_n	Value of the cost at time t	(-)
r	Discount rate	(%)
A_0	Value of repeating cost	
C_{ann}	Annual capital cost	(€/year)
U	Overall coefficient of thermal exchange	

Abbreviations

BF	Biodegradable fraction
BF_W	Biodegradable fraction of the waste
BM	Biological methanation
BMP	Biochemical methane potential
BOD	Biochemical oxygen demand
BoP	Blance of Plant
C&D	Construction and demolition
CAES	Compressed air energy storage
CAPEX	Capital Expenditure
CHP	Combined heat and power
CHW	Coarse household waste
CM	Catalytic methanation
COD	Chemical oxygen demand
CRA	Conestoga - Rovers & Associates
CS	Cold standby
CS	Contaminated soil
CSTR	Continuous stirred-tank reactor
CW	Commercial waste
$DDOC_m$	Decomposable degradable organic carbon
DEA	Diethanolamine
DGA	Diglycolamines
DMPEG	Dimethyl ethers of polyethylene glycol
DOC	Degradable organic carbon
DOC_f	Fraction of the degradable organic carbon
DOC_m	Degradable organic matter
FLH	Full load hour
FR	Waste fraction
GHG	Greenhouses gas
GPC	Gas production cost
HHV	Higher heating value
HLR	Hydraulic loading rate
HS	Hot standby
HW	Household waste

I	Investment
LCC	Life cycle cost
LCCA	Life cycle cost analysis
LFG	Landfill gas
MBR	Membrane biological reactor
MCF	Methane correction factor
MEA	Monoethanolamine
MSW	Municipal solid waste
NAP	National Action Plan
NF	Nano filtration
NMOCs	Non-methane organic compounds
OP	Production
OPEX	Operation expenditure
PBP	Payback period
PEM	Proton exchange membrane
PHS	Pumped hydro storage
PSA	Pressure swing adsorption
PtG	Power-to-gas
PtH_2	Power-to-hydrogen
PV	Present value
PZ	Piperazine
R	Return
RES	Renewable energy sources
RO	Reverse osmosis
S&C	Sewage sludge and compost
SBR	Sequencing batch reactor
SCW	Street cleaning aste
SMR	Steam methane reforming
SNG	Synthetic natural gas
SOEs	Solid oxide electrolyzer
SW	Shredder waste
TN	Total nitrogen
TSO	Transmission system operator
UASB	Up-flow anaerobic sludge blanket

VOC	Volatile organic compounds
w	Water content
WLC	Whole life cost

General Introduction

The greatest environmental problem for the present time is the combustion of fossil fuels such as coal, oil and natural gas. Due to the development and growth of world economic, the energy need of more and more countries is increasing enormously. Presently, the fossils fuels are responsible for the main energy resources approximately 80% of the global demand for use in our daily life, in economic or in industrial activities. Nearly 80% of the worldwide CO_2 release derives from the combustion of such fuels [1]. Use of fossil fuels have many associated risks such as decreasing reserves, emissions of greenhouse gases (GHG) and also dependency on the importation [2]. Towards resolving these severe issues, international treaties like the Kyoto protocol and COP21 are emphasizing on development and utilization of renewable energy sources [3]. Thus, as an encouraging solution, renewable energy sources and biomethane can serve as powerful alternatives to curb the use of fossils fuels [4]. Moreover, the EU members agreed to reach in the heating sector an annual increase of 1 % of renewable energy and a target of 14% of renewable sources in the transportation sector by 2030. The projection is a long-term decarburization up to 2050 [5].

In this perspective, the decomposition of biodegradable waste and substrates in anaerobic conditions is a well-established process for the biogas production and consequent biomethane generation. The leading countries in the production of biogas was Germany (46.7 % of the total produced biogas of the EU) followed by united kingdom and Italy as second and third major producers, with respectively 16.2 % and 11.3 % of the total biogas production in EU [5]. By end of 2017, there were 17783 biogas plants with a trend towards installations with bigger capacities [5]. In about 71% of plants, biogas is obtained from agricultural crops and residues, in about 16% from sewage sludge, in 8% from landfill and in the remaining 5% from other substrates [4].

As a carbon neutral source of energy now, biogas gaining more attractions to be a part of alternatives on the fossil fuels and in reducing greenhouse gases emissions. The energy content of the biogas which in fact comes from CH_4 is captured and utilized in many different services such as: electricity production through cogeneration plants, injection to the grid, used as biofuel or town or non-injected into grid used as biofuel mostly [6]. In all these cases, untreated raw biogas needs to be properly treated from all the impurities as well as separated from carbon dioxide to generate biomethane. The French law on energy transition and growth (LTECV) [1] fixed a target of 10% of the total gas consumption that should be represented by green gas by end of 2030. Biogas properly upgraded would be used in the transport sector or directly feed into natural gas grid reaching end consumers, both solutions adding value to biogas.

In the interest of transition towards sustainable and green energy production, a landfill sourced biogas valorization and production of biomethane has been deeply and broadly studied in this thesis. The contents presented in this manuscript have been classified under five separate chapters each presenting different approaches while with the same objective of biomethane production. The chapters are presented as below:

Chapter 1 takes into account a bibliographic study highlighting state of the art data regarding biogas to biomethane process chain. The current problems in the sector of energy and need of more green energy production in this regard has been pointed out in this chapter. Moreover, different state of the art technologies of biogas upgrading have been presented along with their associated research and development in the future. Biogas upgrading technologies such as physical and chemical adsorption, pressure swing adsorption, membrane technology and cryogenic distillation are explained with an objective of presenting their capacities in terms of converting biogas into biomethane. Technical features of five mostly and broadly implemented biogas upgrading technologies are studied and their technical features are compared in terms of methane recovery, methane content in upgraded gas, removal of nitrogen as well as demand on heat and specific electricity consumption. This chapter includes a literature review on the importance of leachate recirculation as well where the composition of leachate, different landfill leachate treatment technologies and some case studies are presented. Moreover, the present chapter reviewed the power-to-gas technology as an alternative and developed technology in converting landfill carbon dioxide into synthetic methane using intermittent renewable sources of energy to produce hydrogen through water electrolysis technology. More highlights regarding power-to-gas technology would be given in the introduction of chapters 4 and 5.

Chapter 2 includes mathematical modeling of landfill biogas (LFG) production; an approach towards the quantification and estimation of future biogas production capacity of a landfill site. After a broad review and research, four different mathematical models to predict landfill biogas production are selected to carry out the estimation of landfill biogas and methane content of the selected landfill site La Poitivinière. TNO model, Multiphase Afvalzorg model, LandGEM and Tabasaran & Rettenberger models are presented in the Chapter 2 with the aim of estimating the available quantity of biogas from La Poitivinière landfill site. La Poitivinière landfill site started receiving a mixture of industrial and household waste in the year 1990. The year 2032 is the end of waste disposal and is considered the closure of landfill site. Knowing the quantity of yearly waste disposal into landfill in tons and their compositions, two different approaches are presented to determine the methane generation potential of waste. The obtained results with the different mathematical LFG model are compared to the recorded site data in terms of yearly biogas volume. The estimation of landfill gas in cubic meter per

year via mathematical models helps us to find the future biogas flow rate from landfill site and hence energy potential of landfill site.

Chapter 3 covers the approach of biomethane production from landfill raw biogas. A life cycle cost assessment including technical and economic features is carried out for the selected five biogas-upgrading technologies to identify the cost effective and energy efficient one. With heat and without heat valorization scenarios are studied along with sensitivity analysis to find out the most influencing parameters in each upgrading technology. CAPEX, OPEX and other associated costs are found from the literature to estimate the total life cycle cost of each upgrading technology. The life cycle cost analysis are carried out independent of source of biogas whether it is from landfill or anaerobic digester. The selection of an upgrading technology is dependent on the source of biogas and its mixture. Landfill for example contains in some cases up to or more than 10 vol% nitrogen. Given the fact that the reference landfill site in this study i.e., La Poitevinière contains more than 10 vol% nitrogen in raw gas mixture, two different scenarios Membrane+PSA and cryogenic distillation which are adoptable for a landfill biogas upgrading, are evaluated. Biomethane production costs in €/m^3 and €/MWh are found for these two scenarios. In addition, economic and financial analysis of upgrading landfill biogas with these two scenarios are assessed in the Chapter 3. As an enhancement to the methane production potential of landfill site, power-to-gas system are introduced via chapters 4 and 5.

Chapter 4 comprises kinetics of catalytic methanation reaction to produce synthetic methane from the hydrogenation of CO_2 in this process. The interest in the study of kinetics of methanation reaction is to understand the impact of input parameters in the process and the evolution of process outputs such as methane and water correspondingly. A thermodynamic analysis as well as simulation of continuous plug flow reactor with a kinetic model have been carried out in Chapter 4. The influence of temperature and pressure on the conversion rate of CO_2 and CH_4 yield is assessed through a thermodynamic analysis. Gibb's free energy minimization method was used to simulate thermodynamic analysis in ProsimPlus process engineering software. In addition, a steady state continuous plug flow reactor was simulated to validate a kinetic model with the literature in the present chapter. The thermodynamic analysis, kinetics of reaction and selection of an appropriate catalyst play a vital rule in the optimization of this process and in achieving better CO_2 conversion rate.

Chapter 5 involves a techno-economic study on power-to-gas system. The interest to introduce power-to-gas system in this chapter is to seek the possibility to valorize carbon dioxide of landfill site captured and separated at the end of an upgrading technology. This way, CO_2 is valorized along with surplus intermittent renewable electricity to produce synthetic methane via two-step hydrogen production through water electrolysis and synthetic methane production via methanation reactor. An

approach is given in this chapter to estimate the synthetic methane production costs via power-to-gas system. The influencing cost items such as electricity purchase price or operating time of sub-system electrolyzer and methanation unit are assessed and their influence on the gas production cost are presented in the current chapter. The integration of an intermediate hydrogen storage facility in decoupling methanation unit from electrolyzer and to respond better to load fluctuation is important. Intermediate hydrogen storage facility helps to achieve a continuous operation of methanation unit and hence guarantees the continuous production of synthetic methane. Its importance in reducing the full load hours of electrolyzer and possibility to use the cheap intermittent renewable electricity is presented in chapter 5.

A General conclusion and future perspectives of the thesis is given at the end to summarize the results of the presented chapters.

1 Chapter 1: Literature review

1.1 Biogas upgrading into biomethane.

The greatest environmental problem for the present time is the combustion of fossil fuels such as coal, oil, and natural gas. Due to the development and growth of world economic, the energy need of more and more countries is increasing enormously. Presently, the fossils fuels are responsible for the main energy resources approximately 80% of the global demand for use in our daily life, in economic or in industrial activates. Nearly 80% of the worldwide CO_2 release derives from the combustion of such fuels [1]. Use of fossil fuels have many associated risks such as decreasing reserves, emissions of greenhouses gas (GHG) and dependency on the importation [2]. Towards resolving these severe issues, international treaties like the Kyoto protocol and COP21 are emphasizing on development and utilization of renewable energy sources [3]. Thus, as an encouraging solution, renewable energy sources can serve as powerful alternatives to curb the use of fossils fuels [4]. Moreover, the EU members agreed to reach in the heating sector an annual increase of 1% of renewable energy and a target of 14% of renewable sources in the transportation sector by 2030. The projection is a long-term decarburization up to 2050 [5].

In this perspective, the decomposition of biodegradable waste and substrates in anaerobic conditions is a well-established process for the biogas production and consequent biomethane generation. The leading countries in the production of biogas was Germany (46.7% of the total produced biogas of the EU) followed by United Kingdom and Italy as second and third major producers, with respectively 16.2% and 11.3% of the total biogas production in EU [5]. By end of 2017, there were 17783 biogas plants with a trend towards installations with bigger capacities [5]. In about 71% of plants, biogas is obtained from agricultural crops and residues, in about 16% from sewage sludge, in 8% from landfill and in the remaining 5% from other or unknown substrates [4].

The European Biomethane Map 2020 shows a 51% increase of biomethane plants in Europe in two years from 2018 to 2020. According to data and statistics obtained, the analysis of the data shows that the number of biomethane plant in Europe has increased from 483 plants (2018) to 729 units (2020). In this context, 18 countries are producing biomethane in Europe. Germany has the highest share of biomethane plants reaching up to 232 followed by France 131 plants and UK 80 plants [19].

By end of 2020, France counts more than 1070 units of biogas production facilities from which 20% is valorized as biomethane and injected into natural gas grid. This accounts in total of 214 unit's injected biomethane into natural gas grid and shows an increase of +74% in 2020. The remaining 861 units (80%) is valorized in combined heat and power (CHP) facilities. The potential increase observed

in 2019 is even amplified in 2020 reaching in total an extra 79% of injection. Renewable biogas production units and valorization in France by end of 2020 is given in Figure 1-1.

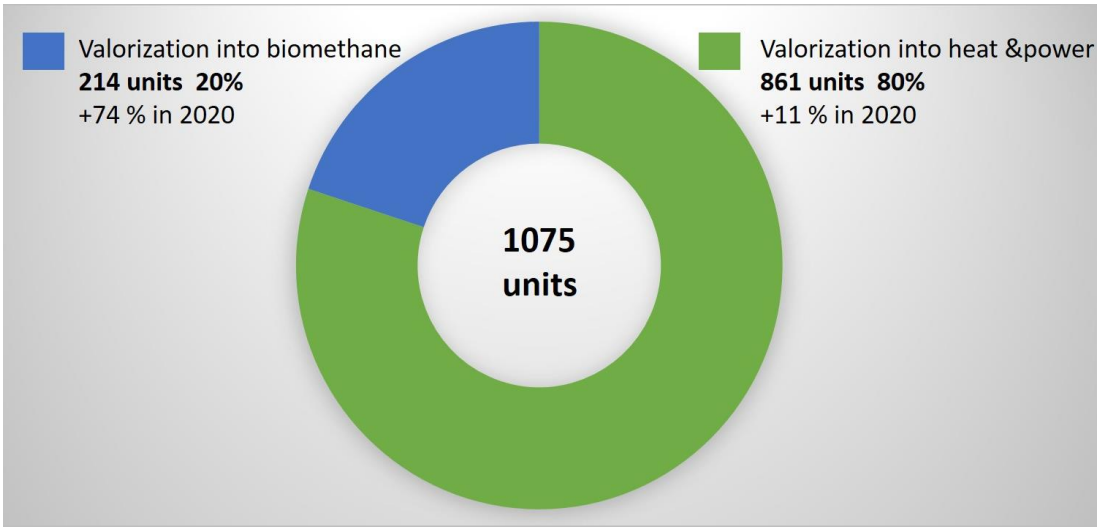

Figure 1-1 : Renewable biogas production units and valorization in France 2020 adopted from [20]

The total number of sites in service and their annual evolution from 2011 until 2020 is given in Figure 1-2. Ninety-one extra sites added in 2020 and reached in total to 2014 sites. In total 3917 GWh/ year capacity of sites were connected into natural gas gird. The total renewable energy production and injection from 214 sites were 2207 GWh/year by end of December 2020. This total energy injection showed +79% increase by end of 2020 and counts for 0.5% of natural gas consumption. The distribution of the total maximum installed capacity by type of injection sites as of 31 December 2020 is given in Figure 1-3. From the total 2014 site, 191 sites (89%) has injected into distribution network and the remaining 23 sites (11%) has injected into transmission network. Landfill sites that are 11 in total have injected 166 GWh/year as of end of 2020 that accounts for 4% of the total injection.

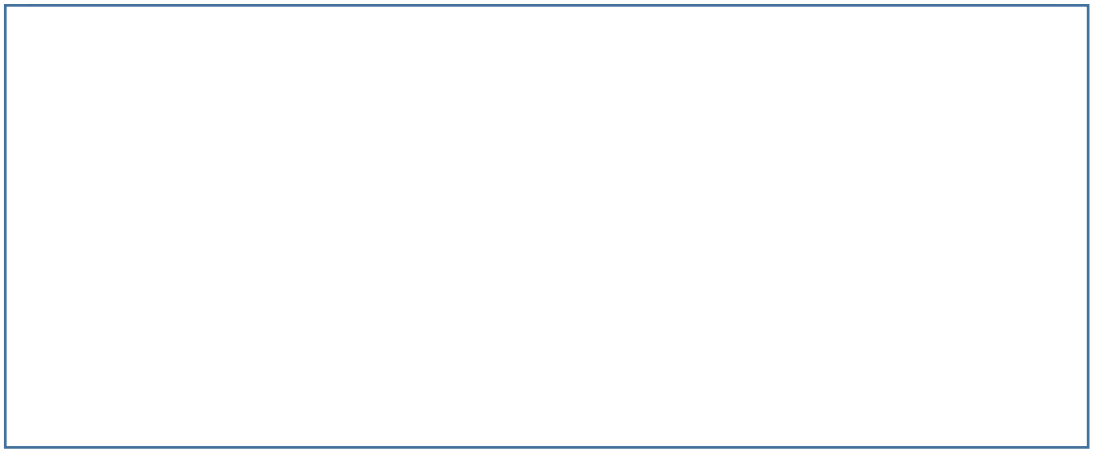

Figure 1-2: Total number of sites injecting biomethane and annual evolution in France from 2011 to 2020 adopted from [20]

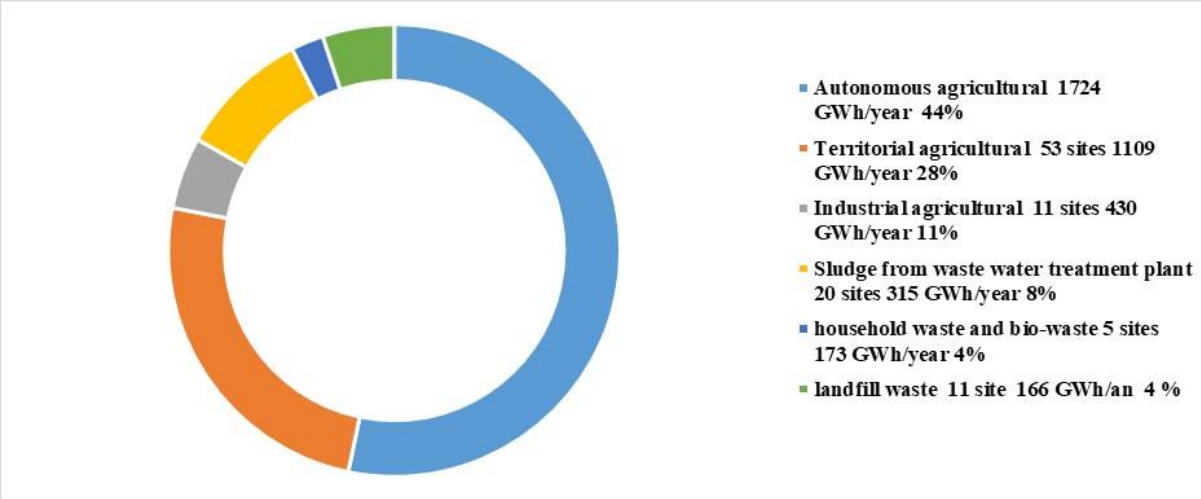

Figure 1-3: Distribution of total maximum installed capacity by type of injection site as of December 2020

As a renewable source of energy, biogas gaining more attractions nowadays to be a part of alternatives on the fossil fuels and in reducing greenhouse gas emissions. The energy content of the biogas that in fact comes from CH_4 is captured and utilized in many different services such as: electricity production through cogeneration plants, injection to the grid used as biofuel or town or non-injected into grid used as biofuel mostly [1]. In all cases, biogas needs to be properly treated from all the impurities to obtain biomethane. Biogas is the result and byproduct of biological decomposition of organic waste in an oxygen absent environment. Biogas is a mixture of mainly methane and CO_2 with hydrogen (H_2), nitrogen (N_2) and other contaminates such as hydrogen sulfide (H_2S), and halogenated carbohydrates and oxygen (O_2) are occasionally present in biogas.

Depending on in what area the biogas is used, different requirements exist in removing the impurities and upgrading to have higher share of CH_4. In most of the cases for example, boilers and cogeneration engines do not require removing CO_2, but if the biogas valorized as vehicle fuel or injected to natural gas grid, it is always recommended to remove CO_2 to reach up to 95% v/v CH_4. Table 1-1 below illustrates the requirements to remove main impurities of biogas depending on its utilization [9].

Table 1-1: Guidelines for impurities removal for specific biogas applications adopted from [9]

Application	**H_2S**	**Siloxanes**	**CO_2**	**H_2O**
Boiler	<250 ppm	Not required	No removal required	No removal required
Cooker	Yes <10 ppm	Not required	No removal required	No removal required
Stationary Engine (CHP)	Yes <250 ppm	Required	No removal required	Avoid condensation
Vehicle Fuel	Yes <5mg/m^3	Required	Recommended <4 %	Removal required <3 %
Natural Gas Grid	Yes	Eventually	Removal required	Removal required

Utilization of biogas as an alternative for natural gas has gained major importance in recent years due to depletion and low quality of natural gas resources. Upgraded biogas can be injected into the natural gas grids [21]. Biogas upgrading as same quality as natural gas by an efficient appropriate method is very important for its injection into the natural gas grids. Countries such as Sweden, Germany, Switzerland, and France have set their own standards for biogas injection into the natural gas grids to prevent corrosion of equipment Table 1-2.

Table 1-2: Biogas requirements for injection into natural gas grid [21]

Component	**France**	**Germany**	**Netherlands**	**Switzerland**
CH_4 (% vol)	≥ 86	≥ 96	≥ 85	≥ 96
CO_4 (% vol)	≤ 2.5	≤ 6	≤ 6	≤ 6
O_4 (% vol)	≤ 0.01	≤ 0.5	≤ 0.5	≤ 0.5
H_2 (% vol)	≤ 6	≤ 5	≤ 0.5	≤ 4
CO (% vol)	≤ 2	-	≤ 1	-
H_2S (mg/Nm^3)	≤ 5	≤ 5	≤ 5	≤ 5
Total sulphur (mg/Nm^3)	≤ 30	≤ 30	≤ 16.5	≤ 30
NH_3 (mg/Nm^3)	≤ 3	-	≤ 3	≤ 20
H_2O (mg/Nm^3)	-	-	-	-
Water dew point (°C)	≤ -5	Soil temp	≤ -8	-
Heavy metals (mg/Nm^3)	≤ 1	≤ 5	-	≤ 5
Siloxanes (mg/Nm^3)	-	-	≤ 5	-

Normally, the calorific value of biogas is 21.5 MJ/m^3, while that of natural gas is 35.8 MJ/m^3. The difference come due to the presence of larger quantity of incombustible part of biogas mainly (CO_2) [3]. Due to presence of large volume of CO_2 in biogas, there is reduced heating value along with increased compression and transportation costs. This drawback limits the economic feasibility of biogas in producing power hence it necessitates the proper treatment technology to be adopted in order to upgrade it to biomethane. Purified biogas not only manage in GHG emissions reduction but in the meantime, it has other advantages such as, emitting lesser hydrocarbons, nitrogen oxides and carbon monoxide compared to gasoline or diesel.

The composition of biogas produced depends on a few factors such as the process design, the type of waste and its varying quantity of organic material put into the landfill or nature of substrate digested in the anaerobic digester. Table 1-3 below lists the typical properties of landfill biogas and its comparison with biogas from anaerobic digester [22].

Table 1-3: Typical properties of the landfill biogas and its comparison with biogas from anaerobic digester.

	Unit	Landfill biogas	Biogas from anaerobic digester
Lower calorific value	MJ/ Nm^3	16	23
	kWh/Nm^3	4.4	6.5
Density	kg/Nm^3	1.3	1.1
Relative density	-	1.1	0.9
Wobbe index, upper	MJ/Nm^3	18	27
Methane range	Vol-%	35-65	60-70
Heavy hydrocarbons	Vol-%	0	0
Hydrogen	Vol-%	0-3	0
Carbon dioxide, range	Vol-%	15-40	30-40
Nitrogen, range	Vol-%	5-40	-
Hydrogen supplied range	ppm		
Ammonia	ppm	5	100
Total Chlorine as Cl^-	mg/Nm^3	20-200	0-5
Oxygen	Vol-%	1	0

1.1.1 Landfill biogas valorization

As said by European commission, over 58 million tons of municipal waste were disposed into landfills in 2017 in Europe. The share of organic waste is 46% from this quantity [7]. Landfill biogas is defined as the natural decomposition of biodegradable organic material under anaerobic environment in a landfill site. Its composition mainly depends on the type and source of waste and is mostly 45% to 60 % methane, 40% to 55% carbon dioxide. The landfill biogas (LFG) also contains trace amounts of inorganic compounds and less than 1% of non-methane volatile organic material. LFG is the main source of methane, a strong greenhouse gas generated by the human activity if not collected it can easily be emitted to atmosphere and causes harm to the environment. Furthermore, methane in nature is combustible and can form potentially explosive mixtures under some certain conditions. This drawback results raising concerns about its leak, migration and release to the atmosphere. The risk of uncontrolled greenhouse gas emissions from landfills are dominant. As a solution into this problem, the disposal of waste into the landfills has decreased 20.6% within the years from 2013 to 2017 in European Union [7]. Few examples of landfill sites valorizing biogas are listed in Table 1-4.

Table 1-4: Example of landfill sites valorizing biogas

Landfill	Utilization	Waste/year	Technologies	Plant capacity (Nm^3/h raw biogas)	In operation service
Claye Souilly	-	-	Membrane/PSA	100	2009
Labessière-Candeil	vehicle fuel	-	PSA	80	-
Saint Florentin	Distribution Grid		Membrane/Cryogenic distillation	160	2017
Saint Maximin	Distribution Grid	200 000	Membrane/Cryogenic distillation	163	2017
Herry	Distribution Grid	-	-	184	2018
Gueltas	Distribution Grid	200 000	Membrane/Cryogenic distillation	255	2018
Pavie	Distribution Grid	40 000	Membrane/Cryogenic distillation	71	2018
Inzinac Lochrist	Distribution Grid	60 000	Membrane/Cryogenic distillation	82	2019
Vert-le Grand	Distribution Grid	-	-	255	2018
Les Ventes-de-Bourse	Distribution Grid	120 000	Membrane/Cryogenic distillation	255	2020
Chevilly	Distribution Grid	60 000	Membrane/Cryogenic distillation	179	2018
Lieoux	Distribution Grid	85 000	Membrane/Cryogenic distillation	194	2020

Three processes are involved in the production of landfill gas that are bacterial decomposition, volatilization and chemical reactions.

Bacterial decomposition:

Most of the landfill biogas is produced with bacterial decomposition. This occurs when the bacteria naturally present in the waste and the soil used to cover the landfill site breaks the organic waste. Organic waste include food, garden waste, street sweepings, textiles and wood and paper products. Bacteria decomposes organic waste in four phases and the composition of gas changes during the decomposition of organic waste within these phases. Figure 1-4 below shows the gas production at each of these four phases. Production phases of typical landfill biogas is given in the Figure 1-4.

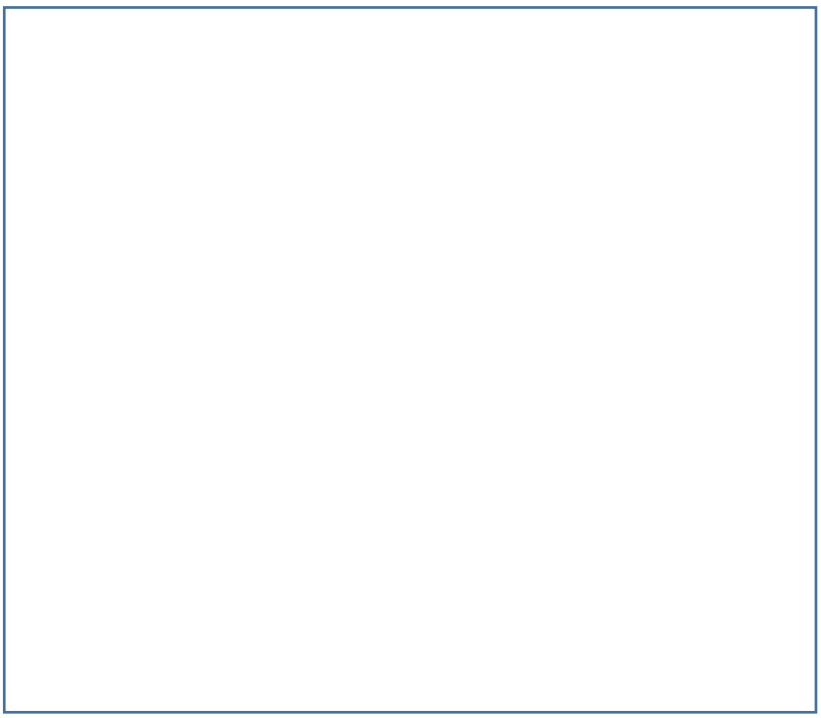

Figure 1-4: Production phases of typical landfill biogas adopted from [23]

Volatilization

Landfill gases can be created when some certain wastes, particularly organic compounds, change from a liquid or solid into vapor. This process is called volatilization. Non-methane organic compounds NMOCs in landfill gas may be the result of volatilization of some chemicals disposed into landfill site.

Chemical reaction:

Landfill gas, including some NMOCs can be created by reactions of certain chemicals present in the waste. For example, if chlorine bleach and ammonia encounter each other within the landfill, a harmful gas is being produced.

The four phases of bacterial decomposition of landfill waste:

Phase I:

During the first phase of decomposition, aerobic bacteria live only in the presence of oxygen consumes oxygen while breaking down the long molecular chains of complex carbohydrates, proteins and lipids that comprise organic waste. The primary byproduct of this phase is carbon dioxide. The level of nitrogen in the beginning of this phase is high but declines as the landfill moves through the four phases. Phase 1 continues until available oxygen is depleted and consumed by bacteria present in the waste. Phase 1 can last few days to months depending on how much oxygen is present in the waste

disposed into landfill. Meanwhile, oxygen level and quantity may vary according to factors such as how loose or compressed the waste was when it was buried.

Phase II:

Phase II decomposition begins when the oxygen is completely depleted and consumed entirely by bacteria. This phase is called anaerobic phase, a process which does not require oxygen to decompose organic matter content of the waste. Anaerobic bacteria transform compounds created by aerobic bacteria into acetic, lactic and formic acids and alcohols such as methanol and ethanol. This landfill becomes highly acidic in this phase. As the acids mix with the moisture present in the landfill, they cause certain nutrients to dissolve, making nitrogen and phosphorus available to the increasingly diverse species of bacteria in the landfill. The gaseous byproducts of these processes are carbon dioxide and hydrogen. Microbial process will return to phase one if the landfill is disturbed or in case if oxygen somehow entered into landfill.

Phase III:

The decomposition of this phase starts when specific kinds of anaerobic bacteria consume the organic acids produced in Phase II and form acetate, which is an organic acid. This process causes the landfill to become a more neutral environment in which methane-producing bacteria begin to establish themselves. Methane and acid-producing bacteria have a symbiotic, or mutually beneficial, relationship. Acid-producing bacteria create compounds for the methanogenic bacteria to consume. Methanogenic bacteria consume the carbon dioxide and acetate, too much of which would be toxic to the acid-producing bacteria.

Phase IV:

Phase IV decomposition begins when both the composition and production rates of landfill gas remain relatively constant. Landfill biogas is being produced at a stable rate in Phase IV, typically for about 20 years; however, biogas will continue to be emitted for 50 or more years after the waste is placed in the landfill (Crawford and Smith 1985). Gas production might last longer, for example, if greater amounts of organics are present in the waste, such as at a landfill receiving higher than average amounts of domestic animal waste.

1.2 Leachate recirculation

Landfill leachate is defined as the liquid effluents generated from rainwater percolation through solid waste disposed of in a landfill as well as the moisture present in the waste and the degradation products of residues. Leachate is counted one of the most dangerous source of emission from a landfill

site. Multicarrier systems are designed and constructed to avoid such emissions into environment. These systems include bottom and lateral lining, waste pre-treatment and extraction and treatment of leachate. Leachate treatment clearly represents one of the big issue to deal with during the design, construction and management of landfill sites. Not only environmental and technical constraints should be considered but also economical ones. In France, as soon as a landfill site comes into operation, environmental monitoring is required and must be continued following site closure for at least 30 years (Decree of 9 September 1997 amended). Post-operation management of closed landfills includes monitoring of emissions (leachate and biogas), receiving systems (for both ground and surface waters), along with general site maintenance (enclosure, covering, vegetation) and maintenance of collection systems for biogas and leachates [24].

Once leachate is treated, it could be discharged into environment but should follow strict regulations and standards in order to not harm the environment, surface and underground water. The concentrated leachate after treatment technology could be reinjected/recirculated into landfill site. The recirculation of concentrated leachate is theoretically similar to the recirculation of law leachate often adopted into bioreactor landfills. Bioreactor is a device that allows maintaining, controlling and optimizing the microbial process by measurements and regulations of parameters. The main objective of the bioreactor is the intensification of biological processes in given conditions. In specific conditions, landfills may be considered as bioreactor when they receive either raw or concentrated leachate. In fact, the pollutant mass associated to raw or concentrated leachate is similar, the only important difference, is the volume of liquid recirculated, hence the pollutants concentrations [25]. Landfill leachate may afford a series of potential advantages:

- Improvement of leachate quality.
- Enhancement of gas production i.e. improving the possibility of gas-to-energy options.
- Acceleration of biochemical processes.
- Control of moisture content, nutrients and microbe migration within the landfill.

In addition to potential advantages mentioned above, recirculation of leachate enhances the decomposition and settlement rates. These provide the landfill owner with additional airspace prior to closure (i.e. a greater mass of waste can be buried per unit volume of landfill) and limits the potential for settlement-induced damage of final cover. Landfill leachate is characterized by several physical-chemical parameters such as pH, suspended solids, biochemical oxygen demand (BOD), chemical oxygen demand (COD), ammonia (NH_3) total nitrogen (TN), chloride, phosphorus, heavy metals and alkalinity.

1.2.1 Factors affecting the characteristics of landfill leachate.

Characteristics of landfill site leachate can be influenced by several factors like landfill age, waste type and also composition, meanwhile, seasonal weather variation; site hydrogeology, dilution by rainfall, precipitation, and degree of decomposition within landfill also influence the characteristics of landfill leachate. Among them, the landfill age is a determinant factor controlling the leachate composition because several parameters dramatically change as the landfill stabilizes [26]. Based on age, conventional landfill leachates are commonly classified into three categories: (1) young (<5 years), (2) intermediate (5–10 years) and (3) mature (>10 years).

As the landfill age increases, the leachate parameters (e.g., pH, BOD, COD, and BOD/COD ratio) change significantly. For instance, the concentrations of BOD and COD decrease with increasing landfill age, likely due to the degradation of organic waste in leachates. It is believed that most of the biodegradable organic matters (evaluated by BOD) are decomposed in stabilization stage, but the non-biodegradable organic matters (contribute to COD) remain unchanged in this stage [26].Consequently, the BOD/COD ratio (biodegradability index) decreases with time. In particular, high COD concentrations (> 10,000 mg L^{-1}) and BOD/COD ratios (0.5–1) are observed in young landfill leachates, whereas the COD concentrations (below 4000 mg L^{-1}) and the BOD/COD ratios below 0.1 are found in mature landfill leachates [26]. In comparison, pH value of the leachate increases with age and the concentrations of heavy metals show a declining rate with age due to higher pH of the leachate. On the contrary, the concentration of ammonia nitrogen does not show an obvious decreasing trend with time, except due to dilution effects.

Leachate composition not only vary with the landfill age, but also from place to place, leading to large fluctuations in the values of representative characterization of parameters. Figure 1-5 demonstrates the typical values of pH, COD, and BOD/COD ratio for leachates from young, intermediate, and mature landfills. It is reported that co-disposal of ash with municipal solid waste may provide a mean to eliminate toxic species in leachates.

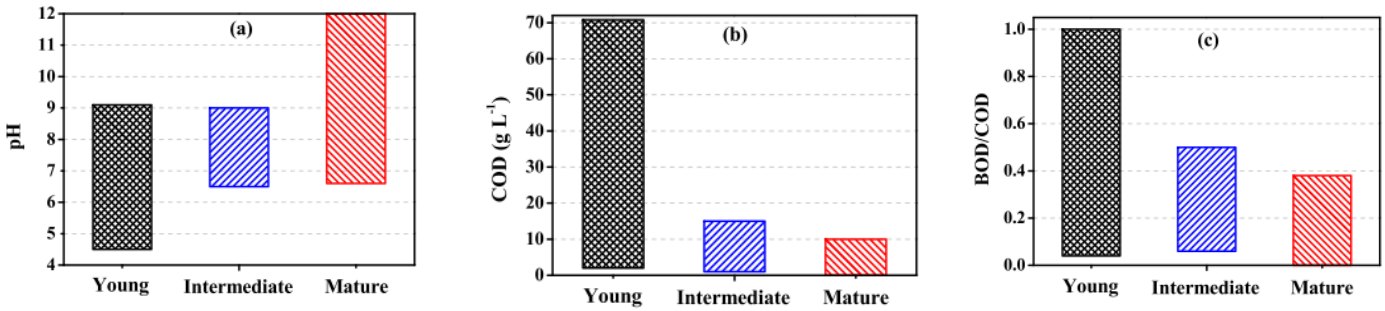

Figure 1-5: Typical values of (a) pH, (b) COD, and (c) BOD/COD ratio for leachates from young, intermediate, and mature landfills. Adopted from reference [26]

1.2.2 Leachate composition

Depending on the stages of waste evolution (i.e., aerobic, anaerobic acid, methanogenic, and stabilization stages), the composition of landfill leachates is extremely heterogeneous and variable. Leachate pollutants are divided into four groups, Table 1-5 illustrates the main pollutants found under four groups. Most of the above pollutants have accumulative, threatening, and detrimental effects on growth of aquatic organisms, ecology, and food chains, thereby leading to enormous problems in public health, e.g., carcinogenic effects, acute toxicity, and genotoxicity.

Table 1-5: Composition of landfill leachate

Dissolved organic matter	Macro inorganic components (mg L^{-1})	Heavy metals <0.01 mg/kg - >1.0*10^4 mg/kg	Xenobiotic organic compounds
e.g., volatile fatty acids humic and fulvic acids	e.g., Ammonia ($NH4^+$-N) 50 – 2200 Sodium (Na^+) 70 – 7700 Potassium (K^+) 50 3700 Calcium (Ca^{2+}) 10 7200	e.g., Chromium (Cr^{3+}) Nickel (Ni^{2+}) Copper (Cu^{2+}) Zinc (Zn^{2+})	e.g., Aromatic hydrocarbons Pesticides Plasticizers

1.2.3 Landfill leachate treatment technologies

Conventional treatments of landfill leachates are generally grouped into three major category: (1) biological processes (aerobic or anaerobic); (2) physical and chemical processes; (3) a combination of biological and physical-chemical processes. Table 1-6 represents the broad classifications of three groups of landfill leachate treatment technologies.

Combination of two or more landfill leachate treatment technologies has been proved effective and efficient than individual treatment for landfill leachates. It can be assigned to the fact

that a two-step or three-step treatment is capable of synergizing the advantages of individual treatments, overcoming their respective limitations. It is well recognized that (1) treatment efficiencies; (2) cost of the treatment system; and (3) environmental impacts of the treatment system are the three major criteria that should be considered for recommending a sustainable treatment technology or combination of treatment technologies for landfill leachates.

Table 1-6: Conventional treatment of landfill leachate

Biological processes	Physical-chemical treatment	Combined treatments
Aerobic treatment Anaerobic treatment	Coagulation-flocculation Chemical precipitation Adsorption Membrane filtration Ion exchange Air stripping Chemical oxidation/ advanced oxidation processes (AOPs) Electrochemical treatment	Combination of two or more physical-chemical treatments Combination of two or more biological treatments Combination of physical chemical and biological treatments

A list of combined physical-chemical technologies for the treatment of landfill leachate is given in Table 1-7.

Table 1-7: Combined physical-chemical technologies for treatment of landfill leachate adopted from [27]

Type of combined treatment	Landfill age	Influent COD (mg L^{-1})	PH	COD removal (%)
Coagulation/Fenton	Mature	417	5.0	73
Nano filtration (NF)/adsorption	Mature	1450	7.3	97
NF/coagulation	Mature	2150	7.5	80
Ozone/adsorption	Mature	4970	8.0-9.0	90
Coagulation-flocculation/Ozonation	Mature	3460	8.5	48
Electro-coagulation/NF	Mature	636	5.7	92
Coagulation-flocculation/Fenton	Mature	7400	8.5	90
Coagulation/photo-oxidation	Mature	5800	7.6	64
Coagulation/Ozonation	Mature	5000	4.0-5.0	78
NF/adsorption/Ozonation	Mature	4000	6.5	99
Ultrafiltration/adsorption	Mature	3050	7.0	97
Reverse osmosis/evaporation	Mature	19.900	6.4	88

Table 1-8 characterizes the treatment performance of landfill leachates by some combined physical-chemical and biological techniques. Using a combined photo-Fenton and biological activated sludge process, about 87±2 % removal of COD and 84±2% removal of BOD by conventional biological process were obtained, while 89 ± 3% removal of COD and 75 ± 1% removal of BOD by photo-Fenton process were obtained [28]. Nevertheless, both processes used alone did not meet effluent discharge standards. With the combined process, it was possible to treat an effluent with high organic load, achieving a removal of 98% COD and BOD and meeting the restrictive standards of release in recipient water bodies [28].

Table 1-8: Treatment performance of landfill leachate by combined physical-chemical and biological techniques. Adopted from [29]

Combined treatments	Initial concentration (mg L^{-1})		Removal efficiency (%)	
	COD	NH_4^+-N	COD	NH_4^+-N
Up-flow anaerobic sludge blanket (UASB)/RO	35.000	1600	99	99
Activated sludge/RO	1153	6440	99	99
Adsorption/nitrification	2450	830	55	93
Coagulation/UASB	11.247	598	80	2.5
Sequencing batch reactor (SBR)/electro-oxidation	3973	1726.6	98	99
SBR/adsorption	3200	1800	43	96
Constructed wetland/adsorption	2301	627	86.7	99.2
Membrane biological reactor (MBR)/UF/electro-oxidation	1485	710	94	77
Trickling filter /electro-coagulation	1332	444	80	94
Photo-Fenton/MBR	24.000	4000	96	88
Activated sludge/coagulation/photo-Fenton	4084	559	96	62-99

1.2.4 Case studies

Leachate recirculation may help to enhance the performance of landfill and optimize microorganism activity but the selection of treatment technology is essential and the characteristics of concentrate needs to be studied and analyzed before reinjection into landfill body. Literature provides few limited full-scale application of concentrate recirculation. Results obtained are varying, in some cases, increase of COD and ammonium nitrogen coupled with an increase in salinity, which might negatively affect both microbial activity in the landfill, and performance of treatment plant has been found. Similarly,

Not only did leachate production not increase significantly but the characteristics of leachate extracted from the well closest to the reinjection point also remained unchanged. Nevertheless, in other cases, the biogas production and methane percentage has increased thanks to concentrate recirculation into landfill body [30].

In the laboratory, leachate recirculation accelerates the biodegradation of organic material and hence the production of biogas respectively. This acceleration did not clearly confirmed experimentally in the landfill site. The reasons could be such as a bad homogeneity in the humidity of waste, system of recirculation and insufficient flow rate of leachate into landfill body [31]. Few case studies are presented where leachate is either reinjected into real landfill site or experimented in lab-scales.

The objectives of the study carried out by N. Sanphoti et al. [32] were to determine the effects of leachate recirculation and supplemental water addition on municipal solid waste decomposition and methane production in three anaerobic digestion reactors. Anaerobic digestion with leachate recirculation and supplemental water addition showed the highest performance in terms of cumulative methane production and the stabilization period time required. In another study carried out by L. Morello et al. [30], the results of lab-scale tests conducted in landfill simulation reactors, in which the effects of injection of municipal solid waste (MSW) landfill leachate reverse osmosis (RO) concentrate were evaluated. Results showed that RO concentrate recirculation did not produce consistent changes in COD emissions and methane production. Simultaneously, ammonium ion showed a consistent increase in leachate (more than 25%) in anaerobic reactors, free ammonia gaseous emissions doubled with concentrate injection, while chloride accumulated inside the reactor. Similarly, in a study carried out by P. S. Calabrò et al. [25], it presents the monitoring study of a landfill site where concentrated leachate obtained during membrane treatment is recirculated. The findings resulting from the first 30 months of monitoring of concentrated leachate recirculation show that leachate production did not increase significantly and that only a few quality parameters (i.e. COD, Nickel and Zinc) presented a moderate increase.

In a recent study by A. Błałowiec et al. [33], the enhancement of biogas production by leachate recirculation has been investigated. In a landfill bioreactor, located in Kosiny Bartosowe, Poland, with capacity of 70 000 ton of municipal solid waste, the research aiming on the determination of the influence of leachate recirculation on biogas generation was done. The Experiments were carried out in two periods: just one month after bioreactor sealing with hydraulic loading rate (HLR) of 2 mm/d corresponding to 104 dm^3/ton year, and one year after bioreactor sealing with HLR of 3 mm/d corresponding to 156 dm^3/ton year. Doubling of biogas production from about 100 to 200 m^3/h and

the increase of methane content from 60 to 65% has been determined when 2 mm/d of HLR of leachate recirculation was applied. The implementation of HLR on the level 3 mm/d increased biogas production from 148 to 270 m^3/d, and methane content from 62 to 64%. Leachate recirculation improved thermal conditions in bioreactor to typical mesophilic values. In this study, the implementation of leachate recirculation into bioreactor landfill body significantly increased the biogas potential to 125 m^3/ton during one month after landfill bioreactor sealing and to 169 m^3/ton after one year landfill bioreactor sealing.

For typical landfill bioreactors, where fermentation is optimized, HLR should be in the range from 100 to 200 dm^3/ton year [34], what was confirmed in the study carried out by A. Błałowiec et al. [33].

1.3 State of the art technologies of biogas upgrading systems

Upgrading of biogas takes place with CO_2 and other impurities removal and as well as enhancement of calorific value of the said gas. The energy content of biogas is directly proportional to CH_4 content, hence removing CO_2 allows to reach higher CH_4 content and to reach a higher calorific value. The technologies, which are mostly used to remove CO_2, are based on absorption either physical or chemical such as water scrubbing or amine scrubbing, adsorption such as pressure swing adsorption and membranes. In addition to conventional biogas upgrading technologies, emerging biogas upgrading technologies exist too. These technologies such as cryogenic, in situ methane enrichment and hybrid are still under research and development and could possibly replace the conventional biogas upgrading in the future. The methods, which are used to purify and upgrade, are mainly distinguished based on their consistency, methane purity at outlet and methane loss during the process of operation. Among the many methods and technologies implemented, water scrubbing has the higher share, followed by pressure swing adsorption and chemical absorption. Pressure swing adsorption and membrane technology offers progressive research potential. The level of maturity and vast area of applicability of the technology is related with lower energy consumption and costs included in the process. The lower the plant consumes energy, the higher the net energy be saved and makes it more suitable in commercial and industrial skills.

Purification of biogas is the removal of contaminants and impurities such as hydrogen sulfide, water, Siloxanes and volatile organic compounds (VOC). Hydrogen gas is corrosive and water vapor may cause corrosion when combined with H_2S on metal surfaces and reduces the heating. H_2S can be removed in a process before CO_2 removal with the help of activated carbon or it is removed sometimes during upgrading process. Water vapor is also removed either by refrigeration or by adsorption with a drying agent [35]. Siloxanes mostly present in landfill gases due to occurrence of defoaming agents

and lubricants. Some type of Siloxanes is water-soluble, and some are not, hence some of them can be removed during upgrading process based on few liquid using technologies such as water scrubbers. In order to get rid of all type of Siloxanes and VOCs an additional cleaning step is required which is achieved by installing activated carbon filter which is by now are the best technology to remove Siloxanes [35], [36]. A second filter can be installed to avoid breakthrough of fully loaded filter.

1.3.1 Absorption process

Absorption technology of biogas upgrading is classified based on nature of absorbent into chemical scrubbing (amine scrubbing) and to physical scrubbing (water scrubbing, organic physical scrubbing).

1.3.1.1 Physical absorption

1.3.1.1.1 Organic scrubbing

Biogas upgrading with absorption technology is either physical or chemical, using organic solvents. These organic solvents used in physical absorption can absorb only CO_2 because CO_2 has higher solubility in organic solvents, but they are not able to remove N_2 or O_2 from the mixture of biogas. Organic solvents such as methanol and dimethyl ethers of polyethylene glycol (DMPEG) can be used as organic solvents in case of physical absorption in upgrading biogas [37]. An appropriate organic solvent should be cost effective, availability and non-hazardous nature for making the system efficient and economical, play an important role in absorption technology. Few of the factors, which makes physical absorption a simple and economical upgrading system, are that it works on small flow rates and does not need a complex infrastructure to operate it.

At the outlet of a physical absorption technology, two streams are collected: one is liquid rich in CO_2 and the other is a gas stream rich in methane. The method under which a physical absorption technology works is that the raw biogas and scrubbing liquid (organic solvents) are kept in contact in counter-currently inside a column.

1.3.1.1.2 Water scrubbing

In this technique of biogas upgrading, a non-reactive fluid such as water is used to remove biogas impurities. Water scrubbing is the mostly and widely implemented biogas upgrading technology in the world. Water is used in this process as a solvent to remove H_2S and CO_2 from biogas and to obtain rich methane gas at the outlet of water scrubbing. Due to high solubility of H_2S and CO_2, it is easier to remove them and separate it from Methane, since CH_4 has lower solubility compared to both CO_2 and H_2S. Although H_2S can also be removed tighter with CO_2 from biogas, but due to having corrosive and poisonous nature, a pre-treatment process is generally adopted in order to remove H_2S first from the biogas and help to capture pure CO_2 stream at the outlet of this process [3].

Once the biogas is firstly pre-treated and removed from H_2S, then it pressurized up to 7-12 bars before introducing to the bottom of the scrubbing column. Water is added from the top of the tower, biogas is fed from the bottom, and it moves in upward direction until it is cleaned and collected at the top of the scrubber tower. Water moves in downward direction counter currently and the CO_2 rich liquid water is collected from the bottom of the tower at atmospheric pressure or sometimes 2-4 bar in a striper or flash tank. Flow of the biogas in counter current direction against water results in dissolving CO_2, H_2S and some quantity of CH_4 in water according to their solubility and partial pressure and results in the increase of CH_4 percentage in the gas flowing upward [38]. Schematic of the physical absorption is shown in the Figure 1-6.

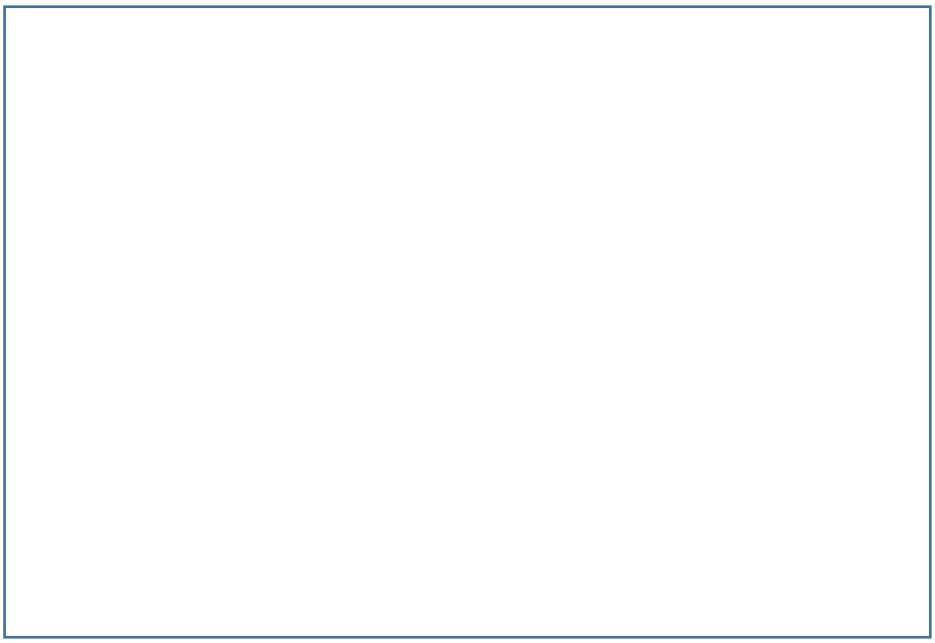

Figure 1-6: Schematic of water scrubbing adopted from [39]

Alternatively, another type of physical absorption, organic physical scrubbing is fundamentally like the concept of water scrubbing followed by regeneration. Organic solvents, which are used in this technology and replaced with water, are methanol and dimethyl ethers of polyethylene glycol (DMPEG) for absorption of CO_2 in organic physical scrubbing. Regeneration of the organic solvent used in this process can be achieved under extremely high temperature and hence can be energy intensive. H_2S needs to be removed and treated before the gas is applied to organic physical scrubbing because it is hard to regenerate from the solvent and in case if it is generated it will negatively impact the capacity of CO_2 absorption [8].

1.3.1.2 Chemical absorption

Chemical absorption varies from physical absorption in the chemical reaction between solvent and absorbed materials. In this process, H_2S and CO_2 are not only get absorbed in the solvent but in

addition, it chemically reacts with the amines present in the solvent. Hence this results in the very low methane losses <0.1% because of high selectivity of solvents towards CO_2 and H_2S [3].

Treating gas with amines also called amine scrubbing and gas sweeting and usually refers to a group of processes that uses aqueous solutions of various alkyl amines (commonly referred to simply as amines) to remove hydrogen sulfide (H_2S) and carbon dioxide (CO_2) from gases [9]. The most frequently used aqueous solutions of amines are monoethanolamine (MEA), diglycolamines (DGA) and diethanolamine (DEA) [40]. Nowadays, mixture of MEA and piperazine (PZ) is commonly used, which is known as activated MDEA (aMDEA).

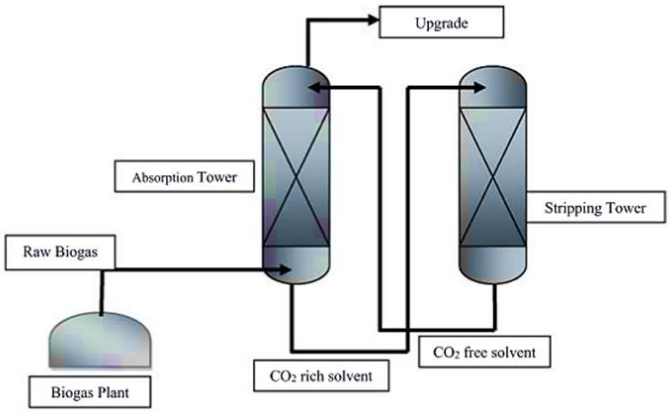

Figure 1-7: Schematic diagram of absorption adopted from [3]

1.3.2 Adsorption process

1.3.2.1 Pressure swing adsorption

Pressure swing adsorption technology works under the mechanism that the gas molecules are adsorbed selectively on the solid surface depending on the different size of molecules. PSA processes has a vast area of application. This technology has been already used for natural gas purification, air separation and in hydrocarbon separation from Petro-chemical and organic synthesis processes. In addition, recently it is also used in upgrading biogas. Since the CH_4 molecule is larger than other gas molecules, PSA processes can be efficiently applied in separating CH_4 from CO_2, N_2, and oxygen.

When pressure swing adsorption is applied to upgrade biogas, it is always necessary to install a pre-treatment of biogas in order to remove H_2S, because hydrogen sulfide is corrosive and toxic and irreversibly adsorbed on the surface of adsorbent materials in PSA. Methane purity up to 98% can reach with PSA and losses of CH_4 are about 2-4% but generally more methane will be lost if higher methane purity is needed [41]. In PSA processes, the adsorbent material is fundamental element. Equilibrium and kinetic adsorbents, by now are commercially available for full-scale applications and can be used for the upgrading of biogas. Activated carbon, zeolite 13, Zeolite 5A, carbon molecular

sieves (CMS) have already been tried and furthermore technological sound materials such as silicate, metal organic framework, silicoaluminophosphate sorbents are being investigated under laboratory scale [40].

The Process of PSA is principally based on four phases forming a cycle called Skarstrom cycle [42]. As this cycle contains four phases and its design comprises four columns. Normally adsorption is done in the first column though the other three (columns 2, 3 and 4) are made to perform different phases of regeneration. In a usual PSA operation once H_2S is removed then the raw biogas is fed into the column at a specific pressure, where adsorbents can adsorb CO_2. After attaining equilibrium, i.e., when the adsorbent is saturated with CO_2, the pressure of the column is being decreases and the loading of CO_2 is decreased.

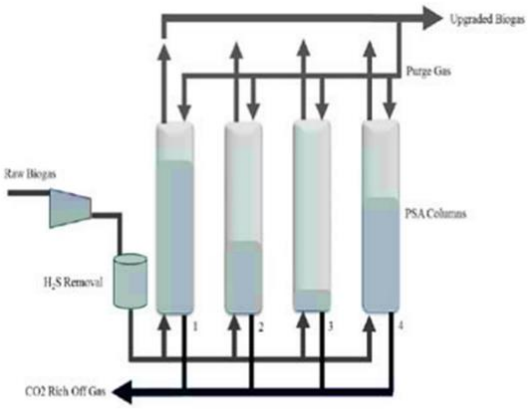

Figure 1-8: Schematic diagram of Pressure Swing Adsorption adopted from [3]

1.3.3 Membrane technology

Membrane technology involves penetration of permeate (liquid or gas) across membrane and is related to the concentration gradient of permeate. The essential approach of membrane separation process is the difference in chemical affinity and particle size of different molecules. Membrane process is a separation technique at molecular scale, and has many merits, such as low cost, energy efficiency and easy process [8]. Different gases to be separated function on the principle of selective permeation. The different gases can certainly be dissolved into polymeric materials and the transport across the membrane takes place when a pressure difference is created on both sides of the membrane. When the rate of permeation is high, the product of coefficient of solubility and coefficient of diffusion is also high. Hence, smaller molecules such as H_2, H_2S and CO_2, which are highly permeable, can permeate at a faster rate than methane. Hence, when raw biogas i.e., with CO_2 is fed through this membrane, it can result into two streams of gases, one is of CH_4 and another one is CO_2. Hydrogen

sulfide removal can be done by two methods either by pre-treatment of gas or selecting a type of membrane that will support permeation of H_2S and CO_2 together [43].

Upgrading biogas by means of membrane process achieved nowadays in vast numbers, because it is easy to operate and does not need any chemicals or heat for the process. The technology works on the concept of penetrating permeate either gas or liquid across the membrane filters and is related on the concentration gradient of permeate. Productivity of the technology depends on selection of the type of the membrane; the technology is lighter, compact and does not require scaled labor for the maintenance of the plant. Other upgrading technologies are somehow dependent on the concentration of the volatile organic compounds (VOCs) present in the biogas, but this is not the case in membrane and the process is independent of the concentration of such volatile organic compounds (VOCs).

Besides many advantages, the membrane technology has disadvantages such as, elevated cost of membrane, degradation of membrane filters with time, and the membrane will get damaged due to the vibration initiated due to colloidal solids [38]. The recent development and research in the field of membrane is to create and build a techno-economically feasible polymer to cope with the different working conditions and to minimize the existing disadvantages. The objective in this research is to be able to enhance permeability of membrane material but in contrast not to compromise its selectivity.

Figure 1-9: Schematic Diagram of Membrane biogas upgrading adopted from [44]

1.3.4 Comparison of biogas upgrading technologies.

The methods that are used for upgrading biogas are compared based on some technical features. Upgrading costs of the established technologies depend on specific technology but more importantly on the plant capacity and characteristics. The amount of the energy needed to upgrade biogas to biomethane is a key consideration while selecting an upgrading method. From Table 1-9 presented, cryogenic distillation is the most energy intensive technology reaching up to 0.76 kWh/Nm^3 electricity demand. The rest of the technologies present the same range of energy need. It is evident from the Table 1-9 that there is no optimal technology considering all parameters. Selecting criterion of

appropriate biogas upgrading technology is not only based on the cost economics. It is also important to keep in mind that selecting these methods also related on the final utilization of bio-methane and percentage of the CH_4.

When the treatment of biogas from landfill is concerned, membrane technology is well suited for this case since the technology can remove nitrogen in addition to separating CO_2 from CH_4. The presence of nitrogen is dominant in the composition of landfill biogas and necessitates to be removed. Moreover, with the future proposed research and developments in the sector of membrane, it is possible to have the integrated H_2S removal with sophisticated membrane filters. This way the investment on activated carbon filters as a pre-treatment step would be avoided. Capturing separated CO_2 is also considered as an advantage and is possible in case of pressure swing adsorption, membrane technology or cryogenic distillation. The captured CO_2 this way could be utilized in many ways and one of which is in the hydrogenation of CO_2 to produce synthetic methane. From the total 47 upgrading plants installed in France until end of 2017, 33 of them are membrane technology [6].

A recent shift is being observed in the market scenario from paradigm's like PSA or water scrubbing towards more balanced technologies such as cryogenic distillation, membrane, in situ methane enrichment and hybrid [3].

Table 1-9: Comparison of biogas upgrading technologies

Characteristics	Unit	Water Scrubbing	Chemical Absorption (amines)	Pressure Swing Adsorption	Membrane Technology	Cryogenic
Electricity demand	(kWh/Nm^3)	0.2-0.3	0.15	0.2-0.25	0.18-0.35	0.76
Heat demand	(°C)	NO	120-160	NO	NO	NO
Operation pressure	(bar)	5-10	0.1	4-7	5-10	10-80
Methane recovery	(%)	98	99-96	98	80-99.5	97-98
Methane content in upgraded gas	(% mol)	>97	>99	>96	>95	>97
Water demand		YES	YES	NO	NO	NO
Demand on chemicals		NO	YES	NO	NO	NO
Ease of operation		Complex	Intermediate	Intermediate	Easy	Intermediate
Removal of N_2		NO	NO	Possible	Possible	Possible
Pre-purification		YES	YES	YES	Recommended	YES
H_2S co-removal		YES	Contaminant	Possible	Possible	YES

1.3.5 Trends in Research & development for the treatment of biogas

1.3.5.1 Upgrading technologies

Due to the high demand in the treatment of biogas, existing upgrading technologies must be enhanced in terms of its function and operation to make them cost effective and competitive between each other. Currently R&D is going on in the field of water scrubbing in improving the efficiency of absorbent and in the purification and separation of CO_2 and further in recycling water [3]. Enhancement and optimization of water scrubbing based biogas upgrading technologies are under current development in order to make the technology competitive in terms of lower energy consumption and reduction in the total cost of plant. One of the energy efficient and cost effective process in this field is to develop novel absorption columns which can provide enhanced mass transfer performance and relatively low pressure drop [3].

Reducing and minimizing the PSA units are the research and developments being carried out currently in the field of PSA. The aim is to enhance the technology and make it adoptable for a small-scale applications by reducing energy use [45]. One of the biggest disadvantage of PSA is that an off gas stream will be generated that requires further treatment to avoid emission in to the environment, treating this off gas stream finally results into an increased cost with the technology. Augelletti et al. [46] modified the size of the PSA, two PSA units were used. Biogas was fed into first unit and the off gas is fed into second unit which contains Zeolite 5A as an adsorbent. They have concluded that the use of double PSA units for biogas upgrading seems to be a remarkably interesting and feasible process to obtain an almost complete separation of biogas components. Indeed, the configuration studied in their work allows obtaining in on one side, biomethane with CO_2 content less than 3% that makes it suitable to inject to natural gas grid and, in addition, an almost pure carbon dioxide stream >99%. The whole process yields a total CH_4 recovery of 99.4% with an energy consumption of (1250 kJ/kg of biomethane) if compared to other biogas upgrading processes based on a single PSA unit. It is worth to mention that the adsorbent development is one of the most important development in the field of PSA.

Research and development are also realized in the field of membranes, one of which is designing novel membrane systems that can cope with the extreme condition. Friess et al [47] designed membranes, which has the ability to function in humid feed and less compressed gas. They used epoxy-amine based ion-gel membranes and it showed an excellent performance in treating humid gases. In a latest study carried out by Park et al. [48] that states a novel biogas upgrading technology using membrane contactor process. They designed a pressure cascaded stripping system

comprised of a polypropylene hollow fiber membrane contractor biogas upgrading unit and observed a higher methane yield 90% and purity 93%.

1.3.5.2 Emerging biogas-upgrading technologies.

1.3.5.3 Cryogenic distillation

One of the emerging biogas upgrading technology is cryogenic one, there are few commercial plants functioning with this technology. The primary concept behind this technology is the difference in condensing temperature of different gases. The raw biogas is cooled and compressed in order to liquefy CO_2. Pretreatment of H_2S and water is necessary to evade freezing and other problems. This technology require large number of equipment and instruments hence increases the capital, and operation and maintenance costs, but it has higher methane purity level up to >99%.

This method of biogas upgrading is used when the component in the gas has different condensing temperatures. For example, methane has a condensing temperature of -161.5°C in atmospheric pressure, while carbon dioxide has a condensing temperature of -78.4°C [39]. When the conditions are given as atmospheric pressure and room temperature, both methane and carbon dioxide are in the gas phase. If biogas is cooled down to -78.4°C, carbon dioxide starts to condense and can be removed in a liquid form. Figure 1-10 gives an illustration of the cryogenic upgrading technology.

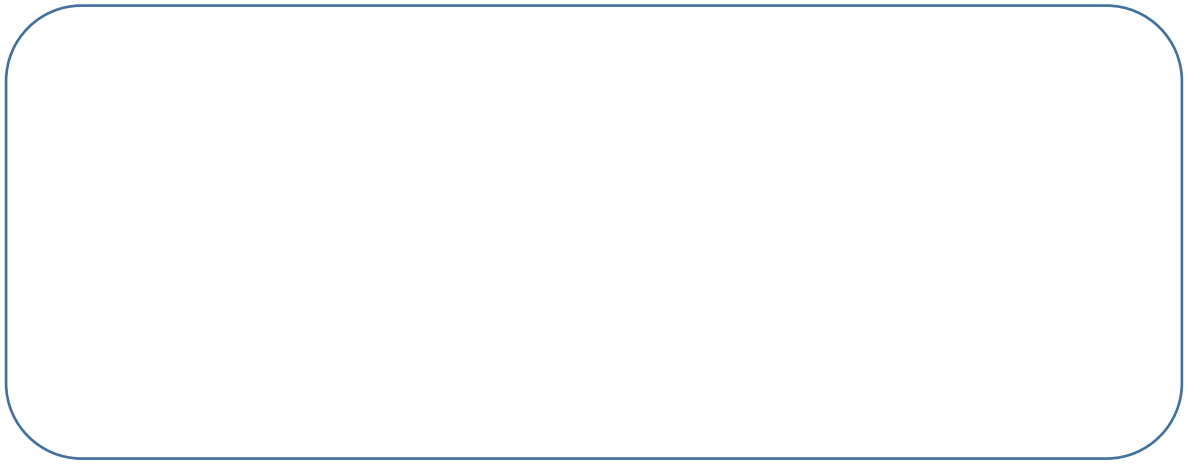

Figure 1-10: Process flow diagram of the cryogenic upgrading technology adopted from [39]

1.3.5.4 In situ methane enrichment

In situ methane enrichment is another emerging biogas upgrading technology, which works on the recirculation of liquid sludge from the digestion chamber to desorption column where it undergoes counter flow of O_2 and N_2 by which CO_2 dissolved in sludge is desorbed. The circulated sludge is then sent back to digester from desorption column for absorption of additional CO_2 present. However, this

concept was put forth for 20 years ago, but it is still in its nascent stage and being tested on pilot scale. The process diagram of the methane enrichment process is illustrated by Figure 1-11.

It is anticipated that the technology is able to give biogas containing up to 94% methane and it could be modified to achieve CO_2 removal efficiency greater that 60% [49]. A simple in situ technique was developed with Brian K. Richards [50] to separate CH_4 and CO_2 from biogas by using their solubility. In this technique, the methane purity was found more than 98% however; leachate recycle rates and alkalinity affect the results of off gas methane content. Steady state performance of bubble column for desorption of carbon dioxide and methane were analyzed by modeling but the experiment results were unsatisfactory. It is believed that main problem was in experimental uncertainties not in model [51]. However this method is still under research in worldwide but more emphasis is on enzyme immobilization, bioreactor mechanics, enzyme cloning and cloning technologies [9].

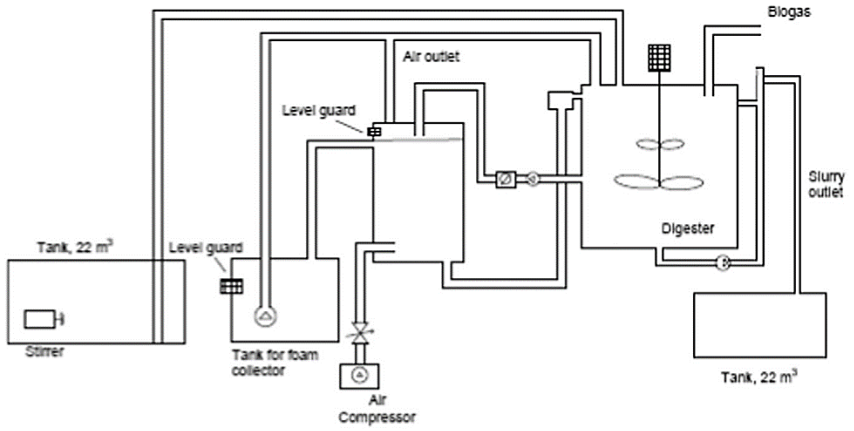

Figure 1-11: Process diagram of methane enrichment process adopted from [52],[9]

1.4 State of art on the power-to-gas technology

Transition into renewable energy coincides with several economic and social challenges. In electricity systems it creates a particular challenge due to the fact that renewable electricity from sun and wind is intermittent because it is related to the weather conditions, while the electricity system requires a permanent balance between inflow and outflow (so called energy balance) [53]. An increasing supply of intermittent electricity, hence, more flexibility within the system. In the main time, the conventional fossil fuel power plants which are currently the main providers of flexibility in main electricity system will be less available in future systems dominated by renewable energy [54].

One option that could provide flexibility in a renewable energy dominated systems is power-to-gas (PtG). PtG can offer three flexibility to the electricity systems. Flexibility with respect to time, location and end-use. The time flexibility of power-to-gas is that it can adopt the timing of using electricity and producing hydrogen. If a power-to-gas plant is equipped with a facility to store hydrogen, the timing of production of hydrogen can be fully adopted to the fluctuations of electricity prices. Meanwhile, the storage facility of hydrogen in a sub-system electrolyzer and methanation could facilitate an independent function of methanation and hence does not rely on the operation of electrolyzer. Furthermore, hydrogen is easily supplied into methanation to produce methane during the high prices of electricity.

A possible way of overcoming renewable energy intermittent challenges is energy storage and integration of it to the power grid. Although tremendous efforts are put in replacing conventional energy resources such as nuclear and fossil fuel with renewables, but still, they have some challenges such as intermittency of wind or solar energy and due to this, they cannot provide base load electric power [2]. Substitute natural gas or synthetic natural gas, or simply SNG is an excellent way of storing extra electrical energy from the grid in the form of chemical gas energy. In addition to SNG, many other energy storage forms exist which are useful to store excess energy: pumped hydro storage (PHS), compressed air energy storage (CAES), fly wheels [13]. A comparison of such energy storage technologies with respect to their storage capacity and their characteristics of charge/discharge time is shown in the Figure 1-12.

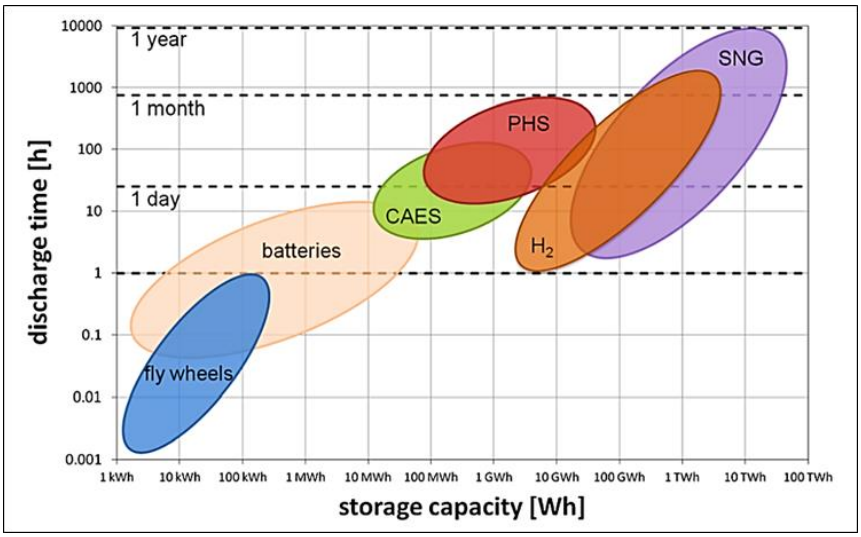

Figure 1-12: Different Energy Storage Systems adopted from [13]

Fundamental factor in an energy storage system is its potential of charge/discharge time and storage capacity. This is achieved only in case of chemical secondary energy carriers such as hydrogen and carbon-based fuels (SNG). Other energy storage technologies such as flywheels, batteries and compressed air energy storage are limited in storage capacity and discharge time [13].

Power-to-gas (PtG) links power gird to gas grid; in this process extra power of the grid is converted to gas with the help of two-step process: production of H_2 with water electrolysis and conversion of H_2 to synthetic methane with CO or CO_2 via methanation. The produced methane in this way is either easily injected to the natural gas grid or used as compressed natural gas (CNG). This way it brings the same value as natural gas grid, and does not need new infrastructure for the transportation since it can be carried and transported within the same gas infrastructure already exists. Figure 1-13 shows an exemplary concept of power-to-gas process.

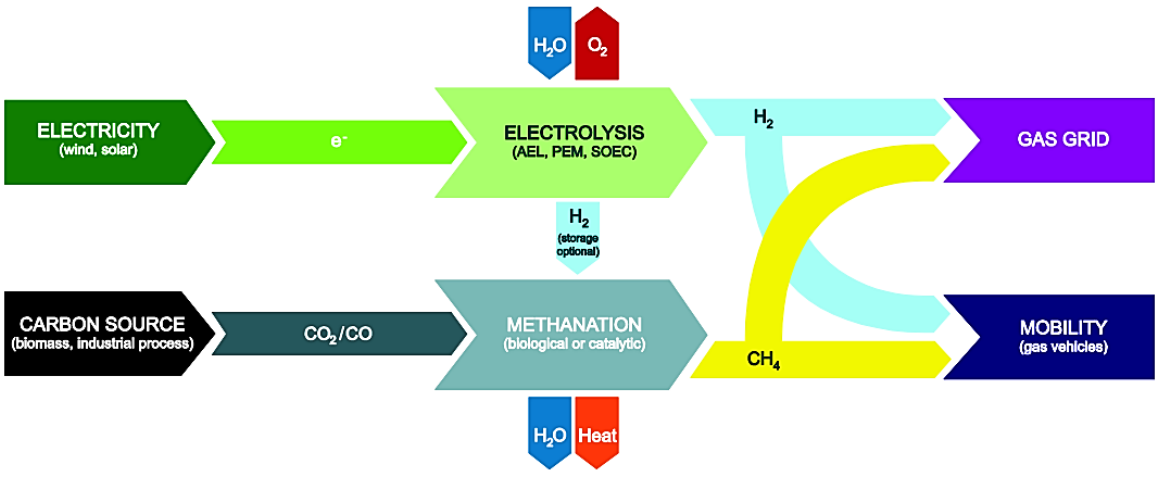

Figure 1-13: Exemplary concept of power to gas process [11].

In addition to converting intermittent electrical power to chemical energy, PtG plays a vital role in dealing and reducing carbon dioxide gas emission into the atmosphere. PtG requires a carbon source either CO or CO_2. There are several sources of carbon exist, like from power plants and refineries, iron, steel and cement industries. Carbon dioxide sources from such industries would require a CO_2 capture and storage and some upgrading technology to remove methanation poisoning gases such as Sulphur [17]. The removal of CO_2 from these gases reduces the energy efficiency and increases the costs considerably. In contrast, power-to-gas does not need larger sources of CO_2 instead; they need smaller sources of CO_2. Even small biogas plants could generate remarkable amount of CO_2 hence this way it helps to store several MWh of energy through power-to-gas technology, but the utilization of CO_2 from relatively small biogas plants would require huge electrolyzer to produce renewable hydrogen [55].

After removing the trace amounts from biogas, the gas what is typically used to produce power with combined heat and power (CHP) plants could be directly used in the methanation and chemically reacted with hydrogen to produce synthetic methane [56]. On the other hand, the CO_2 captured and stored from biogas upgrading plants (biomethane plants) can be valorized as useful commodity in the process of methanation to produce synthetic methane [12]. The essential advantages from using biogas in the power-to-gas process is the low gas treatment cost and ability to use the heat produced from methanation and oxygen from electrolyzer.

A Sankey diagram is presented in the Figure 1-14 to assess the process efficiency of power-to-gas. From the Sankey diagram, two improvement potentials could be seen for power-to-gas. First, the efficiency of water electrolysis could be improved also heat from the methanation reactor could be utilized [11]. To assess the power-to-gas process efficiency, the following system is examined. Current available electrolysis technologies alkaline electrolysis and polymer electrolyte membrane (AEL and PEM) delivering H_2 at 25 bar with an electrical efficiency of 70% are considered. The methanation reactor is operated at 20 bar with an efficiency of 78% (maximum chemical efficiency). CO_2 is already compressed to 20 bar for the methanation reaction (otherwise 2% efficiency loss) [11].

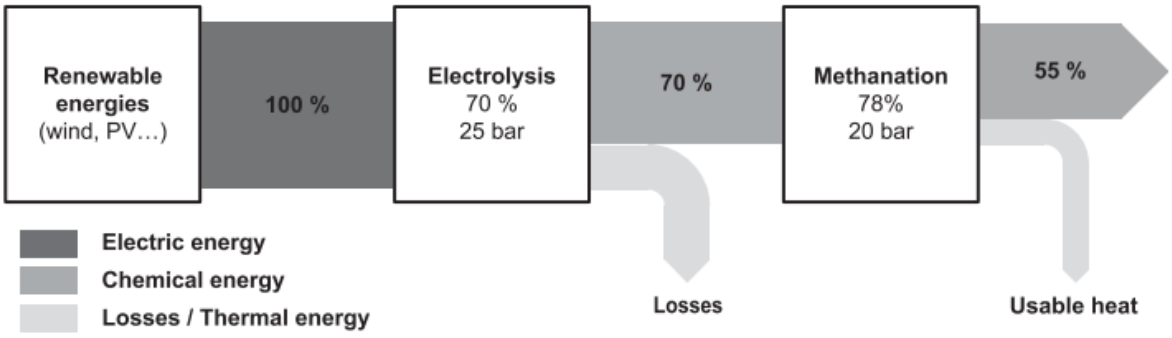

Figure 1-14: Sankey diagram of the PtG process efficiency (heat integration is not taken into account). Adopted from [11].

Jupiter1000 is the first industrial demonstrator of Power-to-gas in France with a power rating of one MW_{el} for electrolysis and a methanation process with carbon capture. The project is coordinated by GRTGAZ and supported by French Environment and Energy Management Agency (ADEME) and European Union. This project is a part of long-term power-to-gas activity in France with the aim of producing more than 15 TWh of gas by power-to-gas system by 2050. A functional diagram of the project is illustrated with the help of Figure 1-15. General design and project definition dates back to 2014 while startup of the project been carried out in the year 2018. Commissioning of alkaline electrolysis has been performed by the year 2020; similarly, the commissioning of PEM electrolysis, construction of CO_2 capture and commissioning of methanation have been scheduled for the year 2021. The project is expected to inject 200 m^3/h of hydrogen and 25 m^3/h of synthetic methane gas into the French natural gas grid. Besides Jupiter 1000, there are several different power-to-gas demonstration and/or pilot projects either been constructed or in the process of construction in France. METHYCENTRE, GRHYD, MINERVE and HyCAUNAIS are the examples of power-to-gas projects in France. Table 1-10 illustrates the demonstration and pilot power-to-gas/Hydrogen projects present currently in France.

Table 1-10: Power-to-X projects in France

Name of the Project	Capacity/electrolysis (kW)	Type of the project& Stage	Start-up	General Description
Juipter1000	1000	Demonstration	2018	PtH_2 and PtG
METHYCENTRE	250	Pilot	2018	PtH_2 and PtG
GRHYD	50	demonstration	2014	PtH_2
MINERVE	10	pilot	2014-2015	PtH_2 and PtG

HyCAUNAIS	1000	Project definition &General design stage	2019	PtH_2 and PtG from landfill gas

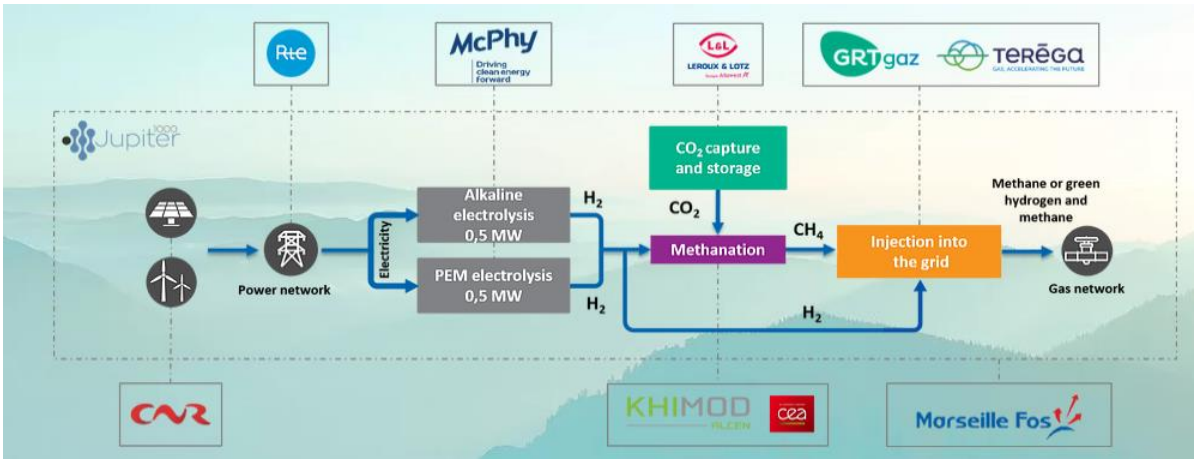

Figure 1-15: Functional diagram of Juipter1000 project adopted from [57]

STORE&GO is currently running three pilot plants with different innovative power-to-gas technologies [53]. Each of the concepts being demonstrated at the three STORE&GO pilot sites involves new methanation technologies and each has been adapted to the respective demonstration site. The plants are integrated into the existing power, heat and gas grid. The characteristics of these three pilot plants are given in the Table 1-11. The STORE&GO project has been funded by the EU under the Horizon 2020 scheme started in 2016 and has been running up to February 2020 in order to figure out the application of different power-to-gas technologies in three different European countries, acting as a reality lab.

Table 1-11: Characteristics of the three power-to-Gas demonstration sites STORE&GO projects [53]

	Demonstration site Falken-hagen Germany	Demonstration site Solothurn/ Switzerland	Demonstration site Troia/Italy
Representative region with respect to typical generation of Renewable Energy Sources	Rural Area in the North East of Germany with high wind power production and low overall electricity consumption	Municipal area in the Alps region with considerable RES from PV and hydro production	Rural area in the Mediterranean area with high PV capacities, considerable wind power production, low overall electricity consumption
Connection to the electricity grid	Transmission grid	Municipal distribution grid	Regional distribution grid
Connection to the gas grid	Long distance transport gird	Municipal distribution grid	Regional LNG Distribution network via cryogenic trucks
Plant size (in relation to the el. Power plant)	1 MW	700 kW	200 kW
Methanation technology to be demonstrated	Isothermal catalytic honeycomb/ structured wall reactor	Biological methanation	Modular milli-structured catalytic methanation reactors
CO_2 source	Biogas or bioethanol plant	Wastewater treatment plant	CO_2 from atmosphere
Heat integration possibilities	Veneer mill	District heating	CO_2 enrichment
Existing facilities and infrastructure	2 MW alkaline electrolyzer, hydrogen injection plant	350 PEM electrolyzer, hydrogen injection plant, district heating, CHP plant	1000 kW alkaline electrolyzer

1.4.1 Methanation: Catalytic versus biological

1.4.1.1 Catalytic Methanation:

SNG or synthetic methane is the product of chemical combination of H_2 and CO_2 in the presence of catalyst. The methanation of biogas takes place via the following chemical reaction. The process is exothermic with $\Delta H = -164.9\ kJ/mol$. In this process, the source of CO_2 sometimes could be biogas, where the existing CH_4 content of biogas remains unreacted but CO_2 content of the biogas goes under chemical reaction with hydrogen to form synthetic methane.

$$CO_2 + 4H_2 \rightarrow CH_4 + 2H_2O \quad (1\text{-}1)$$

Reaction (1-1) is a two-stage reaction including reverse water gas shit and methanation of CO given in equations 1-2 & 1-3. In the first step, carbon dioxide and Hydrogen are converted to carbon monoxide and water via reverse water-gas shift reaction and this reaction is endothermic. $\Delta H = +41.5\ kJ/mol$

$$CO_2 + H_2 \rightarrow CO + H_2O \quad (1\text{-}2)$$

In the subsequent reaction, methane is formed from carbon monoxide and hydrogen. This reaction is called Sabatier reaction and is exothermic with $\Delta H = -206.2\ kJ/mol$

$$CO + 3H_2 \rightarrow CH_4 + H_2O \quad (1\text{-}3)$$

The reaction of catalytic methanation dates to 1902: that means that this reaction is clearly not a discovery and reactors already have been designed for conditions well defined. The novelty consists in the integration of this technology in a new sector: the biogas upgrading.

Hydrogenation of CO_2 is done in the presence of catalyst (usually nickel-based). Catalyst used in reactions helps to reduce the needed activation energy of the said reaction. Catalytic methanation is called thermochemical reaction and usually their operating conditions are: temperature is between 300 to 500°C and pressure varies from 1 to 100 bars [58]. Assuming 5000 $GHSVh^{-1}$ and a 100% of CO_2 conversion, 2MW of heat per m^3 should be removed of catalyst bed [11]. In addition, it is essential to maintain a good control of temperature inside a catalytic methanation rector in order to avoid thermodynamic restrictions and catalyst sintering. Fulfilling this objective, many steady state reactor concepts have been developed but in the scope of this work, the detailed explanations of these reactors will not be given. These steady-state reactor concepts are fixed bed, fluidized bed, three phase and structured reactor. Among them, only fluidized bed and fixed bed reactors are established technologies and rest is still in the development and research stage.

When large-scale and continuous operations are carried out, the most popular technology is the adiabatic fixed-bed reactor; smaller scale or intermittent operation (as with PtG) can be achieved with isothermal reactors [59]. Heat released from the reaction should be controlled to prevent catalyst degradation and maintain a forward reaction, and this is the focus of much research [11],[60]. In the recent experiments the usage of a nickel catalyst have produced conversion efficiencies of 99.06% whilst reacting at 20 bar, 450 °C, and stoichiometric CO_2/H_2 ratios at 1:4 [61]. Operational flexibility is a key problem with catalytic methanation as load modifications can also additionally set off runaway heating or cooling of the reactors and a whole shutdown requires flushing with an inert gas or hydrogen.

A minimal of load of 40% or temperature of 200 °C to keep away from such troubles is desired, to prevent the formation of catalytic poisons and to allow for fast restarts [62] . Catalytic methanation necessitates a high purity feed gas and thus biogas from anaerobic digestion or landfill site has to be cleaned upstream prior to use [11]. Due to the favorable conditions, the presence of a catalyst and the lack of a gas-liquid mass transfer resistance, much faster production rates are achieved with catalytic methanation compared to biological methanation [63]. Catalytic methanation processes also have a lower power requirement per unit of gas produced than that of biological methanation [58].

1.4.1.2 Biological Methanation:

Another approach for the methanation is biological methanation where methanogenic microorganism works as biocatalyst in the process of hydrogenation of CO_2 to synthetic CH_4 [11]. The biological methanation has been known since 1906 but the technical application of the process is still an issue [58]. Biological methanation takes place in a lower range of temperature (40-70°C), which is an advantage for small-scale plants. Moreover, the level of tolerance of microorganism in the process against impurities is high which can be found in the composition of the gases, which are used as feed gas in the biological methanation [58]. Such impurities could be sulphur and ammonia, which comes together with CO_2 if biogas is the source and oxygen, which could be present from the electrolysis. Due to presence of microorganisms in a fermentation broth, hydrogen is poorly soluble in the liquid because of methanation reaction taking place within the aqueous solution [11]. This non-solubility of hydrogen in the liquid and supply of it to the microorganisms present the biggest engineering challenge. Hence, to overcome this mass transfer limitation, many reactor concepts are presently being developed [64].

In the process of biological methanation, continuous stirred-tank reactor (CSTR) is mostly used, because by increasing the stirrer frequency, the mass transfer of H_2 can be enhanced. In addition to CSTR other concepts such as trickle bed and membrane reactor exist, the microorganisms are

restrained. In the process of biological methanation, one of the important factors to evaluate the efficiency of process is the specific methane formation rate (MFR). This factor mainly depends on the microorganism, the type of reactor used, the pressure of the process and PH-value and finally temperature [11] [58].

1.4.2 H_2 production via water electrolysis

The electrolysis of water has been known for more than 200 years and is developed industrially for over a century. Electrolysis of water is the decomposition of water into hydrogen and oxygen under the effect of an electric power. Electricity is used to decompose water into its elemental components: hydrogen and oxygen. Though hydrogen is the most abundant element in the world, it cannot be found in its pure state in the nature. Up to 96% of hydrogen is produced from fossil fuels and only 5% is produced with water electrolysis. Concerning the production of hydrogen from fossil, it has economic reasons and factors involved in it [56].

Electrolysis is the important technology to obtain hydrogen and hydrogen obtained in this way is 99.99% pure once the produced hydrogen is dried and oxygen impurities are removed. Producing hydrogen with electrolysis is the mostly preferred method of hydrogen production since the technology is renewable because it does not rely on the fossil fuel energy and thus helps to fight in coping and dealing greenhouse gas emissions. The technology provides high product and is feasible for both small and large-scale hydrogen production projects [56].

Nowadays, integrating water electrolysis with intermittent renewable energy projects are gaining more attractions, because it holds mutual benefits, that is producing green and clean hydrogen and making use of intermittent wind or solar electrical power otherwise wasted due to demand-supply load variations. For instance, these technologies nevertheless limited to some research and advancement [65].

Production of hydrogen with water electrolysis is an essential and major part of methanation process, where the renewably produced hydrogen is chemically combined in a Sabatier reaction with carbon dioxide to produce synthetic methane (SNG). Here in this section a brief description of main water electrolysis: alkaline, proton exchange membrane (PEM) and the solid oxide electrolyzer (SOEs) will be given to highlight their availability in a commercial scale and their capacity in producing hydrogen.

The concept of electrolysis of water is given in the equation 1-4 below:

$$2H_2O(l) \rightarrow 2H_2(g) + O_2(g) \qquad \Delta H = \frac{285kJ}{mol} \tag{1-4}$$

The simplest method is to connect two immersed electrodes into a source of electrical direct current. Schematic of the electrolyzer technology is given in the Figure 1-15 as below:

Figure 1-16 Schematic of the Electrolyzer Technology adopted from [56]

1.4.2.1 Alkaline water electrolysis

Alkaline water electrolysis is economically more favorable and a best candidate system to produce hydrogen on a large scale from the renewable energies. Specifically, its benefit over other electrolyzer is that the electrolyte and electrode materials are much cheaper and are abundantly available but still with higher energy efficiency and high gas purity [66]. In order to increase the conductivity of the electrolyte, usually ions are added to water to stimulate ion transfer between the electrodes.

In alkaline technology basic ions are added, the most common of which is potassium hydroxide (KOH, which dissolves in $K^+ + OH^-$). The OH^- ion therefore serves for the transfer of charge between the electrodes where the reactions take place. In addition to potassium hydroxide (KOH) in water, the solution of sodium hydroxide (NaOH) in water is another electrolyte type and both these electrolytes are in position of high degree of hydrogen ion concentration. The energy utilization of alkaline water electrolysis spans from 60% to 90%. In case of conventional alkaline water electrolyzer, their maximum operation can be achieved in between 60°C to 90°C. Moreover, a pressure approximately at an ambient temperature. Furthermore, their operating voltages range from 1.8 V to 2.2 V and density of the electric current is below 0.4 A cm^{-2}. Contrasting to conventional alkaline water electrolysis, advanced water electrolysis operates in a range of lower temperature and pressure.

The range of hydrogen production with alkaline water electrolysis are as small as 0.01 m^3/h to as high as 100 m^3/h. Their advantages over other electrolysis are that they are simple to perform, relatively

cheap, suitable for uses both in household and commercial scales. Figure below shows the schematic of an alkaline water electrolyzer.

A treatment unit should demineralize the water supplied to the alkaline water electrolysis. The impurities present in the water remain in the system and over the period, it concentrates. The gases hydrogen and oxygen produced in this technology contains impurities that come from alkaline solutions. The hydrogen obtained at the outlet of alkaline water electrolyzer is washed by separators to remove traces of electrolyte solutions such KOH, NaOH then purified to remove oxygen and it is finally dried. Schematic of alkaline Water electrolyzer is given in Figure 1-17.

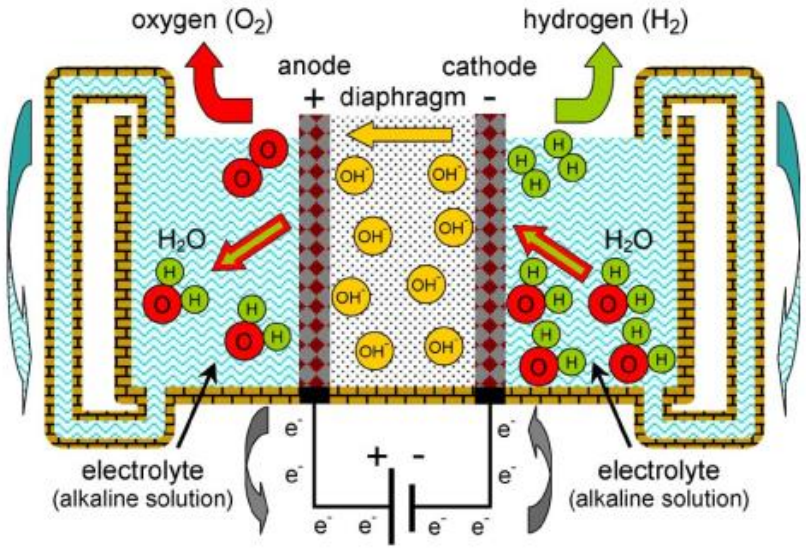

Figure 1-17 © [2012] IEEE- Schematic of the Alkaline Water electrolyzer adopted from [65]

1.4.2.2 Proton Exchange Membrane Electrolyzer (PEM)

Proton exchange membrane electrolyzer dates back to 1950s, and during this period these were primarily used for life supports in closed environment such as in space, submarines and leveraging oxygen rather than focusing on hydrogen production [67]. The electrolyzer stack includes 100 cell, and each cell consists of polar plates, cathode, anode, electrolyte, gas diffusion layer and catalyst. The principle operation of PEM water electrolysis cell is shown in the schematic given in Figure 1-18. Water is oxidized at anode to produce oxygen, electrons, and protons that spread through the membrane to the cathode where they are reduced and produces hydrogen that can bubbles toward the cathode [65]. The following reactions take place at cathode and anode sides of the PEM [67].

$$Anode: H_2O \rightarrow 2H^+ + \frac{1}{2} O_2 + 2e^- \quad (1\text{-}5)$$

$$Cathode: 2H^+ \rightarrow +2e^- \quad (1\text{-}6)$$

$$Overall\ Reaction: H_2O_{(l)} \rightarrow H_{2(g)} + \frac{1}{2} O_{2(g)} \quad (1\text{-}7)$$

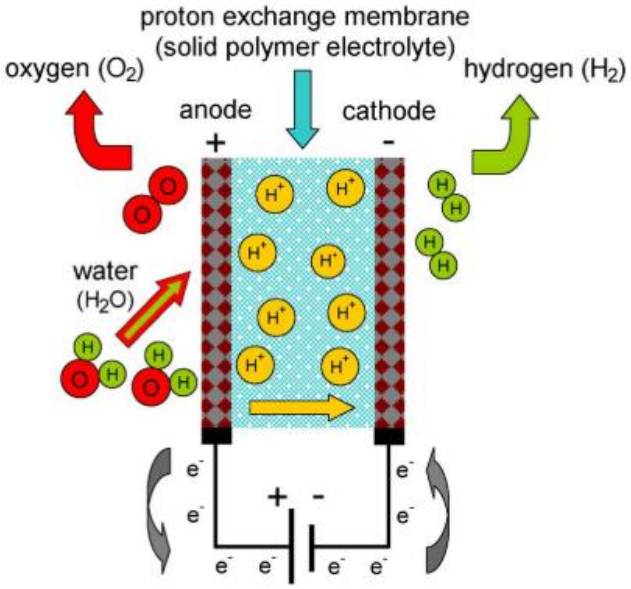

Figure 1-18 © [2012] IEEE- Schematic of the PEM electrolyzer adopted from [65]

PEM electrolyzer are commercially available only for low-scale production applications. Maximum hydrogen output is in the order of 30 Nm^3/h with a power consumption of 174 kW [68]. These devices can operate at current densities that are quite higher than their alkaline counterparts, achieving values even above 1.6 A cm^{-2}. The presence of the polymeric membrane limits the electrolysis temperatures to values usually below 80 °C. Some models reach pressures up to 85 bar [69]. Purity of hydrogen could go up to 99.99% in case of PEM water electrolysis cell without the use of some auxiliary equipment [70]. In addition, the risk of formation of flammable mixtures are low due to the presence of low gaseous permeability of the polymeric membranes; hence, it is possible to operate at extremely low current densities. One of the interesting aspects of PEM electrolyzer is their capability to function under variable power feeding regimes. This is because the proton transport across the polymeric membrane reacts rapidly to the fluctuations of power. But this is not the same case in alkaline electrolyzer, where the ionic transport in the liquid electrolytes shows a greater inertia [71].

Even though the PEM electrolyzer exists commercially but in the small-scale still, they have few disadvantages that needs specific consideration in a shorter time. One of the drawbacks is their high investment costs, which is mainly due to the membrane used, and the noble metal-based electrodes. Moreover, another drawback is they have shorter life of operation compare to alkaline technology [72].

1.4.2.3 Solid Oxide Electrolysis (SOE)

Solid oxide electrolysis is also referred to high temperature electrolysis and is the most newly developed technology of hydrogen production. This technology is still under development and is in the laboratory scale. The high temperature helps to reduce the equilibrium cell voltage and electricity, but the heat demand of the electrolysis increases with temperature increase [73]. The low electricity demand of the electrolyzer is one of the significant advantages of SOEs. It is possible to achieve higher overall efficiency of the process and fulfill heat demand of the process by combing to the exothermal reactions in power to gas process [74]. However, the specific cell area and the investment per hydrogen unit produced will increase with the heat integration. The signification of high temperature operation means that the product stream leaving electrolyzer is a mixture of hydrogen and steam; this in fact requires additional processing and, in this manner, the capital cost of the technology will increase. Furthermore, these kind of electrolyzer are not established against fluctuating and intermittent sources of electrical power [65].

The reaction of one mole of water is shown in the reactions below with oxidation of water occurring in anode and reduction of water occurring in cathode.

$$Cathode: H_2O_{(g)} + 2e^- \rightarrow H_{2(g)} + O^{-2} \quad (1\text{-}8)$$

$$Anode: O^{-2} \rightarrow \frac{1}{2} O_{2(g)} + 2e^- \quad (1\text{-}9)$$

The principal operation of the solid oxide electrolyzer is to split water in the form of steam into pure H_2 and O_2. This way steam is feed into the porous cathode. On the application of a voltage, the feed steam travels to the cathode-electrolyte interface and is reduced to form H_2 and oxygen ions. The formed hydrogen gas then diffuses backward through the cathode and is finally collected at the surface of cathode as hydrogen fuel, whereas oxygen ions are conducted through the dense electrolyte. This requires that the electrolyte used should be sufficiently dense so that the steam and hydrogen cannot diffuse through and lead to the recombination of the H_2 and O^{-2}. At the interface of the electrolyte-anode, the oxygen ions are oxidized to form pure oxygen gas, which is then collected at the surface of anode [75]. The schematic representing the operating mechanism of SOE is given in Figure 1-19.

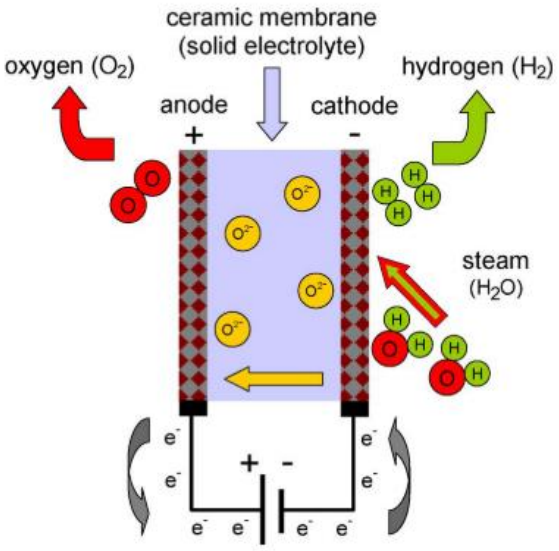

Figure 1-19 © [2012] IEEE- Scheme of the operating principle of a solid oxide (SOE) electrolysis cell adopted from [65]

The leading present-day constraint for the industrial application of SOEs is the limited long-term stability of the electrolysis cells [76]. The greatest challenge associated with SOEs are the degradation of its material in a rapid manner and limited long-term stability and both of these disadvantages are due to high temperature operation of the electrolyzer [65]. The research and development efforts should be focused on this issue in the short term [65].

2 Chapter 2: Mathematical Modeling of Landfill Biogas Production

Determination of amount of landfill gas (LFG) that can be produced from a landfill site is the most challenging task in the planning as well as operation stages of landfill gas system. The design elements of a gas collection and control system and the feasible applicable method for the control and/or use of LFG are determined based on the amount of LFG produced and its amount of methane content in the produced LFG.

In the active landfill cell units, LFG emissions can be measured by field measurements (i.e. measuring LFG flow and its composition in the test wells in the site). Although field measurements could give accurate results about LFG measuring, but it is a time consuming and costly method. Therefore, mathematical modeling approaches have been developed to estimate LFG generation and recovery based on the past and/or future waste quantities. LFG production is predicted with a rough approximation method as well. A rough approximation method takes into account the amount of waste in place as the only variable [78]. A rough approximation method of estimating LFG production is based on the data received from many but often very different projects and is derived from the waste quantity to biogas flow. It does not reflect type of waste, climate and other characteristics present at the specific landfill site. This method is recommended to be used as a primary screen tool for initial planning of the project because the accuracy of this method is only between +/- 50% [79]. USEPA (1996) reported that industry experts, working in this field, showed that LFG generation rates change from 3 to over 12 m^3 of gas per ton of waste per year (in average 6 m^3/ton/y)[78] [79] [80].

Two specific approaches exist for the mathematical estimation of the gas production rate: gas production rate is given as a) a simple empirical function or b) a combination of simple functions of an overall kinetic parameter. Mathematical modeling of LFG production is classified under zero-order and Monod first-order equations [78].

Zero-order:

In this kind of model, the biogas generated from landfills is remained constant versus time. On this basis, waste age and waste type do not have any effect on the rate of gas production through the models. This assumption causes a critical inaccuracy in the results. Examples of zero-order models are EPER Germany, SWANSA zero order and IPCC model [80].

First-order:

Almost all the available and globally used models, which are able to forecast the biogas production from the landfills, are among the ones developed based on the first order decay model. These models take into consideration the waste quality (i.e. moisture content, carbon content, age of waste and the

ability of waste to be digested). The developed first order models also consider the quantity of waste and landfill conditions (i.e., climate, temperature and precipitation). The effect of depletion of carbon in the waste through time is accounted for in a first order model [80]. Examples of first order models are TNO, Multi-phase model, Afvalzorg, LandGEM, Tabasaran & Rettenberger model, GasSim, SWANSA, and EPER Model France.

In the LFG modeling, the availability and quality of data representing waste characteristics and condition of landfill sites are significant sources of uncertainty. Subsequently, each model has been developed based on different approaches and assumptions. This is another factor in the development of several models for the estimation of LFG generation.

Because of its economic outcomes and energy potential of the chosen landfill site, it is important to estimate the amount of methane production from this landfill area. To do so, four of the first LFG models have been selected to calculate the methane potential and biogas production of the La Poitevinière landfill site. The description of these models has been given as below:

2.1 TNO Model

LFG formation from a given amount of waste is assumed to decay exponentially and the effect of depletion of carbon in the given amount of waste through time is accounted for in a first-order model [81].The mathematical expression of the first order model is given as below:

$$\alpha_t = \vartheta 1.87 A C_0 K_1 e^{-K_1 t} \quad 2.1$$

Where,

α_t Landfill gas production at a given time (m^3 LFG. y^{-1})

ϑ Dissimilation factor 0.58 (-)

1.87 Conversion factor (m^3 LFG. kgC^{-1}degreaded)

A Amount of waste in place (Mg)

C_0 Amount of organic carbon in waste (KgC. Mg $waste^{-1}$)

k_1 Degradation rate constant (y^{-1})

t time elapsed since depositing (y)

The TNO model estimates LFG production based on the degraded organic carbon in the waste.

Table 2-1: Organic carbon content used in the TNO single-phase model

Waste category	Organic carbon content (kgC.Mg^{-1})
Contaminated soil	11
Construction and demolition waste	11
Shredder waste	130
Street cleaning waste	90
Sewage sludge and compost	90
Coarse household waste	130
Commercial waste	111
Household Waste	130

2.2 Multiphase model Afvalzorg

Multi-phase model (Afvalzorg) is based on the TNO model, which estimates LFG production from a landfill site on the basis of biologically degradable organic carbon ratio in the waste and the cumulative amount of waste [78]. Different types of waste contain different fractions of organic matter that degrade at different rates. The advantages of a multi-phase model is that the typical waste composition can be taken into account [82]. As in TNO model, eight waste categories are also taken into account in the multi-phase model (Afvalzorg). For the considered eight waste categories, three different fraction rates are distinguished. For each fraction, LFG production is calculated separately.

The waste categories, fractions and rate constants used in the Afvalzorg multi-phase model are described in Tables 2-2. Only rapidly, moderately and slowly degradable organic matter has been taken into consideration. The total organic matter content is higher than the sum of these three categories due to the presence of organic matter that is not considered biodegradable under anaerobic conditions. Examples are humic substances, lignin and plastics. The multi-phase model is a first-order model and can be described mathematically as below:

$$\alpha_t = \vartheta \sum_{i=1}^{3} cAC_{0,i} K_{1,i} e^{-K_{1,i} t} \qquad 2.2$$

Where,

α_t Landfill production gas at a given time (m^3 LFG . Y^{-1})

ϑ Dissimilation factor 0.58 (-)

i Waste fraction with degradation rate $k_{1,i}$ (kg$_i$.kg^{-1}waste)

c Conversion factor (m^3 LFG. kgC^{-1}degreaded)

A Amount of waste in place (Mg)

C_0 Amount of organic carbon in waste (KgOM. Mg $waste^{-1}$)

$k_{1,i}$ Degradation rate constant (y^{-1})

t Time elapsed since depositing (y)

Table 2-2: Organic matter content used in the Afvalzorg multi-phase model

	Minimum organic matter content (kgOM.Mg^{-1})				Maximum organic matter content (kgOM.Mg^{-1})			
	Rapid	Moderate	Slow	Total	Rapid	Moderate	Slow	Total
CS	0	2	6	40	0	9	8	42
C&D	0	6	12	44	0	8	16	46
SW	0	6	18	60	0	11	25	70
SCW	0	18	27	90	12	22	40	100
S&C	9	38	45	150	11	45	48	160
CHW	8	39	104	260	19	49	108	270
CW	13	52	104	260	19	54	108	270
HW	60	75	45	300	70	90	48	320

2.3 LandGEM model

EPA's LandGEM is a Microsoft Excel-based software application that uses a first-order decay rate equation to calculate estimates for methane and LFG generation. LFG generation estimates are based on the methane content of the LFG. LandGEM assumes that the methane generation is at its peak shortly after its initial waste placement (after a short time lag when anaerobic conditions are established in the landfill site). This model likewise assumes that the rate at which methane is generated from landfill then decreases exponentially (first-order decay) as organic material is consumed by bacteria[83][84].

$$Q_{CH4} = \sum_{i=1}^{n} \sum_{j=0.1}^{1} k\, l_0 \left(\frac{M_i}{10}\right) e_{ij}^{-kt} \qquad 2.3$$

Where,

Q_{CH4} Flow rate of methane generation (m^3/year)

i 1-year time increment

n (year of the calculation) – (initial year of waste acceptance)

j 0.1-year time increment

k methane generation rate ($year^{-1}$)

L_0 potential methane generation capacity (m^3/Mg)

Mi mass of waste accepted in the i^{th} year (Mg)

t_{ij} age of the j^{th} section of waste mass Mi accepted in the i_{th} year (decimal years)

Model inputs

Only three of the variables in the LandGEM first-order decay model require user inputs. These variables are (k, L_0, M_i)[84].

K (methane generation rate constant)

This constant describes the rate at which waste placed in a landfill decomposes and produces LFG. The constant of methane generation is expressed with the unit 1/year or y^{-1}. At higher values of constant rate *k*, the methane generation at the landfill increases (as long as the landfill is receiving waste), and then declines more quickly after the landfill decrease. The value of *k* is a function of (1) waste moisture content, (2) the availability of nutrients for methane generation bacteria, *PH* and (4) temperature[84]. Moisture conditions within a landfill intensely influence the *k* value and decay rates. The *k* values and waste decay rates are very low at desert sites, have a tendency to be higher in moister climates and reach maximum under moisture-enhanced conditions. Annual precipitation is often used as replacement for waste moisture because of absence of data on moisture conditions within a landfill. Air temperature can also affect the *k* values, but to a lesser extent. Internal landfill temperatures are relatively independent of the outside temperatures and typically range from approximately 30 to 60 °C.

L_0 (Potential Methane Generation Capacity):

The total amount of methane gas potentially produced by a metric ton of waste as it decays is depicted with L_0 or potential methane generation capacity. EPA proposes some appropriate values for L_0 which ranges from 56.6 to 198.2 m^3 per metric ton or megagram (m^3/Mg) of waste [84]. Except in the dry climate conditions where lack of moisture can limit methane generation, in this condition the value of L0 depends almost entirely on the type of waste present in the landfill. The value of L_0 is directly proportional to the organic content of the waste, the higher the organic content of the waste, the higher the value of L_0. It is worth to mention that the value of L_0 is determined on the dry organic

content of waste and not the wet weight measure and recorded in the landfill site, as water does not generate LFG.

M_i (Annual Waste Disposal Rate):

Anticipated waste disposal rates are the primary determining factor of LFG generation in any first-order decay-based model. LandGEM does not adjust annual waste disposal estimates to account for waste composition. Adjustments to account for waste composition are typically handled by adjustments to the L_0 value.

Figure 2-1 adopted from [84] shows an example gas curve for a landfill with approximately 2 million tons waste-in-place expected at closure. The potential gas generation was modeled in the two scenarios, using identical landfill parameters, except that *k* was varied between values for dry conditions (0.02 yr^{-1}) and a value for wet conditions (0.065 yr^{-1}). The graph expresses the significant difference in gas generation that can occur based on moisture conditions at the site.

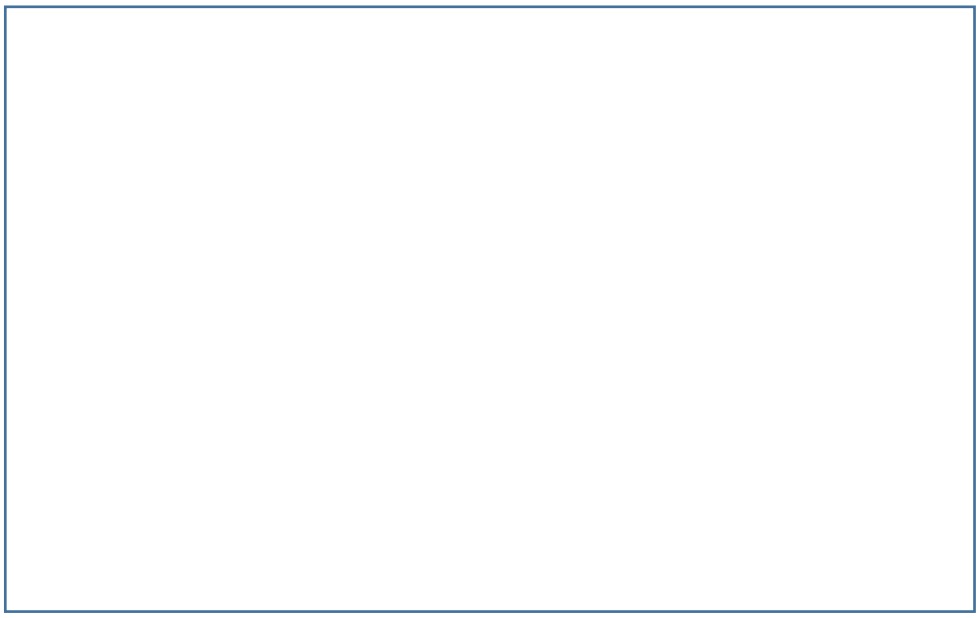

Figure 2-1: LFG generation variance by *k* values adopted from [84]

Landfill Gas Emission Model LandGEM is a biochemical model implemented by US EPA that considers the waste composed of an only class, thus requiring an only kinetic constant for methane (*k*) and a potential methane generation per ton of waste (L_0). It is important to note that, the default values, *k* and L_0, are representative of American landfills and thus, may not be applied directly to European landfills without a calibration on monitored case studies [85].

2.4 Tabasaran & Rettenberger model

Tabasaran & Rettenberger model simulates carbon degradation by a first order decay approach as given in the below mathematical expression. The expression is a relationship originally developed for the anaerobic digestion of sewage [78]. Due to the portion of substrate that is used for cell synthesis, it may vary with temperature in sewage digestion. The model equation contains a temperature correction in the equation. However, anaerobic digestion in landfills is different as compared to anaerobic digesters, the temperature correction is irrelevant for landfills [86].

$$G_t = 1.868 C_{org}(0.014T + 0.28)(1 - 10^{-k.t})M_t \quad 2.4$$

Where,

G_t Total LFG production at a given time (m^3)

T Temperature in degree Celsius (°C)

C_{org} Organic carbon in waste (kg OC/ton waste)

k Degradation rate constant (y^{-1})

Mt waste in place in a given time

2.5 Basic methodologies to estimate methane generation potential

2.5.1 Determination of Methane Generation Potential (L_0)

Different methodologies exist to determine the methane generation potential. Three different methodologies will be broadly explained here. These methodologies are: US EPA method, CRA method and IPCC method.

2.5.1.1 EPA Method

The biodegradable fraction (BF) of the waste can be obtained through tests that quantify the biochemical methane potential (BMP). The *BF* value can be calculated using the ratio between the BMP value and the values predicted by stoichiometric equations (here called C_m), which assumes a complete conversion of organic matter to gaseous products [87]. The C_m values vary according to the component considered, but they are normally between 400 and 500 L CH_4/dry-kg. According to [88], values of C_m of 414.8 and 424.2 L CH_4/dry-kg can be considered for cellulose and hemicellulose, respectively. Table 2- 3 adopted from [87], presents the *BF* values for different components of waste suggested by several authors. Values of C_m for the waste as a whole can be calculated using the waste composition (dry basis) and the values of BF values suggested by [87]. Table 2-4 gives the values of C_m calculated with the equation suggested in [89].

Following the concepts given above, if the biodegradable fraction of the waste as a whole, BF_W, and the value of C_m are known, the waste methane generation potential, L_0, can be easily calculated. Equation 2.5 is presented to find the value of BF_W. The dry basis fraction of each component in the given waste composition, *FR*, is multiplied by its *BF* value and finally the value of BF_W is found by summing all the components considered [87]. From the equation 2.6, the waste average value of c_m is calculated.

$$BF_{w} = \sum_{i=1}^{n} BF_i \times FR_i \quad 2.5$$

$$C_m = \frac{\sum_{i=1}^{n} BF_i \times FR_i \times C_{mi}}{BF_w} \quad 2.6$$

$$L_0 = \frac{BF_w \times C_m}{1 + w} \quad 2.7$$

$$L_0 = C_{org} \times 0.93 \quad 2.8$$

Table 2-3: BF values suggested in the technical literature[87]

BF						
Paper	Cardboard	Food waste	Garden waste	Wood	Textiles	Reference
0.44	0.38	0.58	0.45	0.61	0.40	[89]
0.19-0.56	0.39	0.70	0.70-0.34	0.14	-	[90]
0.30-0.40	0.44	-	0.20-0.51	0.30-0.33	0.17-0.25	[91]
0.40	0.41	0.64	0.35	0.17	0.32	[87]

Table 2-4: Methane generation (c_m) and water consumption in MSW [87]

Waste Organic Component	C_m (m^3 CH_4/dry-Mg)	H_2O Consumption (H_2O kg/dry-kg)
Food waste	505.01	0.26
Paper	418.51	0.20
Cardboard	438.70	0.16
Textiles	573.87	0.41

Leather	759.58	0.64
Yard wastes	481.172	0.28
Wood	484.94	0.24

2.5.1.2 IPCC Method

IPCC (2006) presents another simplified model in which the methane generation potential is estimated with a mass balance method that includes the determination of the degradable organic carbon (DOC) content of the waste. One key input in the model is the amount of degradable organic matter (DOC_m) in the selected waste which is disposed into the landfill site. If the type of disposed waste is municipal solid waste, this is estimated using information on the different waste types/materials (food, paper, wood, textile, etc.) included in the MSW composition. The equations for estimating the methane generation potential is given as below. The basis for the calculation is the amount (here given in mass fraction, dry basis) of decomposable degradable organic carbon ($DDOC_m$) as defined in Eq. 9. $DDOC_m$ is the part of the organic carbon that will degrade under the anaerobic conditions.

$DDOC_m$ is equal to the product of the fraction of degradable organic carbon in the waste (DOC), the fraction of the degradable organic carbon that decomposes under anaerobic conditions (DOC_f), and the portion of the waste that will decompose under aerobic conditions (prior to the conditions becoming anaerobic) in the landfill, which is interpreted with the methane correction factor (MCF).

Equation 2.10 may be used to calculate the $DDOC_m$ value of the waste as a whole considering data presented in Table 2-5 (IPCC, 2006) for different waste components and the waste composition (dry basis). *FR* is the fraction (dry basis) of each component in the waste composition. Table 2-6 presents suggested values for MCF according to the type of landfill. Comparing the two approaches presented here, it may be said that DOC_f and BF have a similar meaning and that DOC and BMP are closely related.

$$DDOC_m = DOC \times DOC_f \times MCF \quad (2.9)$$

$$DDOC_m = MCF \times \sum_{i=1}^{n} DOC_i \times FR_i \times DOC_{fi} \quad (2.10)$$

DOC_f is an estimate of the fraction of carbon that is ultimately degraded and released from landfill, and reflects the fact that some degradable organic carbon does not degrade, or degrades very

slowly under anaerobic conditions. DOC_f is usually assumed as 0.5 (on the assumption that the landfill environment is anaerobic and the DOC values include lignin). DOC_f value (as BF) is dependent on many factors such as moisture, temperature, PH, composition of waste, etc. In addition, equation 2.11 shows the calculation of DOC_f value and this calculation was adapted from Tabasran & Rettenberg model. T is the temperature and is given in degree Celsius °C.

$$DOC_f = 0.014 \times T + 0.28 \quad (2.11)$$

In the IPCC (2006) model, the methane generation potential, L_0 (m^3CH_4/Mg of MSW), maybe calculated using equation 2.12 below. F_{CH4} is the CH_4 volume concentration in the gas, 16/12 is the molecular weight ratio of CH_4 and ρ is the methane density, which may be adopted as 0.717 kg/m^3 for practical purposes. w is the waste water content, dry basis. Values of DOC and dry matter content suggested by IPCC (2006)[87] [92] is presented in the Table 2-5 . Some MCF values suggested by IPCC (2006) [93] is presented in Table2- 6.

$$L_0 = \frac{DDOC_m \times F_{CH4} \times {}^{16}/_{12}}{\rho \times (1 + w)} \quad (2.12)$$

Table 2-5: Values of DOC and dry matter content suggested by IPCC (2006) [87] [92]

MSW Component	Dry Matter Content In % of Wet Weight	DOC Content In % of Wet Waste		DOC Content In % of Dry Waste	
	Default	Default	Range	Default	Range
Paper/cardboard	90	40	36-45	44	40-50
Textiles	80	24	20-40	30	25-50
Food Waste	40	15	8-20	38	20-50
Wood	85	43	39-46	50	46-54
Garden and park waste	40	20	18-22	49	45-55
Nappies	40	24	18-22	60	44-80
Rubber and leather	84	39	39	47	47
Plastics	100	-	-	-	-
Metal	100	-	-	-	-
Glass	100	-	-	-	-
Other, inert waste	90	-	-	-	-

Table 2-6: Values of MCF suggested by IPCC (2006)[93]

Type of Site	MCF Default Values
Managed- anaerobic	1.0
Managed- semi-aerobic	0.5
Unmanaged- deep (> 5m waste) and /or high-water table	0.8
Unmanaged – shallow (<5m waste)	0.4
Uncategorized landfill	0.6

2.5.1.3 Conestoga - Rovers & Associates (CRA) Method

This method is prepared by CRA for British Colombia Ministry of Environment. According to this method, L_0 value of MSW was estimated through waste characterization and also decomposability of waste material disposed into the landfill site. According to [94] methane generation potential for decomposable, moderately inert and relatively inert are given respectively 160, 120 and 20 m^3 methane per ton of MSW. Waste characterization and the corresponding methane generation potential L_0 (m^3CH_4/ton) is given in Table 2-7. In the CRA method, the weighted average of waste composition is calculated in order to categorize the given waste into a proper category.

Waste categorization

According to CRA method, Waste landfilled should be segregated into the following three categories by mass:

- Relatively inert waste includes metal, glass, plastic, soil, contaminated soils, and water treatment plant screened fines.
- Moderately inert waste includes paper, wood, wooden furniture, rubber, textiles, and construction and demolition material.
- Decomposable waste includes food waste, yard waste, and slaughterhouse waste.

Table 2-7: Waste characterization and potential methane capacity [94]

Waste Characterization	Methane Generation Potential L_0 (m^3methane/ton)
Relatively Inert	20
Moderately Inert	120
Decomposable	160

2.5.2 Determination of Methane Generation Rate Constant (k)

The fraction of waste refuse which decays during a given period of time and that produces methane gases is presented by *k* values. The simplest way to estimate the methane quantity of the LFG is to estimate a single *k* value for the whole landfill site [85]. From the laboratory studies it can be seen that, fast-decaying organic material (like food waste) can decay at 5 times the rate of medium decay rate materials (like paper) and 20 times the rate of slowly decaying rate materials (like textile)[95]. The *k* values obtained from the data collected from US landfills range from 0.003 to 0.21 as per [96]. Table 2-8 represents the relationship between methane generation rate constant (*k*) and annual precipitation [97]. Table 2-9 shows some *k* values suggested with IPCC (2006).

The value of k is a function of the following factors:

- Waste moisture content
- Availability of nutrients for methane generating bacteria.
- PH
- Temperature

Table 2-8: Relationship between methane generation rate constant (k) and annual precipitation adopted from [97]

Annual precipitations (mm/year)	k (per year)
0-249	0.040
250-499	0.050
500-999	0.065
At least 1000	0.080

Table 2-9: Methane generation constant rate of various waste according to various climate conditions (IPCC)[93]

Waste type		Dry boreal and temperate climate[1]	Wet boreal and temperate climate[2]	Dry tropical climate[3]	Wet tropical climate[4]
		Range	Range	Range	Range
Slowly degrading waste	Paper/textiles waste	0.03-0.05	0.05-0.07	0.04-0.06	0.06-0.085
	Wood/straw	0.01-0.03	0.02-0.04	0.02-0.04	0.03-0.05

Moderately degrading waste	Other (non-food) organic Putrescible/garden and park waste	0.04-0.06	0.06-0.1	0.05-0.08	0.15-0.2
Rapidly degrading waste	Food waste/ sewage sludge	0.05-0.08	0.1-0.2	0.07-0.1	0.17-0.7
Bulk Waste		0.04-0.06	0.08-0.1	0.05-0.08	0.15-0.2

[1] Annual precipitation is lower than potential evapotranspiration.

[2] Annual precipitation is higher than potential evapotranspiration.

[3] Less than 1000 mm annual precipitation.

[4] More than 1000 mm annual precipitation.

Boreal and temperate means that the mean annual temperature is below 20 °C.

Tropical means the mean annual temperature is in excess of 20°C.

CRA also suggested different degradability values (k values in y^{-1}). These values can be found in the Table 2-10 below for 3 categories of wastes.

Table 2-10: Methane Generation Rate Selection Matrix [94]

Annual Precipitation	Methane Generation Rate (k) Values		
	Relatively Inert	Moderately Inert	Decomposable
<250 mm	0.01	0.01	0.03
>250 mm <500mm	0.01	0.02	0.05
>500 mm <1000mm	0.02	0.04	0.09
>1000 mm <2000 mm	0.02	0.06	0.11
>2000 mm <3000 mm	0.03	0.07	0.12
>3000 mm	0.03	0.08	0.13

The values presented in Table 2-10 above, should be corrected based on the storm water management, leachate recirculation and/or storm water injection, cover properties, and landfill operational practices. Table 2-11 below shows the three-water addition factor. A value of 0.9 represents downward if little to no storm water is infiltrating into the waste or added to the waste mass. Similarly, a value of 1.0 represents unity if a portion of storm water infiltrates and/or there is partial recirculation of leachate into the waste mass. Finally, a value of 1.1 illustrates upward if storm water infiltrates and leachate is recirculated.

Table 2-11: Water Addition Factor [94]

Landfill Conditions	Water Addition Factor
Low to negligible water addition to the waste mass "dry tomb type landfill"	0.9
Partial infiltration or water addition to the waste mass	1.0
Addition of water into the waste mass "bioreactor type landfill"	1.1

2.6 Description of the Study Area:

La Poitevinière landfill site, owned and operated by Groupe Brangeon, is located in Beaupréau-en-Mauges which is a commune in the Maine-et-Loire department in western France. It has an area of 86 hectares and from the overall area, 57 hectares are divided into landfill cells. In the remaining surface, a leachate treatment station and a combined heat and power plant to produce heat and electricity are installed. The wastes come mainly from Maine-et-Loire department and neighboring departments: Loire-Atlantique, Deux-sèvres and Vendée.

The landfill has an active storage of about 57 hectares. This area is divided into landfill cells and receives a mixture of non-recyclable, nontoxic industrial and household wastes. The landfill site started receiving waste in 1990 and it is expected to continue to be operated till 2032. The yearly amount of waste disposed into overall landfill cells in the la Poitevinière site is given in Figure 2-2 below. The quantity disposed into landfill site has followed an increasing trend from 1990 to 2020 reaching up to 120000 ton per year. However due to European Union regulation on the quantities of waste landfilled, the future waste disposal will follow a decreasing trend. The waste disposal in the landfill in the closure year 2032 will be of only 40000 ton/year. The expected future quantity of waste disposed into the landfill cells is represented with the same Figure 2-2 which corresponds between years 2021-2032.

For the purpose of estimating the methane generation potential from the disposed waste into landfill site, the analysis of the composition of the waste was carried out. The quantity of the different composition of waste disposed into landfill cells was recorded year by year in the site and an average value was taken for the estimation of methane generation potential and landfill biogas production from the landfill site with LFG mathematical modeling.

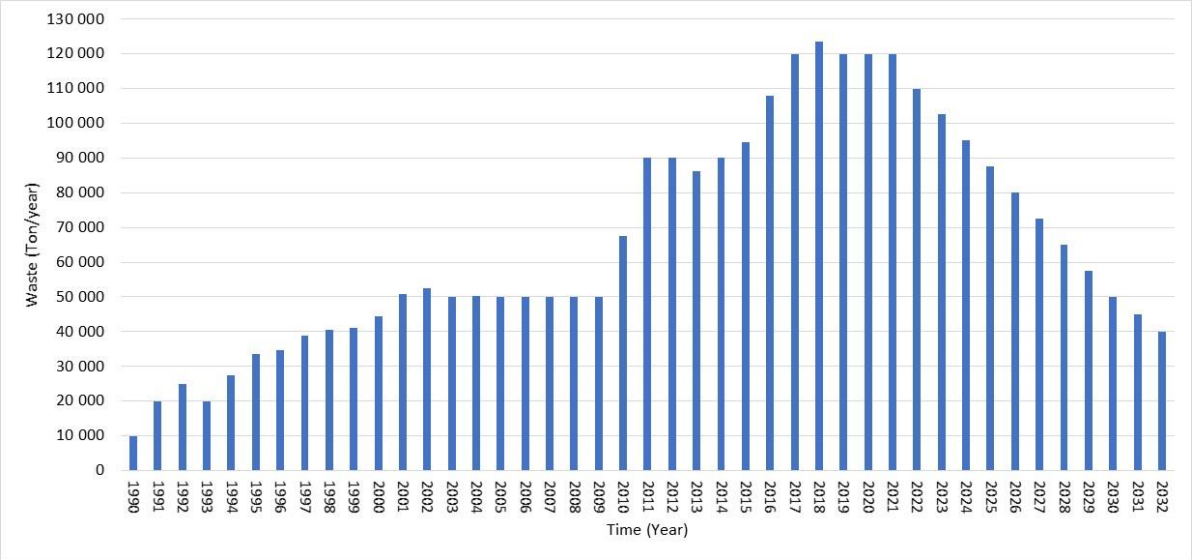

Figure 2-2: Total amount of waste disposed into landfill site between 1990-2020

Annual Average waste composition in La Poitevinière landfill site is given in the Table 2-12. Waste composition of this landfill site is firstly classified into three categories: Decomposable, Moderately inert and relatively inert as suggested by CRA method. The detailed waste type of each category is given in Table 2-14 along with annual average composition in the section results and discussions. La Poitevinière landfill site received up to 35% of decomposable waste between the years 1990-1996. The average annual quantity of decomposable waste was only 12% for the period 1997-2011. And later, the landfill received almost negligible amount of decomposable material for the period 2012-2020 which is 3 percent only.

From the past records of the waste type and compositions, an average annual of last five years of the disposed waste compositions is taken for the years 2021-2032. The quantity of moderately inert material in the disposed waste in contrast has increased from 65 to 90%. For the last and next 10 years, the waste disposed in the La Poitevinière landfill site contains mainly industrial waste. Hence, it is important to know the detailed composition of industrial waste disposed into La Poitevinière landfill site. The industrial waste disposed consist of paper, cardboard, textiles, leather and wood. For instance, the accurate data on the percentage fraction of each consisting piece is missing which is why an assumption of percentage fraction of industrial waste is made and presented in the Table 2-13.

Table 2-12: Annual average composition of waste in the La Poitevinière landfill site

year	Annual Average (%) Waste Compositions		
	Relatively Inert	Moderately Inert	Decomposable
1990-1996	0	65	35
1997-2011	9	78	12
2012-2020	6	91	3
2021-2032	5	92	3

Table 2-13: Assumption made on the Percentage fraction of industrial waste disposed into La Poitevinière Landfill site

Elements	Fraction percentage (%)
Paper	25
Cardboard	20
Textiles	20
Leather	15
Wood	20

2.7 Results and discussions

2.7.1 Estimation of LFG model inputs

Two different methodologies were investigated in order to estimate the methane generation potential of the selected landfill site waste. The methane generation potential found with two different methods later used as an important input parameter for the estimation of landfill biogas production by different first-order mathematical models. As a first method, the landfill gas generation assessment guidelines by Conestoga-Rovers & Associates (CRA) prepared for British Colombia Ministry of Environment was used [94]. According to this method, methane generation potential L_0 value of a waste is estimated via the waste characterization and decomposability of the waste fractions. CRA suggested three different methane generation potential values for decomposable, moderately decomposable and inert which are 160, 120 and 20 m^3 of CH_4 per ton of waste. Methane generation potential L_0 value with CRA method for the La Poitevinière landfill site waste is found to be 115.7 m^3CH_4/ton of waste given as in the Table 2-14.

Annual percentage mean of each waste type presented in the Table 2-14 is multiplied with L_0 values proposed with CRA to find out the L_0 of each individual waste type. All the individual L_0 values are summed to find out the methane generation potential of the concerned waste. Similarly, the

weighted averages of waste compositions were calculated to identify the waste category as given in the last column of the Table 2-14. From the estimations, the CRA ID of this waste was found to be 1.973, which shows that the waste is moderately decomposable.

Table 2-14: Methane generation potential L_0 assumed from CRA method (2012-2032)

	Waste Type	Annual Mean (%)	CRA Category	L_0 (m^3/ton)	L_0	Weighted sum of CRA Category
Decomposable	Household waste	1.8	3	160	2.8	0.053
	WTP sludge	0.03	3	160	0.043	0.001
	Sweepers	0.6	3	160	1	0.019
	screening	0.3	3	160	0.5	0.009
Moderately Inert	Gravel and aggregate	5.4	2	120	6.5	0.109
	Solid recovered fuel	1.9	2	120	2.3	0.038
	Waste sorting refusal	0.7	2	120	0.8	0.014
	Industrial waste	83.8	2	120	100.6	1.676
Relatively inert	Construction and demolition material	5	1	20	1	0.050
	Other	0.4	1	20	0.1	0.004
				Total	**115.7**	**1.973**

As a second methodology to estimate the methane generation potential of the waste, the method proposed with US EPA [87] was applied. According to this method, methane generation potential L_0 value is estimated from stoichiometric calculations that are obtained from biodegradable fraction of waste composition. Dry matter content in the % of wet weight given by IPCC (2006) [87],[93] is used. The biodegradable fraction for the waste component given in [87] is used in this method. The methane generation (cm_i) and water content (w) data were taken from IPCC 2006. The L_0 value estimated with EPA method is presented in the Table 2-15. In accordance with this method, the methane generation potential L_0 value was found to be 86.8 m^3 CH_4/ton of waste.

Table 2-15: Methane generation potential estimation based by US EPA method

Waste component	FR*	Waste Fraction	FR_i	BF_i	cm_i	FR_i x BF_i
Food waste	0.4	0.087	0.035	0.64	505.01	0.022
Yard waste	0.4	0.026	0.010	0.42	481.17	0.004
Paper	0.9	0.21	0.186	0.39	418.5	0.073
Cardboard	0.9	0.17	0.149	0.40	438.7	0.060
Textiles	0.8	0.17	0.132	0.31	573.87	0.041
wood	0.85	0.17	0.141	0.30	484.94	0.042

*Dry matter content in % of wet weight (IPCC) 2006

$$BF_w = \sum_{i=1}^{n} BF_i \times FR_i = 0.242 \quad (2.13)$$

$$C_m = \frac{\sum_{i=1}^{n} BF_i \times FR_i \times C_{mi}}{BF_w} = 470.5 \quad (2.14)$$

$$L_0 = \frac{BF_w \times C_m}{1+w} = 86.8 \quad (2.15)$$

$$C_{org} = L_0/0.93 = 93.3 \quad (2.16)$$

The hypothetical organic carbon content in the solid waste could be estimated according to the methane generation potential which is suggested by [82] and shown in equation 2-15. This value is estimated as 93.3. Methane generation rate constant (*k*) values of La Poitevinière landfill site was estimated based on waste fractions and the average annual precipitation of the region. Average annual precipitation in the region of La Poitevinière landfill site for the period 2001-2020 is about 740 mm. No additional information about the hydrological balance was available. LFG generation rate constant (*k*) for La Poitevinière landfill site was calculated based on the waste characteristics given in Table 2-10. For TNO, LandGEM and Tabasaran& Rettenberger models, the LFG generation rate constant (*k*) value was estimated as 0.04 $year^{-1}$. For Multi-phase (Afvalzorg) model, the rate constant values for slow, moderate and fast degradation were taken as 0.02, 0.04 and 0.09 $year^{-1}$. Table 2-16 sums up all the inputs used in different models. LFG generation rate constant (*k*) values can range from 0.005 to 0.4 $year^{-1}$. Based on IPCC (2006) [93].

Table 2-16: Parameters for each model with US EPA and CRA methodologies

Model	Input	EPA method	CRA method
Multi-phase (Afvalzorg)	k_{slow}	0.02	0.02
	$k_{moderate}$	0.04	0.04
	k_{fast}	0.09	0.09
	C_0	93.3	124.4
	ϑ	0.58	0.58
	c	1.87	1.87
	T		20
TNO and Tabasaran & Rettenberger Model	k	0.04	0.04
	C_0	93.3	124.4
	ϑ	0.58	0.58
	c	1.87	1.87
	T		20
LandGEM	k	0.04	0.04
	L_0	86.8	115.7
	T	20	20

2.7.2 LFG Estimations

Two different methane generation potential L_0 values were estimated with CRA and EPA methods. The highest L_0 value was estimated with CRA method. The base for the CRA methodology was characterized by the impact factors according to the organic and inorganic contents of the waste. For example, food and garden wastes had an impact factor of 3 because their potential of producing methane was greater than other solid waste type. On the other hand, inorganic wastes such as ash and metal had an impact factor of 1. The moderate level of decomposition was identified by an impact factor of 2 [98].

The lowest L_0 was estimated by EPA method. The biodegradable fraction BF of the waste was related to the anaerobic conditions therefore this parameter was sensitive to the ambient conditions such as PH, temperature and moisture content of the waste [98]. According to [87], the values of L_0 (C_0) were significantly different between the estimations of $L_0(C_0)$ done by adopted parameters and the estimation of $L_0(C_0)$ done by measured parameters from laboratory results for EPA method. Furthermore, similar study was carried out by Gulden GOK for NIGDE landfill site [98]. The $L_0(C_0)$ values were estimated 135 and 73 m^3CH_4/ton of waste by CRA and EPA method. Moreover, in a study carried

out with Isin (2012) for Izmir Harmamndali landfill [98], the L_0 (C_0) values was estimated 57 m^3CH_4/ton of waste. When analytical methods are not used, the CRA method can be proposed for saving time instead of literature acceptance.

Figure 2-3 shows the landfill gas generation obtained with the lowest adopted L_0 that was recommended with EPA. The values of k and L_0 are taken as 0.04 and 86.6. According to this method, the L_0 value is obtained from the chemical reaction of decomposition of organic material present in the given waste. As per this method the lowest landfill gas generation was calculated with the TNO model and the highest LFG was obtained with LandGEM model. The maximum estimated LFG with LandGEM is 12.4 million m^3/year biogas at 2019. Similarly, the peak of LFG was estimated with the rest of the models was at the year 2024. Maximum estimation of LFG did not occur at the closure year 2032 since the waste disposed at this year was noticeably reduced to 40000 ton per year. Multiphase and Tabasaran & Rettenberger models showed almost the same maximum LFG at the year 2024.

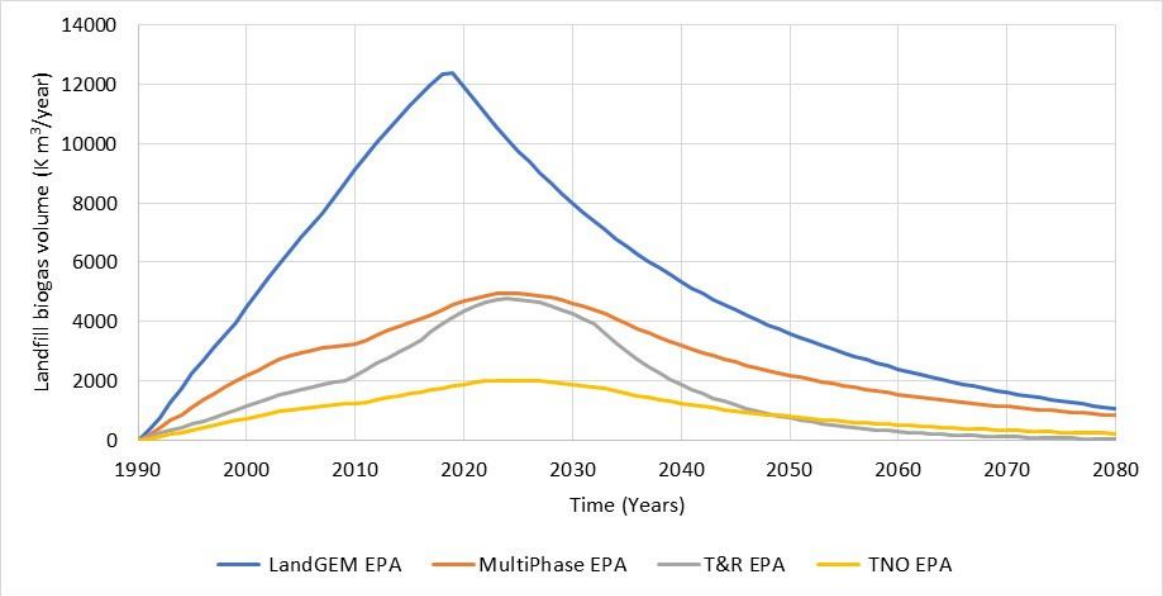

Figure 2-3: LFG generation obtained by EPA method with different models at L_0 = 86.6 and k = 0.04

Figure 2-4 shows the landfill gas generation obtained with the highest adopted L_0 that was suggested with CRA. The Figure 2-4 illustrates a similar pattern as Figure 2-3. As per this method lowest landfill gas generation was calculated with TNO method and the highest LFG was obtained with LandGEM model. The maximum estimated LFG with LandGEM was at year 2019. Similarly, the peak of LFG estimated with the rest of the models was at the year 2024. Methane and LFG volumes were higher than the EPA method which is due to the higher L_0 taken in this method. La Poitevinière landfill site may have one million m^3 of CH_4 gas in 2024 according to TNO model for L_0 equal to 86.6 m^3 CH_4/ton. This quantity of methane gas is more than 2 million with Multiphase and T&R models for the same L_0

value with EPA method. Table 2-17 presents the different results obtained by four models with different L_0 values adopted by EPA and CRA methods.

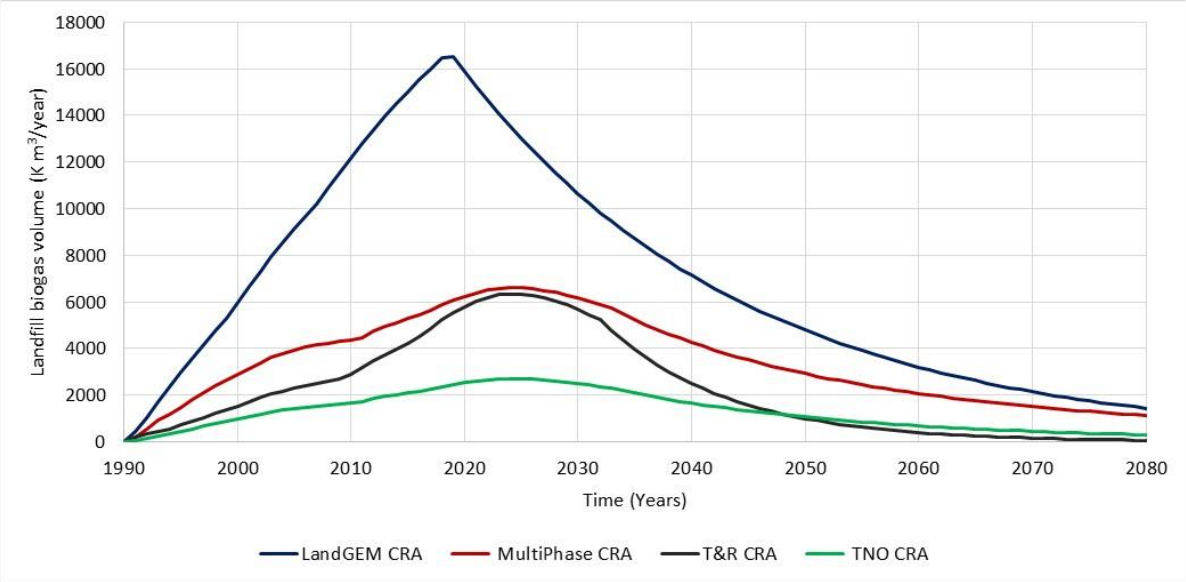

Figure 2-4: LFG generation obtained by CRA method with different models at L_0 = 115.7 and k = 0.04

Among the four first-order mathematical models with two L_0 values by EPA and CRA, the total lowest estimated LFG for the La Poitevinière landfill site is with TNO model at 89 million m^3/year by EPA and 119 million m^3/year by CRA. The maximum methane generation at 45 volume percentage is 0.9 million m^3 by EPA and 1.2 million m^3 CRPA method.

Table 2-17: Results of different models with different methane generation potential (L_0 values)

Multi-phase (Afvalzorg)			
Method	Total LFG Yield (million m^3)	Total Methane Yield (million m^3)	Maximum Methane Generation (million m^3)
EPA	237	106.8	2.22 in (2024)
CRA	317	142.4	2.97 in (2024)
First Order Model (TNO)			
Method			
EPA	89	40.1	0.9 in (2024)
CRA	119	53.5	1.21 in (2024)
Land GEM Model			
Method			
EPA	475	213.7	5.58 in (2019)

CRA	633	284.8	7.43 in (2019)
Tabasaran & Rettenberger Model			
Method			
EPA	151	68.1	2.14 in (2024)
CRA	202	90.8	2.85 in (2024)

Figure 2-5 shows the LFG and methane gases estimated with both EPA and CRA methods by TNO model. TNO showed the lowest estimation of landfill gas among the four studied mathematical models. According to the field measurements carried out at La Poitevinière landfill site, the methane volume of LFG was approximately 45% which is an average annual value. Methane gas volumes with EPA as well as CRA methods were calculated with 45 volume percentage from the estimated LFG gas and illustrated in the Figure 2-5. It can be seen from the Figure 2-5, the economic feasible lifespan of LFG energy recovery from the site will end at almost 2060.

A methane reserve between the closure year 2032 and 2060 was calculated to show the remaining methane potential of site after the closure year. Table 2-18 presents the remaining methane potential calculated with CRA method for four models. The methane volume of the LFG was approximated at 45% which is the case in the La Poitevinière landfill site. It can be seen from Table 2-18 that methane potential (methane reserve) is between 20 to 35% with different models for the period 2032 until 2060. The maximum remaining methane potential was obtained with Multiphase method and the rest of the models showed a similar value for the methane potential.

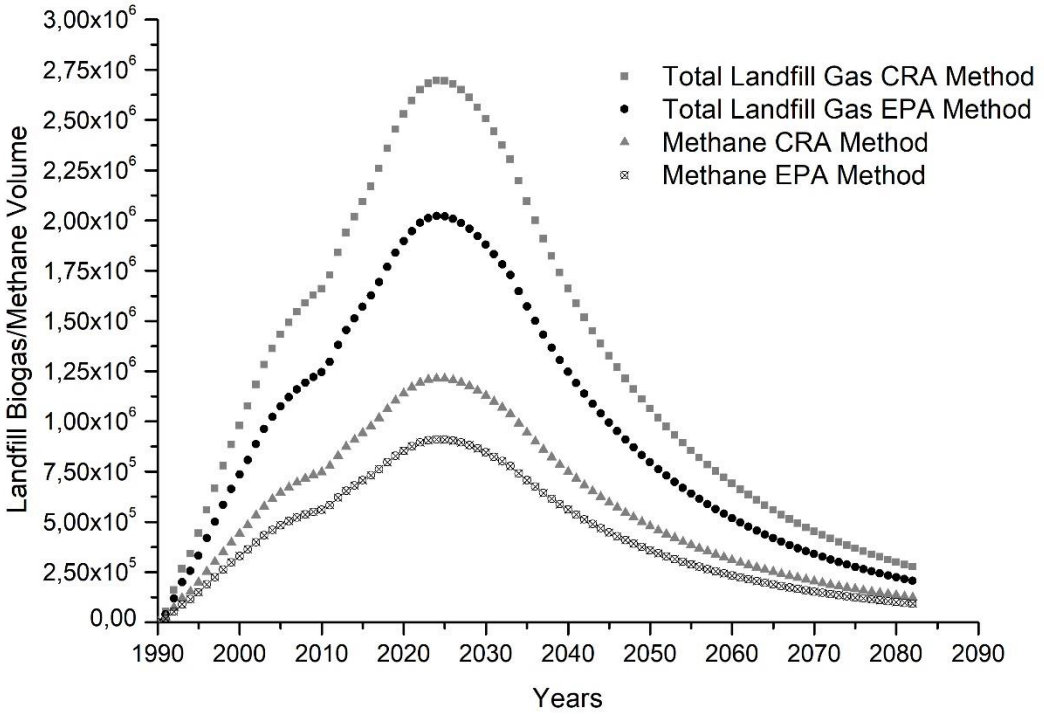

Figure 2-5: LFG and methane gas production obtained with CRA and EPA by TNO model

Table 2-18: Methane potential remaining after landfill closure year

	Methane Potential with CRA method (million m^3)			
Years	LandGEM	Multiphase	T&R	TNO
1990-2060	264.14	127.82	89.18	35.77
2033-2060	73	44.36	22.57	7.88
(After closure year till 2060) %	27.6	34.7	25.3	22

Model LFG estimates were compared to actual site data. The actual site data recorded from the site for last 10 years is only available for the years 2010 to 2020. The actual site data presented as in Table 2-19 is the yearly total accumulated biogas recorded at the site. LandGEM model, Multiphase and Tabasaran & Rettenberger models estimate LFG in high volume compare to the real volume of biogas recorded in the landfill site. TNO model when compared to actual site data showed lesser deviations compare to other models. Outputs of both EPA and CRA with two different L_0 values were compared to actual site data. Lesser deviation was achieved when k value was varied from 0.04 to

0.065. The comparison of model outputs to the actual site data is presented in the Table 2-19. Percentage deviation compares model estimates to actual site data, with negative indicating model estimation is lower than actual site data. The graphical comparison of LFG estimates to actual site data is given in Figure 2-6. Actual site data is presented with blue dots for the years between 2010 and 2020 which is the period where the data is available. It can be seen from the Figure 2-6 that TNO model with CRA method at k = 0.065 would deviate less and approaches to the actual site data.

Table 2-19: Models output deviations to actual site data

		% deviation of TNO model estimates to actual site data		
Year	Actual site data	CRA Method		EPA Method
		k = 0.04	k = 0.065	k = 0.04
2010	1 476 663	12	10	-16
2011	1 887 700	-8	-12	-31
2012	2 571 000	-28	-33	-46
2013	1 675 547	16	6	-13
2014	2 137 213	-6	-15	-29
2015	2 160 544	-3	-15	-27
2016	1 816 393	19	2	-10
2017	1 915 915	18	-1	-12
2018	1 705 881	38	14	4
2019	1 722 065	42	14	7
2020	1 942 098	30	2	-2

Figure 2-7 shows the landfill biogas production for three different sets of years. The first set is 2010-2020 for the period where the actual site data is available. The second set of years is from 2021 to 2032 which is the next 10 years till the landfill closure year and finally the third set of years is from 2033 to 2060 to evaluate the energy performance of landfill site after closure year for about 30 years. For the second set of years 2021 till the closure year of landfill 2032 which represents the next 10 years of waste disposal into the site, the lowest estimated landfill biogas with EPA method is 23 million m^3 by TNO model. Accumulated biogas of the actual site for the last 10 years between 2010 and 2020 is 21 million m^3. Similarly, accumulated biogas presented in the Figure 2-7 for the first set of years 2010-2020 is 17 million m^3 by EPA and 23 million m^3 by CRA for the same TNO model. From this comparison, the TNO model seems to be coherent with the actual site data. In the third set of years for 2033-2060 after the closure of landfill site, the landfill biogas is estimated at 27 million m^3 by TNO.

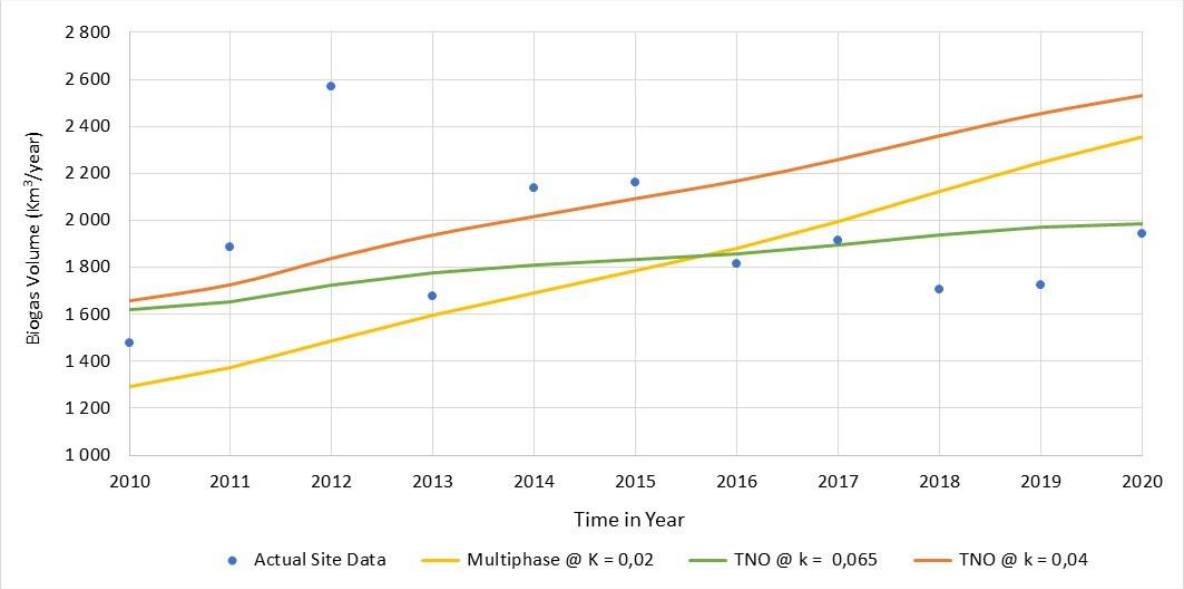

Figure 2-6: Comparison of LFG models with CRA method to Actual Site Data

The methane production for the sets of years by four models with CRA method is illustrated in Figure 2-8. The methane volume in the LFG was approximated at 50% which is a future prediction and possible increase in the methane volume of landfill biogas. The Figure 2-8 illustrates that there is clearly huge difference in the methane volume estimations done with four different models. This is because each model has been developed on different approaches and assumptions. The lowest methane volume though coherent with the actual site data was estimated with TNO at 10 million m^3 for the set of year 2021-2032 and 9 million m^3 for 2033-2060. This estimation is almost 3 times with T&R method. Temperature of the landfill site plays an important role in the T&R model in addition to k and L_0 values. The detailed data on the temperature profile of the site is missing and the uncertainty made in this case is the selection of an average temperature of 20 °C for the years 2010-2018 for the entire landfill site.

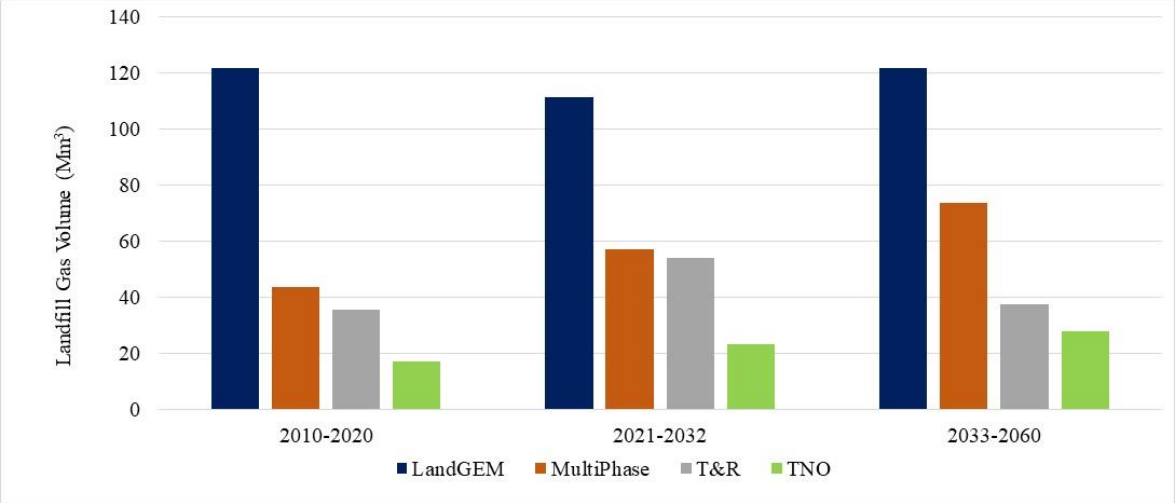

Figure 2-7: Landfill Gas volume production by sets of years obtained by CRA Method

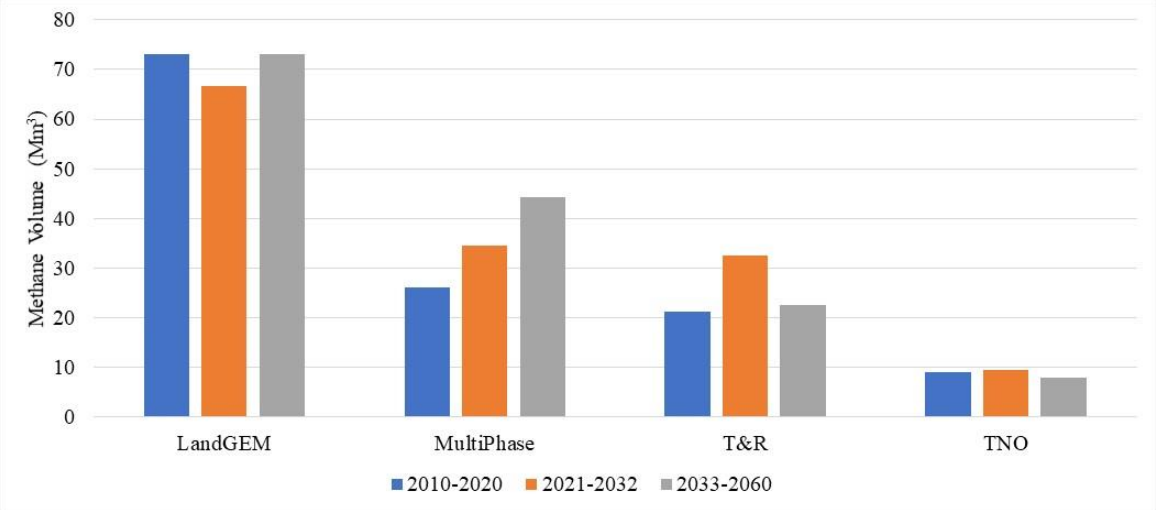

Figure 2-8: Methane Production by sets of years obtained by CRA Method at 50 volume % CH_4 in LFG

2.8 Conclusion of chapter 2

The study carried out in this chapter clearly shows a huge difference in LFG/CH_4 estimations obtained from four different LFG mathematical models. It is commonly approved today that each model has been developed based on different approaches and assumptions. The models selected for this study were Monod first order decay equation which are also called first order decay models.

First order models have a linear relation with the maximum potential of methane production per weight of waste as well as an exponential relation with decay rate and time. Mathematical modeling of landfill biogas production is a useful approach to assess the lowest and highest biogas

productivity in order to analyze the viability of biogas exploitation for energy purposes. The maximal average hourly biogas flow rate recorded at the site for the year 2020 is 220 Nm^3/h. Although the existence of LFG collection system provides historical flow measurements but it does not provide information on future LFG collection potential. The estimated maximal average biogas flow rate with TNO model by CRA method at k = 0.04 for the year 2032 is 270 Nm^3/h reaching a maximum 310 Nm^3/h at year 2025. The estimated hourly landfill gas potential with different models by two different L_0 values EPA and CRA and at different k values for TNO model is illustrated by Figure 2-9 below.

A comparison made between TNO model and actual site data provides a coherency between model outputs and actual site data for the time period 2010-2020. The percentage deviation is lesser in case of CRA method with k = 0.065 given as in Table 2-19. Nevertheless, this coherency and lesser deviation does not fully validate the accuracy of estimations carried out with LFG modeling. This study in this stage probably not be the final word about the different models applied to the La Poitevinière landfill site. But the application of proposed models allowed the generation of a range of biogas potential for the future. With the results of any first order LFG model, relevant individuals can calculate the energy potential of biogases produced in the landfill site so as to study the feasibility of waste to energy projects. The absence of information on the hydrological balance and consequently, on the water content of the waste required the insertion of uncertainties and approximations in the estimation of biogas potential carried out with LFG modeling.

For the present LFG modeling carried out, the compositions and types of waste disposed in the landfill site is broadly studied. Methane potential generation and organic content of the waste was estimated with two different methods: CRA and US EPA. Likewise, the LFG generation rate constant of La Poitevinière landfill site is estimated based on the waste characteristics and climatic conditions of the region. The waste compositions for the incoming years till the closure year 2021-2032 was estimated based on an average value of the last five years data from waste compositions and waste types. The reduction in the disposal quantity of waste into landfill site containing only 3 percent of rapidly biodegradable fraction could decrease the production of biogas from the landfill site results in the lesser biogas volume produced in the site.

The more precise and accurate estimation of LFG would be using a model which considers the temperature variation in time and depth and landfill settlement.

To perform an appropriate modeling of biogas generation process, an appropriate biodegradation rates (k_i) was needed. The selection of these parameters depends strongly on the specific landfill in which the models are applied to and may require a calibration on each landfill. The accurate choice of these parameters represents the main problem for an accurate LFG modeling.

Indeed, the biodegradation rates are functions of moisture content, which represents the most important factor in the process of anaerobic decomposition. The absence of well-made gas extraction/monitoring system for the landfill site made a calibration on this specific case impossible.

The mathematical modeling carried out in this study is important to do a future estimation of biogas potential from this landfill site. A range of maximal hourly biogas flows based on yearly average estimated biogas would be proposed for the next chapters to assess the feasibility of its exploitation for energy purposes. The variability of the expected maximal hourly biogas flow rates accounts for the absence of detailed inputs and the uncertainties encountered in the mathematical modeling.

From the seven scenarios illustrated in the Figure 2-9, it can be seen that the biogas flow rate is estimated below 200 Nm^3/h for most of the cases after the landfill closure year. A range of maximal biogas flow rate between 100-500 Nm^3/h is considered for the further biogas valorization objectives in the next chapters. LFG model estimations in (Nm^3/h) for La Poitevinière landfill site from 2020-2060 is given in Figure 2-9 below.

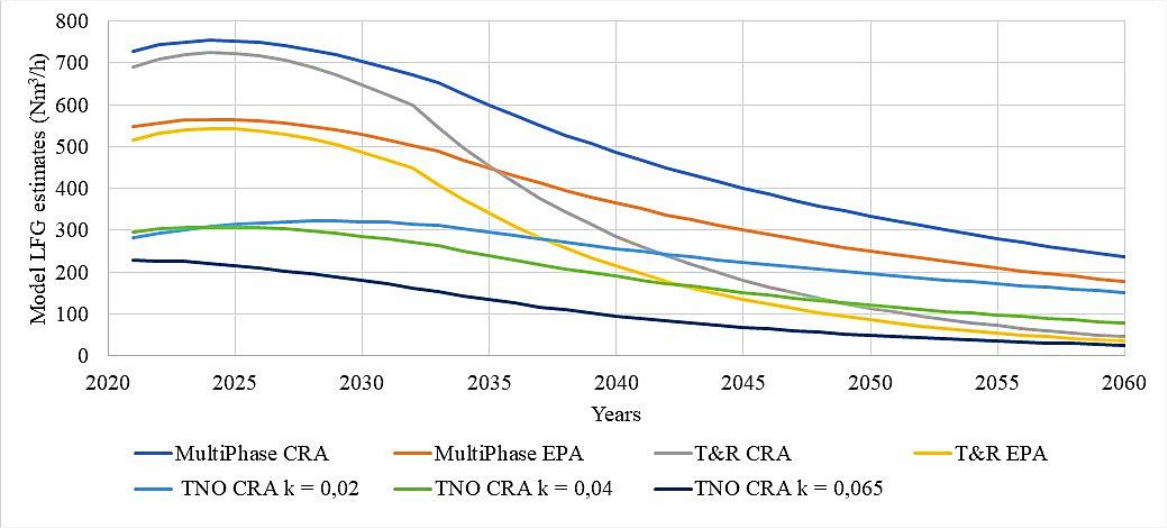

Figure 2-9 LFG Model estimations (Nm^3/h) for La Poitevinière Landfill site from 2020-2060

3 Chapter 3: Biomethane Production from Landfill Gas

3.1 Introduction

Converting organic waste into biogas through biodegradation processes is in high demand and yields a carbon neutral green gas called biomethane when cleaned from impurities and upgraded by removing CO_2. Biogas nowadays mainly being produced via anaerobic digestion which helps to avoid sending organic waste to be incinerating as well as landfilling. Nevertheless, landfills still receive some quantity of mixed waste and gas is being generated from these sites although, either they are closed already or exposed to waste reduction disposal in the future. Moreover, there exist many landfill sites where produced gas is cleaned from impurities and valorized. In most of the cases, landfill biogas is valorized in the combined heat and power (CHP) process thanks to a more favorable regulatory and incentive framework. However, landfill biogas is also converted into biomethane by removing impurities such as hydrogen sulfide, nitrogen, water vapor and separated from carbon dioxide to the required level to meet the natural gas grid injecting criteria. Both solutions adding value to biogas.

The produced gas either from anaerobic digester or landfill site contains methane, carbon dioxide, and minor parts of impurities whose type and content depend on the biogas source. Moreover, the type and amount of such impurities would also help to select which biogas cleaning technology (and, to some extent also upgrading technique) is more suitable for gas purification. Biogas can be cleaned from these impurities and upgraded by removing carbon dioxide to substitute either natural gas in the national gas grid or liquid natural gas for vehicles in the transport sector. “Cleaning” is referred to the pre-treatment that allows the removal of all impurities but carbon dioxide, while “upgrading” involves of CO_2 removal. The most widely used technologies for biogas upgrading are water scrubbing, pressure swing adsorption, membrane, amine scrubber and cryogenic separation. These five technologies are broadly assessed in this chapter.

The first purpose of this chapter is to evaluate mentioned five biogas upgrading technologies independent of source of biogas. A life cycle cost assessment considering all technical features and economic features of the technologies is carried out to find out most cost-economic and energy-efficient technology. Moreover, sensitivity analysis is also performed with the aim of finding the most important parameter in the technology and its impact on the total life cycle cost assessment. Life cycle cost assessment with heat recovery and without heat recovery cases are also evaluated to find out the influence of heat recovery in some of the technologies. The assessment of these five technologies is carried out using literature data. In addition to that, some assumptions are made and several data are included to make the assessments more realistic and specific to some particular site.

The second purpose of this chapter is to assess the existing biogas upgrading technologies which could be adopted and selected for a site-specific landfill site. Some of the technologies may not be easily proposed for landfill sites either they are not capable to remove simultaneously nitrogen and carbon dioxide, or they are too expensive. The landfill site chosen for this study contains more than 10 vol % nitrogen in the raw biogas mixture.

As a part of the biogas upgrading system, N_2 rejection or removal may be required, depending on the biogas inlet N_2 levels and the required biomethane specifications. Because of the potential intrusion of ambient air that contains N_2 when biogas is collected from landfills, N_2 is typically more of an issue in landfill biogas (LFG) as compared to biogas from anaerobic digesters. N_2 is difficult and expensive to remove from biogas given the fact that the diameters of N_2 and CH_4 are similar, which are approximately 3.6 angstroms and 3.8 angstroms, respectively [99].

Nitrogen rejection units remove N_2 gas from biogas streams via pressure swing adsorption (PSA) or membranes technologies. The typical biomethane conditioning process initially removes trace-level contaminants and most of the CO_2, while allowing in this step N_2 to pass through the system with the CH_4. A secondary N_2-specific rejection system may be required at the end of the gas conditioning system to remove N_2 to acceptable end use levels. Some biogas conditioning systems remove N_2 simultaneously with CO_2 using adsorbents that have a high kinetic selectivity toward N_2 and O_2 nevertheless, inlet N_2 vol% in this case is limited to less than 10 percent. For $\geq$ 10% inlet N_2, a secondary N_2-specific removal system is suggested so far [100].

A specific case of landfill biogas upgrading into bio-methane process would be hence studied that is adoptable for the case of La Poitevinière landfill biogas. Based on biogas analysis tests carried out previously on the La Poitevinière LFG, it is found that the said gas contains N_2 up to 20 vol%. The reported N_2 content is an average value and is based on different test analysis carried out. Consequently, simultaneous removal of N_2 together with CO_2 from the said gas would not be possible due to higher content of N_2 in the inlet gas. To account for this case, a specific N_2 removal via PSA unit is selected. Simultaneous removal of N_2 and CO_2 would be possible in case of cryogenic upgrading unit. These technologies yet separate N_2 and CO_2 in the same system nevertheless they are expensive and energy intensive.

N_2 removal processing can reduce the CH_4 recovery rates. The impact on CH_4 recovery varies depending on the inlet N_2, outlet N_2 specifications and the technology used to remove the N_2. In one example, the CH_4 recovery drops from 90 to 81.5 percent when an N_2 and O_2 removal unit is added to the process[50], [101].

3.2 Results and discussion

3.2.1 Biomethane production and upgrading technologies

The main components in biogas upgrading technologies are identified through a detailed literature review and are presented in chapter 1. Two different sources of biogas are considered for this chapter: biogas from a reference landfill containing more than 10 vol % nitrogen in the gas mixture and biogas from an anaerobic digestion tank with almost no nitrogen in the raw biogas. Biogas upgrading is an additional option, while alternative options would include utilization of biogas for direct heating, or in a combined heat and power plant especially when source of biogas is considered from a landfill site.

However, studies have shown that the best climate benefit is obtained when biogas is upgraded and removed from carbon dioxide and converted into biomethane and either injected into natural gas or green transportation fuel. In the objective of this study, the process of biogas upgrading is assessed no matter whether the source of biogas is a landfill site or an anaerobic digestion tank. Type of the landfill site or the reactor used in the production of biogas from anaerobic digestion or the associated costs in the production of raw biogas is out of scope of this study. The assessment carried out here assumes that the upgrading technology is integrated into a biogas producing plant whether landfill site or anaerobic digester.

3.3 Life cycle cost analysis

This section of chapter 3 presents the results obtained from life cycle cost analysis (LCCA). Various biogas upgrading technologies whose technical and economic data obtained from a detailed up-to date literature are analyzed in order to find the most-cost effective system. In total, five different biogas upgrading technologies were assessed for life cycle costs analysis. Upgrading technologies that have been compared are water scrubbing, amine scrubbing, membrane, pressure swing adsorption and cryogenic technology. Moreover, the life cycle cost analysis carried out in this chapter evaluated heat recovery from different biogas upgrading technologies. Life cycle cost analysis with and without heat recovery is presented. This section of present chapter investigates two different scenarios for the calculations on the life cycle cost of upgrading units:

Scenario with heat recovery: heat is recovered from the upgrading unit, and used in other parts of the biogas production process.

Scenario with no heat recovery: heat is not recovered from the upgrading unit.

3.3.1 Input data

Table 3-1 contains all the inputs used in this study. The input data given in Table 3-1 correspond to the plant data, obtained in [39] and literature [8],[102]. The data given in this Table is an average of the

data found in several different sources. These input data are used for each different biogas upgrading technology in order to drive the LCCA.

Factors that are included in this analysis are:

- Annual cost
  - Energy-Electricity
  - Energy-Heat
  - Water consumption
  - Activated Carbon
  - Amine
  - Maintenance/Service
  - Methane loss
- Initial Cost
  - Investment cost

Table 3-1: Initial Input data used for life cycle cost analysis of different biogas upgrading technologies

		Water Scrubber	Amine scrubber	Membrane	PSA	Cryogenic
Investment cost	€	1 100 000	1 250 000	1 177 230	1 386 667	2 300 000
Energy-electricity	kWh/Nm^3	0.27	0.28	0.285	0.24	0.65
Energy-heat	kWh/Nm^3	-	0.6070		-	-
Energy-Herat recovery	kWh/Nm^3	-0.0688	-0.3231	-0.145	-	-0.8450
Water Consumption	m^3/year	665	135	-	-	300
Active carbon	Kg/year	-	1030	1375	697	1 100
Amine	Kg/year	-	660	-	-	-
Maintenance/service	€/year	15 000[102]	59 000	42 000	31 000	167 000
Methane loss	%	1	0.4	0.5	1.25	0.3

3.3.2 Assumptions and additional data

Besides the technical and economic data of the different upgrading units addressed from the literature, some additional data were used. In addition, certain assumptions were necessary in order to conduct the LCCA. These assumptions and data are presented in Table 3-2.

Table 3-2: Input data and assumptions to conduct life cycle cost analysis

Plant life	15	years
Availability-stream factor	0.94 corresponding to 8200 h	hour [103],[6]
Discount rate	6	%[39]
Biogas Production	1640000	m^3 raw biogas/year
Methane content	50	%
Amine cost	23	€/kg
Tap water cost	3	€/m^3
Electricity purchase price	100	€/MWh [104],[105]
Pre-treatment (Activated carbon cost)	5.5	€/kg specific cost @1.85 g/Nm^3raw biogas [5]

Most of the upgrading technologies are pre-fabricated and delivered in a container. They are initially designed for different flow rates of raw biogas with a given minimum and maximum range of flow rates. The minimum flow rates for the considered upgrading units are ranging from 0 to 260 m^3/h, while the maximum goes as high as 700 m^3/h. when performing LCCA for the five above mentioned upgrading units, the raw biogas flow rate is set to 1640000 m^3 biogas annually. This corresponds to a flow rate of approximately 200 m^3/h. The average purchase price for tap water is set to 3 €/m^3 [106]. When calculating the price for the energy, there are several factors that need to be considered. Here in this study, the associated costs for electrical grid rent to the supplier who delivers the electricity is not considered.

The electricity price varies over time and the consumption quantity, but an average price for the last five years is considered for the LCCA [105]. It is assumed that the investment costs for LCCA are paid all at once, and the construction time has not been taken into account. The annual operational costs are assumed to remain constant each year throughout the lifetime of the upgrading plants. This is done due to lacking information regarding changing cost for maintenance and consumables over time. For the calculations where heat recovery is included, it is assumed that all excess heat produced from the upgrading unit can be utilized in other parts of the biogas production process. Further costs for utilization of the excess heat, have not been considered. Cost of additional equipment such as pipelines and other components, might reduce the benefits of heat recovery.

3.3.3 Life cycle cost

LCCA is used to find out the economic perspective of an upgrading system throughout its entire life. The objective of performing life cycle cost analysis includes quantifying the life cycle cost, and using it for further technology evaluation or decision making.

ISO 15686-5:2008 defines LCC as the *"cost of an asset or its parts throughout its life cycle, while fulfilling the performance requirements".* LCCA can be used as a tool for long-term financial assessments throughout the lifespan of a system. Rather than saving money in a short- term perspective, the LCCA finds the best long-term economic option [39]. The monetary investment, long-term expenses and income are analyzed in this cost-based process. The LCC can be compared for various designs or options in order to find the most cost-effective system [107]. If an economic comparison is established for different options, requirements and boundaries must be set.

Following steps have been suggested by [107] for conducting LCCA:

1. Establishing objectives for the analysis
2. Determining the criteria for evaluating alternatives
3. Identifying and developing design alternatives
4. Gathering cost information
5. Developing a life cycle cost for each alternative

Figure 3-1 shows a graphical overview of the elements that are included in the LCCA and the whole life cost (WLC) [108]. The LCC includes the cost for construction, operation, maintenance and end-of-life. These elements can be adjusted and more costs might be added for the specific case. With respect to future income, it is only considered for WLC analysis but not for LCC analysis.

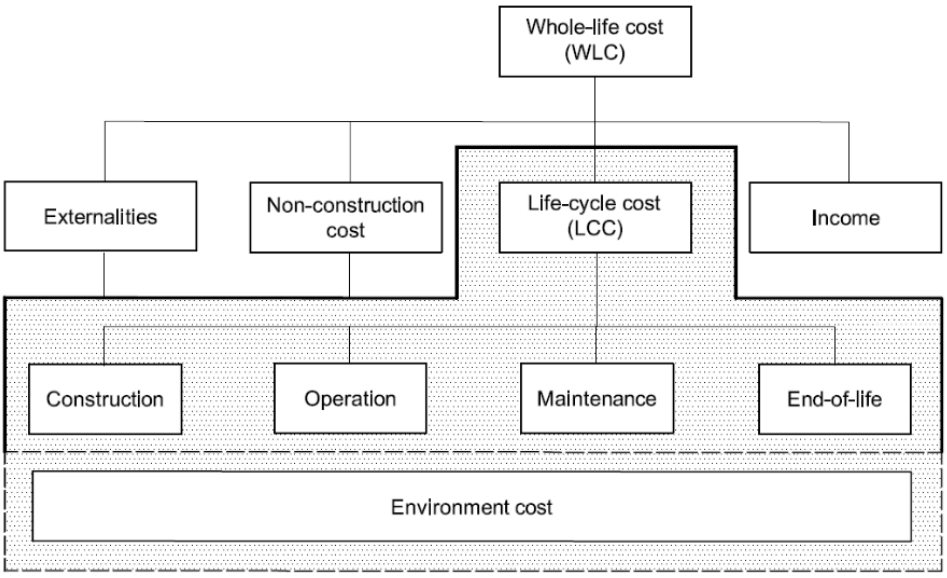

Figure 3-1: Graphical overview of LCCA and WLC elements [108]

All the monetary costs which occur in the future period of the project should be discounted, in order to be able to compare different cash flows from different time periods of the project [109]. For this purpose, the present value of all cost elements is calculated.

To find out present value of a future cost, the following formula is used [109]:

$$PV = A_n \frac{1}{(1+r)^n} \tag{3.1}$$

Where:

PV = present value

A_n = Value of the cost at time t

n = times in year

r = Discount rate

For annual costs that are repeating throughout the lifetime, the following formula is used [109]:

$$PV = A_0 \frac{(1+r)^n - 1}{r(1+r)^n} \quad (3.2)$$

Where:

PV = present value

A_0 = Value of repeating cost

n = Total times in year

r = Discount rate

To make the LCC analysis result as comprehensive as possible, two situations have been analyzed for five different upgrading units. One with heat recovery, and the other without heat recovery. It is possible to design biogas plants for the use of excess heat, and hence it is possible to include the reduction in costs due to heat recovery from biogas upgrading plants. Some of the upgrading technologies produce a large amount of excess heat, and in order to compare different upgrading technologies, the use of this excess heat should be included in the analysis. If the heat recovery is not taken into account when comparing different technologies, the result cannot be justified for a real case. When considering both scenarios with and without heat recovery, it is easier to consider the actual operating cost of the upgrading plant in context with the whole biogas plant.

3.3.4 Life cycle cost analysis (LCCA) with heat recovery

The annual cost is calculated for the different elements of the upgrading units and added together in order to find the total annual cost. Furthermore, the present value for the total annual cost is calculated for all upgrading plants, as presented in Tables 3-3 and 3-4. The present value is then added to the investment cost, which sums up to the total life cycle costs for all the respective upgrading units.

Figure 3-2 shows a graphical representation of life cycle cost (LCC) when heat recovery is included. The investment cost and present value for annual costs are presented with two different colors. The cryogenic upgrading unit is estimated to have the highest LCC. With an annual cost of 1400 K€ and an investment cost of 2300 K€, this system has a LCC over 3700 K€. However, due to the extremely high heat recovery rate, this unit does not have the highest total annual costs. The unit with the highest annual cost is the amine scrubber. The reason why the cryogenic upgrading unit has a higher LCC than amine scrubber, is the investment cost of the technology. As seen from Figure 3-2, water scrubber has the lowest annual cost. This is due to the heat recovery, as well as the relatively low maintenance cost. Similarly, water scrubber reported to have the lowest investment cost as well. Membrane and PSA technologies estimated to have similar annual and investment costs and hence

they have almost the same total life cycle reaching up to 2000 K€. The second highest total life cycle cost among the five evaluated technologies is amine scrubber.

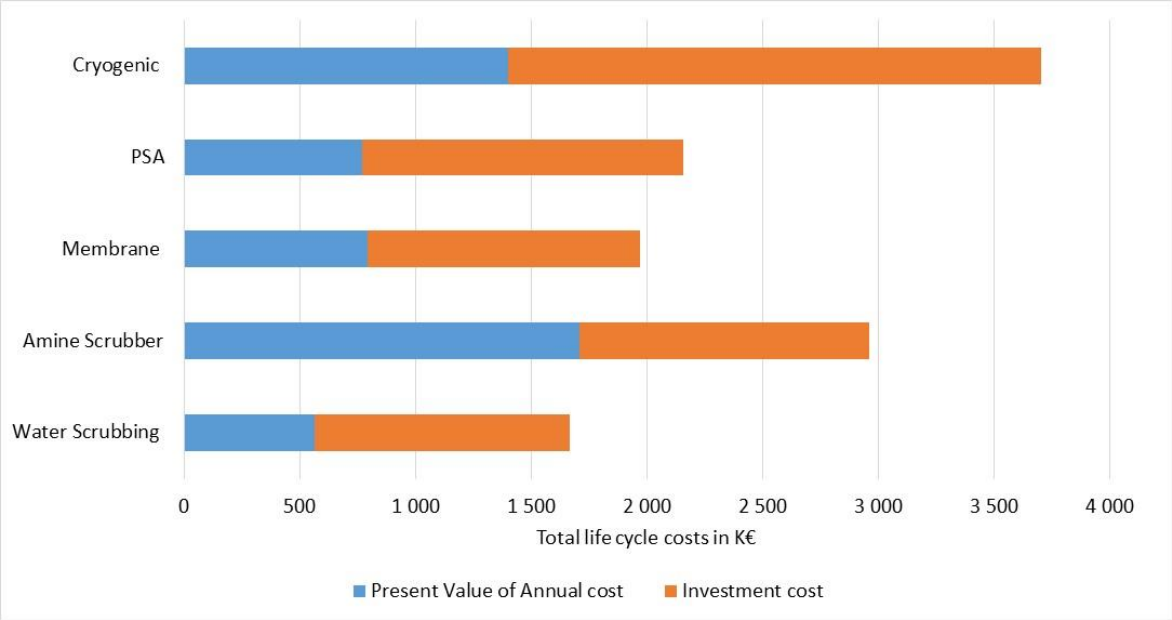

Figure 3-2: Total life cycle cost with heat recovery of five upgrading technologies

Table 3-3: Calculated life cycle cost analysis of five different upgrading technologies with heat recovery scenario

		Water Scrubbing	Amine Scrubber	membrane	PSA	Cryogenic
Investment cost	€	**1 100 000**	**1 250 000**	**1 177 230**	**1 386 667**	**2 300 000**
Annual cost of Investment	€/year	113 259	128 703	121 211	142 775	236 814
Energy-electricity	€/year	44 280	45 920	50 430	38 813	106 600
Energy-heat	€/year	0	99 630	0	0	0
Energy-Heat recovery	€/year	-11 283	-52 997	-23 780	0	-138 580
Water Consumption	€/year	1 995	405	0	0	900
Active carbon	€/year	0	5 665	7 563	2 556	6 050
Amine	€/year	0	15 180	0	0	0
Maintenance/service	€/year	15 000	59 000	43 500	31 000	167 000
Methane loss	€/year	8 118	3 247	4 059	6 765	2 435
Annual cost	€/year	**58 110**	**176 051**	**81 772**	**79 134**	**144 405**
Present Value of Annual cost	€	**564 377**	**1 709 847**	**794 185**	**768 569**	**1 402 501**
Total cycle cost	€	**1 664 377**	**2 959 847**	**1 971 415**	**2 155 236**	**3 702 501**

Table 3-4: Calculated life cycle cost analysis of five different upgrading technologies without heat recovery scenario

		Water Scrubbing	Amine Scrubber	membrane	PSA	Cryogenic
Investment cost	€	**1 100 000**	**1 250 000**	**1 177 230**	**1 386 667**	**2 300 000**
Annual cost of Investment	€/year	113 259	128 703	121 211	142 775	236 814
Energy-electricity	€/year	44 280	45 920	50 430	38 813	106 600
Energy-heat	€/year	0	99 630	0	0	0
Energy-Heat recovery	€/year	0	0	0	0	0
Water Consumption	€/year	1 995	405	0	0	900
Active carbon	€/year	0	5 665	7 563	2 556	6 050
Amine	€/year	0	15 180	0	0	0
Maintenance/service	€/year	15 000	59 000	43 500	31 000	167 000
Methane loss	€/year	8 118	3 247	4 059	6 765	2 435
Annual cost	€/year	**69 393**	**229 047**	**105 552**	**79 134**	**282 985**
Present Value of Annual cost	€	**673 962**	**2 224 563**	**1 025 142**	**768 569**	**2 748 425**
Total cycle cost	€	**1 773 962**	**3 474 563**	**2 202 372**	**2 155 236**	**5 048 425**

3.3.5 Life cycle cost analysis (LCCA) without heat recovery

The annual cost for the upgrading units with excess heat is greater when heat recovery is not considered. The estimated annual cost and life cycle costs for the scenario without heat recovery is presented in the Table 3-4. A graphical representation of the LCC for the scenario without heat recovery is illustrated in the Figure 3-3. By excluding the option for heat recovery, the results of LCCA changed for some upgrading technology.

The units that produces excess heat, are the ones affected by elimination of heat recovery. Water scrubber, amine scrubber, membrane and cryogenic technologies are the ones showed higher LCCA due to elimination of heat recovery option. The greatest change in LCC is found for the units with the highest heat recovery. The annual cost for the cryogenic unit is increased by 140 K€ resulting an increase of 1300 K€ in LCCA. Similarly, amine scrubber generates an increased annual cost of 50 K€ which equals a total increase of 510 K€ for the entire life cycle cost of this unit. Besides the units without excess heat, the lowest change in LCC was found for water scrubber which is due to low excess heat recovery capacity of the unit. By excluding heat recovery, PSA and water scrubber appear as the most cost-effective upgrading technologies.

The annual cost for the upgrading units with excess heat is greater when heat recovery is not considered. The calculated annual cost and life cycle cost for the scenario without heat recovery is presented in Table 3-4. A graphical presentation of the LCC for the scenario without heat recovery are illustrated in Figure 3-3.

3.3.6 Comparing scenarios

By comparing the results from analyzing two different scenarios, it is clear that the heat recovery has a rather big impact on the LCC for some of the upgrading technologies such as cryogenic technology and amine scrubber. Figure 3-4 shows a graphical representation of two different scenarios. For the cryogenic and amine scrubber, the change with and without heat recovery options were significant. A 36 and 20 % increase in the total life cycle costs were estimated for cryogenic and amine scrubber in scenario with elimination of excess heat. Water scrubber and membrane also produce some excess heat which can be recovered. The difference in LCC with and without heat recovery for these upgrading units was 110 K€ and 230 K€ respectively.

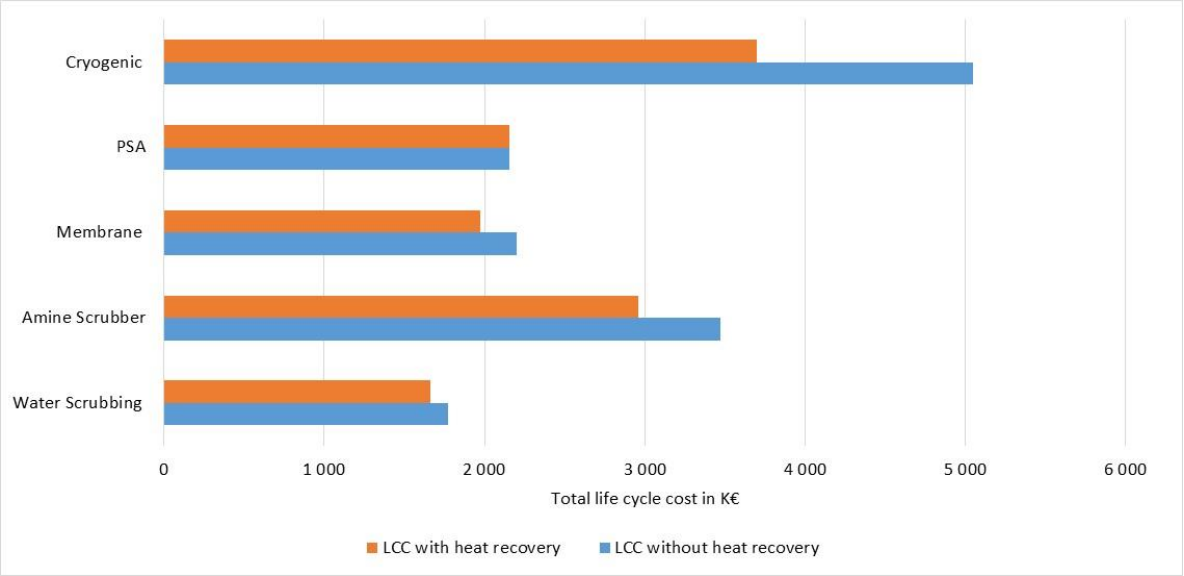

Figure 3-3: Comparing scenarios with and without heat recovery

3.4 Sensitivity analysis

Performing a sensitivity analysis, makes it possible to identify which input data that has the greatest impact on the LCC and analyze the consequences on the output results. It tests the outcome of the LCCA by changing some of the input parameters in the initial analysis. Two parameters are considered in the current sensitivity analysis. These are electricity price and discount rate.

3.4.1 Changing electricity price

The electricity cost can vary extensively throughout the year and is therefore a critical factor. The total electricity cost is therefore set to a minimum value of 60 €/MWh and 130 €/MWh (0.06 and 0.13 €/KWh). Increasing electricity price results in an increasing LCC for all upgrading units, except for cryogenic technology. An increasing electricity price results in a decreasing LCC for the cryogenic upgrading unit, since the heat recovery is larger than energy need for the operation of the unit (Fig.3-4).

Nevertheless, the other units, namely water scrubber, amine scrubber, membrane and PSA show a steady increasing LCC with increasing electricity price. The changing electricity price has the greatest impact on the LCC for amine scrubber. With changing electricity price from 0.06 to 0.12 €/KWh the LCC for amine scrubber increased from 2600 K€ to 3200 K€. The lowest change on the LCC from changing electricity price is for cryogenic technology. Membrane, water scrubbing and PSA show a slight increase in the LCC by increasing electricity price. Increase in LCC in function of electricity price with heat recovery is given in Appendix A1.

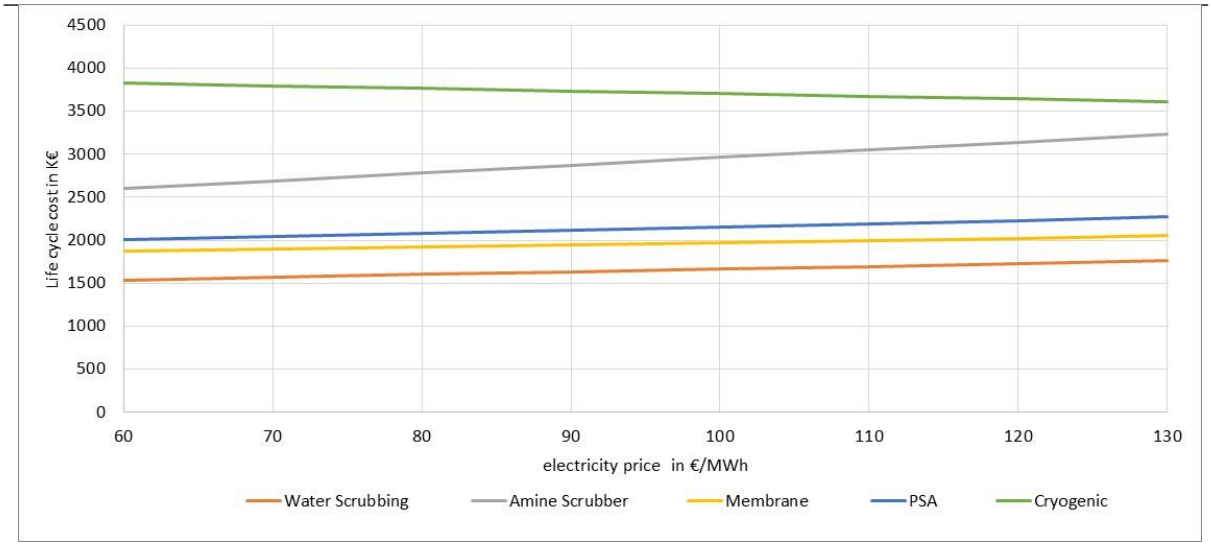

Figure 3-4: Sensitivity analysis for electricity costs with heat recovery

Figure 3-5 presents the results of sensitivity analysis for electricity cost without heat recovery scenario. The trend in the change of life cycle costs due to changing electricity prices for the case without heat recovery scenario found to be similar to the case with heat recovery scenario. Here in this case, the most affected upgrading units due to change of electricity price are amine scrubber and cryogenic technology. The rest of the technologies water scrubbing, membrane and PSA presented a slight increase in the life cycle costs due to increase in electricity price. The increase in the life cycle costs are due to increase in total annual costs which is again due to higher energy costs of the upgrading units. Increase in LCC in function of electricity price without heat recovery is given in Appendix A2.

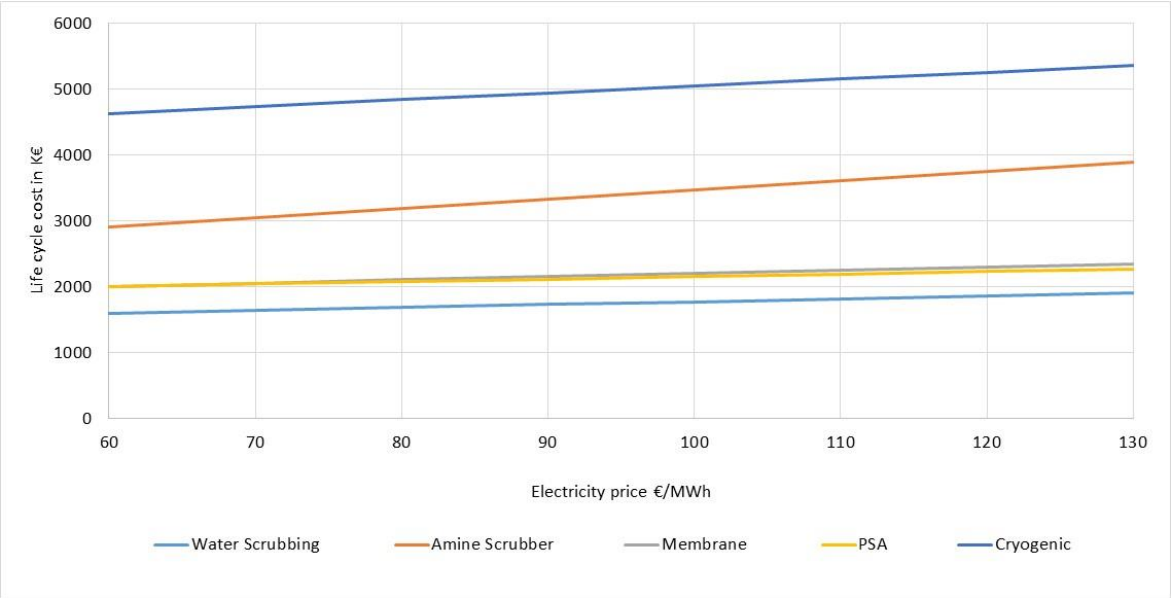

Figure 3-5: Sensitivity analysis for electricity costs without heat recovery

3.4.2 Changing discount rate

The discount rate affects all the parameters from the annual cost. The present value of the annual cost is calculated by multiplying the total annual cost with the discount factor as given by Equation (3.2). Appendices A3 & A4 shows the results from sensitivity analysis with and without heat recovery scenarios. Changes in the discount rate cause a proportional change in the present value for the annual cost. An increase in the discount rate, results in a decrease in LCC. The LCC for all upgrading plants decreases, when the discount rate is increased.

The largest change in LCC are seen on the upgrading units that have the highest annual cost. When heat recovery is included, the highest annual cost is for amine scrubber. It is clear that the amine scrubber also ends up with the largest change in LCC, when the discount rate is changed. The second mostly affected unit by changing discount rate is cryogenic technology. Amine scrubber and cryogenic technology both have presented 26 and 35% reduction in LCC respectively when discount rate increased from 2% to 10%.

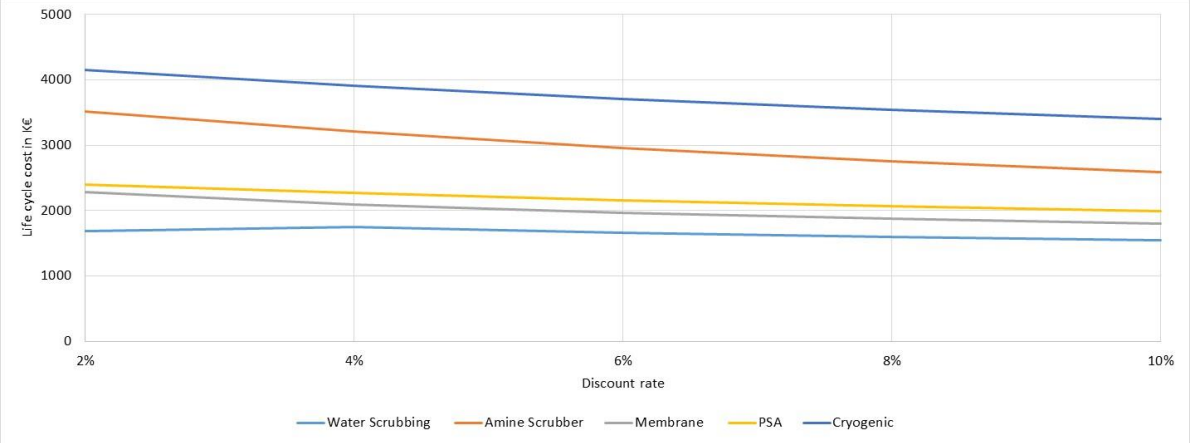

Figure 3-6: Sensitivity analysis for discount rate with heat recovery

For the case when heat recovery is not included, the cryogenic upgrading unit has the largest annual cost. This is also reflected on the result from the sensitivity analysis, where the cryogenic upgrading is the unit that is most affected by changes in the discount rate. Amine scrubber has high annual costs, and is therefore highly affected by changing discount rate. When the discount rate is changed from 2 % to 10 %, the LCC for amine scrubber and cryogenic technology decreases with 1200 K€ and 1400 K€ respectively. The reduction in PSA and membrane is in the rage 400 and 500 K€ when the discount rate is changed from 2 % to 10 %.

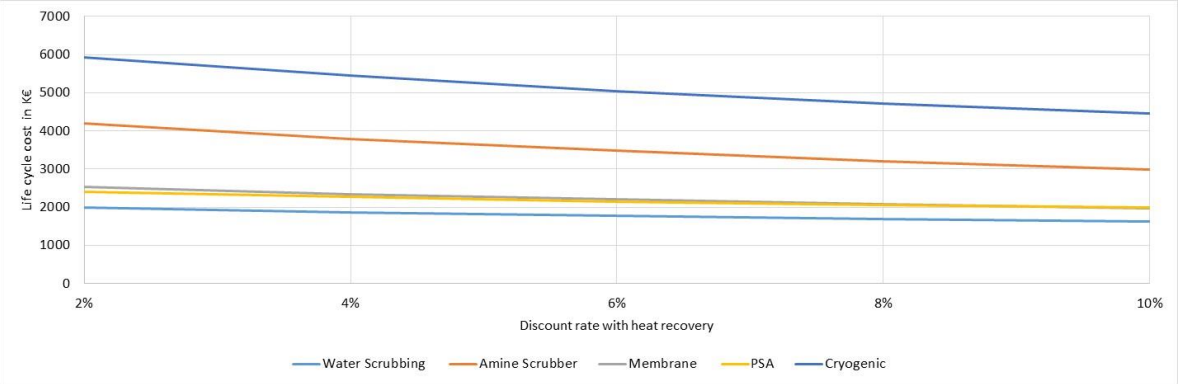

Figure 3-7: Sensitivity analysis for discount rate without heat recovery

3.5 Financial aspects of biomethane production

A new project involves spending an investment (*I*), and then earing a return (*R*), over the life time period of the project. As an example, installing or construction of an upgrading plant requires spending of money now in the hopes of earning money subsequently in the future. Similarly, the total costs of upgrading for the selected range of inlet biogas flow rate and total sales of revenue from selling the total produced biomethane to gas gird are assessed.

The specific costs of producing biomethane in €/Nm^3 and in €/MWh for selected upgrading technologies and different raw biogas flow rate are also calculated. Several additional costs are not clearly included in the calculations, either because they were supposed to be specific to the certain sites, too uncertain or included already in the maintenance and operation costs. These excluded costs include for compression costs in the event of grid injection and fees for gas grid connection [123]. Planning, wages, regulatory issues and breakdowns are not included either. The introduction of other costs increases uncertainty without additional accuracy.

3.5.1 Economic analysis

In this paragraph, an economical evaluation of a specific case: a landfill site biogas optimization into biomethane is performed. The produced biomethane from a landfill site is economically evaluated with the objective of injecting it into natural gas grid. Due to lack of supporting mechanisms such as incentive or feed-in tariffs in the location of landfill site, i.e. France, the economic analysis is only carried out for injecting into natural gas grid. The schematic considering the source of biogas from landfill and its upgrading into biomethane is given in Figure 3-8.

Table 3-5 presents three different possible combination of biogas upgrading technologies able to upgrade raw landfill biogas containing more than 10 Vol % nitrogen in the raw gas mixture. Among

the three given scenarios, cryogenic technology has the capacity to remove CO_2 and N_2 simultaneously and presents a higher final CH_4 recovery than scenario 1 and scenario 2 given in Table 3-5.

Moreover, cryogenic technology has the lowest life cycle costs compared to scenario 1 and 2 as illustrated with the help of Figure 3-9. Cryogenic upgrading unit with heat recovery scenario has the lowest total life cycle cost compared to other scenarios. Nevertheless, when heat recovery of the technology is not considered, cryogenic technology in this case would have the highest total life cycle cost compared to both Membrane + PSA and PSA+PSA scenarios. Hence, for the economic evaluation, cryogenic technology has been selected and further analysis carried out correspondingly. Heat recovery scenario of the technology has been considered since it give lower life cycle cost compared to without heat recovery scenario due to the valorization of extra heat in the system.

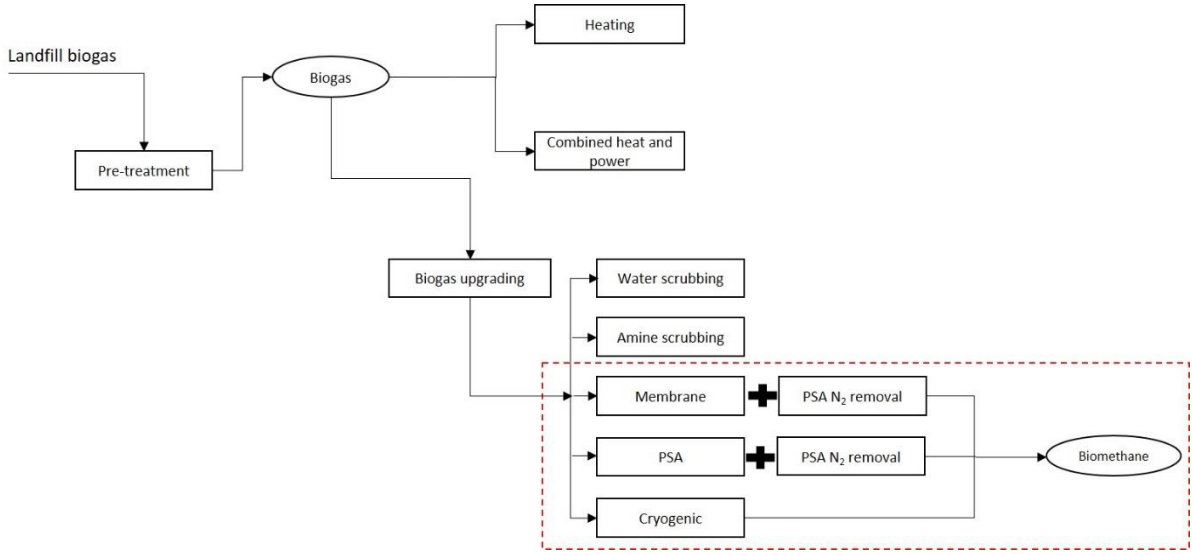

Figure 3-8: Schematic of landfill biogas upgrading process to biomethane

Three different scenarios including different biogas upgrading technologies are analyzed in order to estimate the lowest possible specific cost of upgrading for the landfill site specific case. Due to the presence of higher amount of nitrogen in the raw landfill biogas, a separate N_2 removal PSA process is added.

Table 3-5: Comparison of different scenarios for landfill site biogas upgrading

Scenarios	Biogas upgrading technologies	Final CH_4 recovery (%)
Scenario 1	CO_2 removal membrane technology + N_2 removal PSA	81.5
Scenario 2	CO_2 removal PSA + N_2 removal PSA	81.5
Scenario 3	Cryogenic technology (simultaneous CO_2+N_2 removal)	99

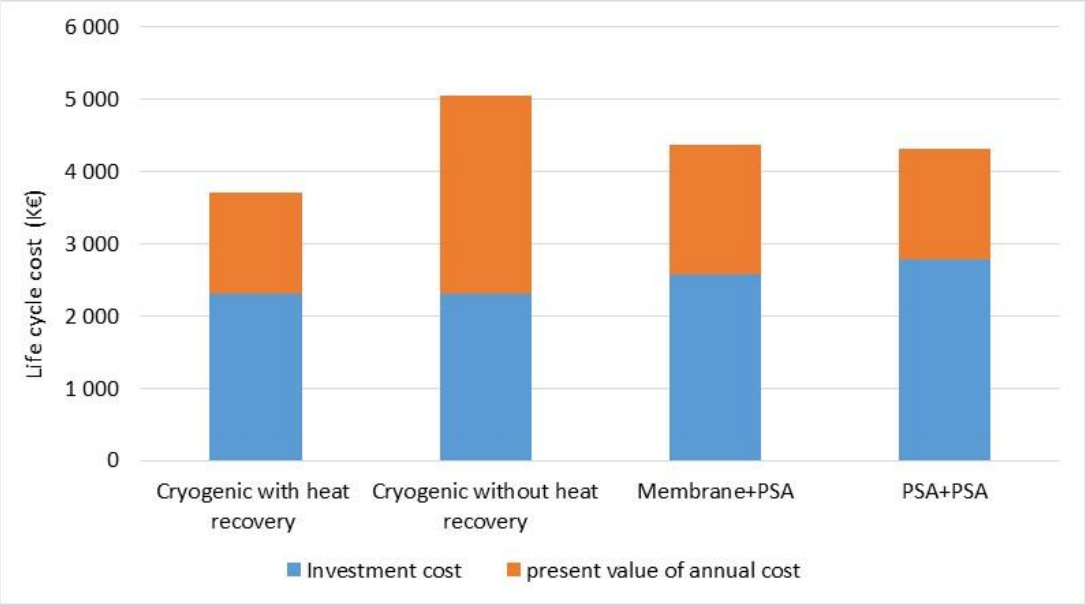

Figure 3-9: Total life cycle cost comparison of landfill biogas upgrading scenarios

In order to calculate the overall specific cost of upgrading, annual capital cost with the help of Equation (3-3) is calculated where C_{ann} is the annual capital cost, *r* is the interest rate and *n* is the depreciation life. In case of cryogenic technology it results C_{ann} = 236000 €/year; and in case of Membrane + PSA it results C_{ann} = 263000 €/year. Table 3-6 represents all the annual operating costs associated in the process. With 50 % CH_4 in the raw biogas and 95 % CH_4 recovery with cryogenic technology, the annual biomethane produced is 779000 m^3. Therefore, the overall specific costs for cryogenic technology with heat recovery option is 0.50 €/m^3 for a 200 Nm^3/h of raw biogas flow rate. This total specific cost of upgrading is 0.76 €/m^3 for cryogenic technology without heat recovery.

Biogas cost in the estimation of total specific upgrading cost is taken as zero €/m^3 which is because the source of raw biogas is considered a landfill site (Table 3-6). A stream factor of 92% and an interest rate of 6% is taken into consideration for the calculations of overall costs of upgrading. A depreciation period of 15 years to find out the annual capital cost is incorporated in the calculations. Table 3-7 illustrates the estimated total specific costs in case of scenario 3 and scenario 2.

$$C_{ann} = CAPEX \frac{r(1+r)^n}{(1+r)^n - 1} \quad (3.3)$$

Table 3-6: Annual operating costs and other techno-economic assumptions of the landfill biogas upgrading technologies

	Cryogenic technology	Membrane + PSA
Methane recovery	95%	81.5%
Plant availability- stream factor	8200/(365*24) = 92%	
Interest rate	6%	
Specific cost of electricity	0.10 €/KWh	
Depreciation life	15 years	
Maintenance cost	167000 €	74500 €
Electricity cost	106600 €	89200 €
Heat recovery cost	-138580 €	-
Biogas cost	0 €/m^3	0 €/m^3
Annual capital cost	236000 €/year	263000 €/year

Table 3-7: Specific cost of biomethane production with the considered scenarios from landfill raw biogas

	Technologies		€/m^3	€/MWh
Scenario 3	Cryogenic technology	With heat recovery	0.46	42.2
		Without heat recovery	0.76	70.6
Scenario 2	Membrane + PSA	-	0.61	56.1

Figure 3-10 shows how the increase of plant size (biogas flow rate in m^3/h) leads to a decrease of the unit production cost of biomethane in case of all three scenarios. It is evident that increasing the plant size from 200 Nm^3/h to 400 Nm^3/h, the unit specific cost decreases of 40% in case of cryogenic without heat recovery and decreases of 50% in case of cryogenic with heat recovery. The total annual costs for different biogas flow rates is given in Appendix B1.

The economic results obtained within this work that is given in Table 3-7 could not be compared with the literature data since such kind of specific case of landfill site biogas upgrading does not exist yet in the literature. In spite of that, in section 1.4.2, a payback period comparison is made with the financial and economic data provided with a cryogenic technology manufacturer. The name and the data is not used in this report due to the issue of confidentiality.

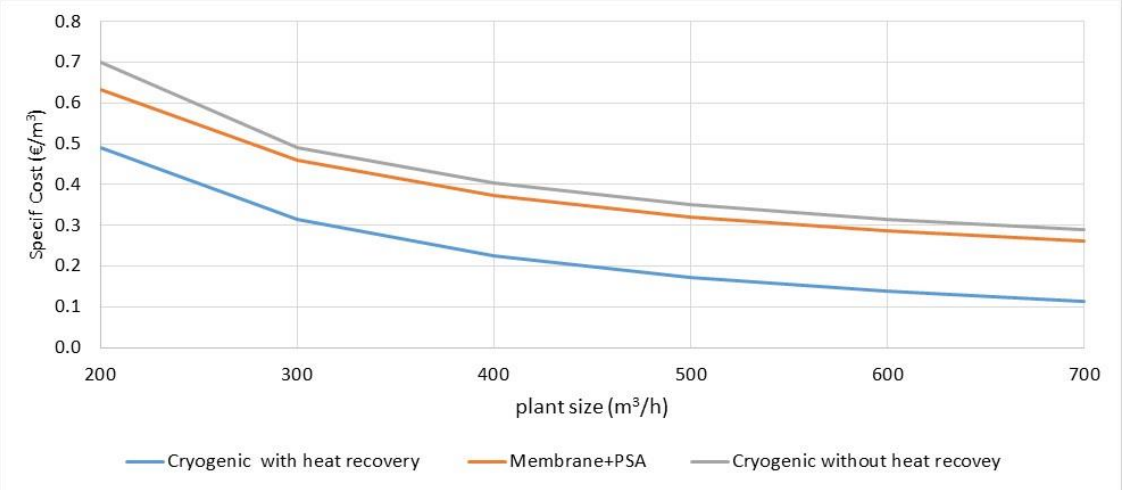

Figure 3-10: Specific cost of biomethane production as a function of plant size (Nm^3/h)

But instead, the economic results obtained with the selection of most cost-effective technology is compared with the literature data. The most cost effective technology in terms of lower LCC and lower annual costs presented in section 1.2.3 is selected and again the total specific cost of upgrading is calculated with the same approach as already explained above. In this case, the source of the selected raw biogas is not a landfill site but instead a typical biogas cost is added which is found in the literature. The typical biogas cost corresponds to the cost of producing raw biogas through anaerobic digestion tanks. The most reasonable values found are presented in the Table 3-8. As reported in [110], *"The higher biogas production costs are for biogases that are produced using a significant share of maize silage (an input source that has a non-negligible cost on the market). For manure-derived biogas, lower costs result being manure a freely available feedstock at the plant site. The biogas production cost could take equal to zero for raw sewage biogas from mixed urban/industrial sludge."*

According to [111], the production costs from waste water treatment plants might be even taken equal to zero. In fact, the main purpose of waste water treatment plant is the inertization of the putrescible matter of the sludge, which occurs in digestion tanks. Biogas is thus a by-product of this inertization process[110]. The assumption used as biogas specific cost is an average of the values reported in the Table 3-8 and amounts to 0.20 €/m^3. Therefore it results an annual cost of 328 000 €/year at 200 Nm^3/h or 164000 €/year at 100 Nm^3/h of raw biogas flow rate.

Table 3-8: Typical biogas costs addressed in the literature

Source	€/m^3	€/KWh
Thrân et al., 2014[112]	0.107	0.018
Thrân et al., 2014[112]	0.214	0.036
Thrân et al., 2014[112]	0.131	0.022
Trendewicz and Braun, 2012[113]	0.059	0.010
Budzianowski and Budzianowska, 2015[114]	0.274	0.046
Budzianowski and Budzianowska, 2015[114]	0.387	0.065
P. Rotunno et al. [110]	0.265	-
Average	0.20	

Referring back to section 1.2, water scrubbing has the lowest both annual and total life cycle costs among the five studied upgrading technologies in both with and without heat recovery scenarios. Annual capital cost of the technology and total cost of biogas production is added and total cost is divided with the annual production capacity of technology to finally find out the specific cost of upgrading. Biogas cost at 0 €/m^3 and biogas cost at 0.20 €/m^3 scenarios are illustrated to show the difference between both scenarios. Table 3-9 gives the overall costs found in the calculation of specific costs of upgrading.

Table 3-9: Annual operating costs and other techno-economic assumptions for the water scrubbing technology

	Water scrubbing technology
Methane recovery	95%
Plant availability- stream factor	8200/(365*24) = 92%
Interest rate	6%
Specific cost of electricity	0.10 €/KWh
Depreciation life	15 years
Maintenance cost	15000 €/year
Electricity cost	44280 €/year
Other costs	10000 €/year
Biogas cost	164000 €/year at 100 Nm^3/h
Annual capital cost	113260 €/year

In Table 3-10 the economic results obtained in this work are compared with overall specific costs available in literature[110]. Other sources [115],[116],[117] indicate an overall specific cost of

upgrading between 0.2 and 0.49 €/m3 but they do not represent a significant term of comparison for many different reasons: cost data referred to plants with a greater size than the one analyzed in this work; upgrading technology is different from the pressured water scrubbing; unspecified utilization of biomethane; annual time of plant operation is not specified.

Although the indicated data are affected from such lack of information, the specific cost range identified is comparable to the one calculated in this work (0.3 - 0.60 €/m^3) for gas grid injection scenario at raw biogas flow rate 0 €/m^3 and 0.2 €/m^3. Share of different cost items in the specific cost of biomethane production is given in Figure 3-11. Biogas cost at 0.2 €/m^3 plays a significant role in the total share of specific cost of biomethane production and the share increases by increasing the plant size. The share is 51% when plant size is at 100 Nm^3/h and increases into 200 Nm^3/h when plant size double from 100 to 200 Nm^3/h. the second greatest share comes from annual capital cost from 22% to 35%.

A: 200 Nm^3/h

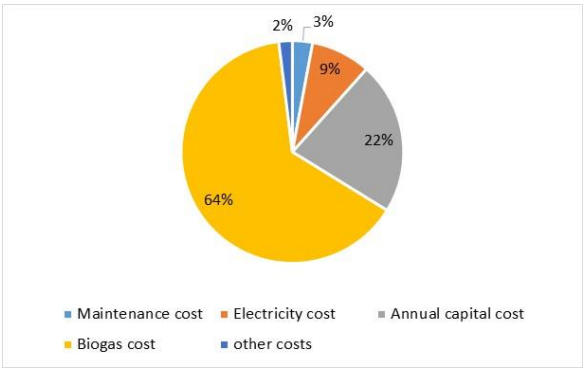

B: 100 Nm^3/h

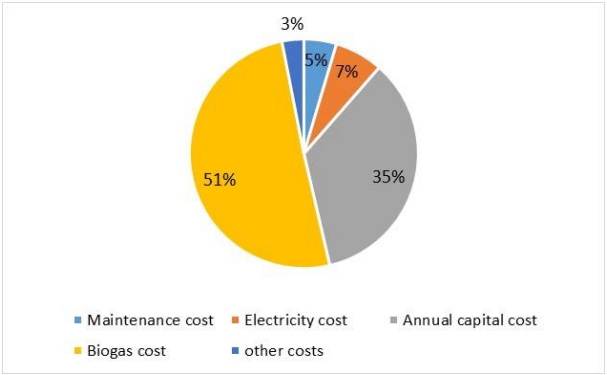

Figure 3-11: Share of cost items in the specific cost of biomethane production with water scrubbing at biogas flow rate A: 200 Nm^3/h and B: 100 Nm^3/h

Table 3-10: Specific cost of biomethane for grid injection and comparison with data reported in literature [110]

	This work (€/m^3)	Literature [110] (€/m^3)
Grid injection scenario		
Biogas cost at 0 €/m^3	0.30	0.26
Biogas cost at 0.20 €/m^3	0.60	0.54

3.5.2 Payback period

3 **Income through sale of upgraded biogas**

In 2010, the National Action Plan (NAP) for renewable energy laid the foundations for a new purchasing obligation for biomethane injected into natural gas networks, which is similar to that which was

established for electricity [6]. In November 2011, the 8 Decrees and Orders allowing the biomethane injection channel to be developed in networks were published [20]. They were incorporated into the French Energy Code. The biomethane sector therefore benefits from two economic tools:

• A regulated and guaranteed purchase price for 15 years for producers;

• A guarantees of origin system, which ensures biomethane can be traced and accentuates its value for consumers.

Introduction of feed-in tariff for biomethane injected into natural gas networks

Thanks to this system, a producer is guaranteed to sell the biomethane produced by its installation to a natural gas supplier at a rate fixed by Decree for a period of 15 years. The producer will benefit from a purchase price of between 46 €/MWh and 139 €/MWh, compared with an average of 99 €/MWh in 2016 [6]. The price depends on the production facility's size, referred to as the maximum capacity of biomethane production (expressed in Nm^3/h) and the nature of the waste or organic matter being treated. For anaerobic digestion facilities, purchase prices are made up of a reference tariff and an "input" premium.

Income is generated through sale of upgraded biogas to utilities where it is injected into natural gas grid [118]. The amount of upgraded biogas depends on the methane loss and methane concentration of upgraded biogas. Grid injection scenario exists in France for storage facilities for non-hazardous waste such as landfill sites. The reference tariff is adopted in case of non-hazardous waste and it misses the premium tariff because of the fact that the biomethane produced from a landfill site. The given tariff for storage facilities for non-hazardous waste is between 45 €/MWh and 95 €/MWh depending on the storage facilities maximum production capacity. Income generated through sales of upgraded biogas where it is injected to natural gas grid in case of cryogenic technology is calculated here with the help of below equation. The term income generated through sales of upgraded biogas is also referred as "total sales of revenue".

$$Total\ sales\ of\ revenue\ \left(^{€}/_{year}\right) = upraded\ biogas\ {}^{Nm^3}/_{h} * price\ {}^{€}/_{MWh} * working\ hours\ \left(^{h}/_{year}\right) \quad (3\text{-}4)$$

Upgraded biogas (Nm^3/h) is expressed in terms of energy content in HHV = 10.9 KWh/Nm^3. 8200 hours of annual operation is considered. Using above formula, income through sales of upgraded biogas is calculated and given in Table 3-11. For different raw biogas flow rates presented in Table 3-11, different biomethane prices depending on the storage facilities maximum production capacity is used. Net income is the net revenue when total annual costs of specific biomethane production is deducted from total sales of revenue. Net income is used to calculate the annual cumulative cash flow

and payback period of the different scenarios at different raw biogas flow rates. The detailed calculations including total annual costs and total annual net income is given in Appendix B2.

Table 3-11: Income through sales of upgraded biogas

Flow rate (raw biogas)	Earnings or annual total sales of revenue (€/year)	
	Cryogenic technology	Membrane + PSA
200	592 040	511 024
300	777 053	670 719
400	962 065	830 414
500	1 110 075	958 170
600	1 221 083	1 053 987
700	1 295 088	1 117 865

Similarly, simple payback period formula is used to estimate the length of the time required to recover the cost of investment done in each scenarios. Simple payback period formula is given in Eq. (3.5). Annual cash flow is the net income or (Total sales of revenue/year- Total costs/year).

$$simple\ payback\ period\ (PBP) = \frac{Cost\ of\ investmnet}{annual\ cash\ flow} \quad (3.5)$$

Although the initial investment is the same for both cases, Figure 3-12 shows that the payback period is lower in case of biogas cost at 0 €/m^3. For the given characteristics in case of water scrubbing, the initial investment is recovered with two years which is more than 5 years in case of biogas cost at 0.20 €/m^3.

In the same way, payback period and cumulative cash flow estimations are conducted for landfill biogas upgrading scenarios. PBP is performed in case of cryogenic technology for both, with heat and without heat recovery scenarios (Fig. 3-13). A range of 200-500 Nm^3/h of plant size is considered for these estimations. At 500 Nm^3/h, with heat recovery scenario, the cost of investment is recovered within only 3 years. This is because, the plant in this case is expected to earn more which is due to high income through sale of huge amount of upgraded biogas. For the same scenario, when plant size is 200 Nm^3/h, the total initial investment cost is recovered in more than 10 years. The fact that the heat is recovered and valorized, the total annual cost reduces and net income increases. A 200 Nm^3/h plant size with no heat recovery scenario will not recover the initial investment even in 15

years which is simply due to high annual expenses and lower income through sale of upgraded biogas. In contrast, when the plant size is 500 Nm^3/h, the payback period in this case is expected to be at more than five years. Cumulative cash flows for landfill biogas upgrading scenarios at different biogas flow rates are given in Appendices C1-C4.

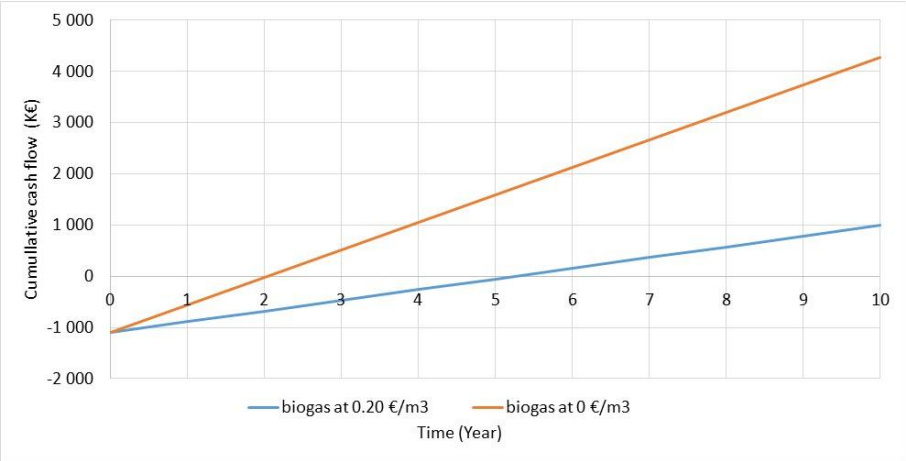

Figure 3-12: Payback period for biogas upgrading technology: water scrubbing at biogas cost 0.20 €/m^3 and 0 €/m^3

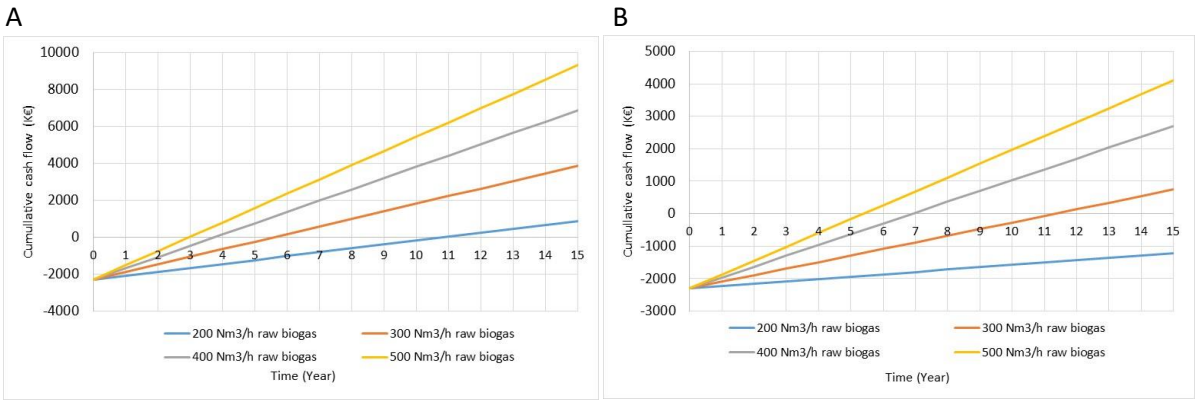

Figure 3-13: payback period of gas grid injection for landfill biogas upgrading scenarios A: cryogenic with heat recovery B: cryogenic without heat recovery

3.5.3 Conclusion and perspectives

Chapter 3 assessed five different biogas upgrading technologies. The technologies that are analyzed in this chapter are water scrubbing, amine scrubbing, membrane technology, pressure swing adsorption and cryogenic technology. These are the biogas upgrading technologies which already exist in commercial scale. The mentioned above five different technologies are analyzed from a life cycle point

of view. Total investment costs, annual operation and maintenance cost and technical and economic features for the upgrading technology were obtained from different literature sources. Through the data collection from the different available literature, it was established that the investment cost for upgrading units was ranging widely. An average of the many investment costs for upgrading units is used for the current assessment. The objective of carrying out a life cycle cost analysis was to find out the most cost-effective and economically profitable technology.

Among the five assessed technologies, water scrubbing has the lowest investment cost, while the cryogenic upgrading unit appears as the most expensive unit. Four of the technologies could recover heat, which include, water scrubbing, amine scrubbing, membrane and cryogenic technology. Three of the technologies presented water consumption, which include water scrubber, amine scrubber and cryogenic technology. The highest methane loss was found to be for the PSA, while the amine scrubbers had the lowest loss.

According to life cycle cost analysis carried out in this chapter, water scrubbing and amine scrubber are the most cost-effective units both in heat recovery included and excluded. If recovered heat is not utilized, the results remain the same for both scenarios. The least cost-effective unit turned out to be the cryogenic upgrading, which is due to either higher total investment or higher total annual cost of the units. The specific energy consumption of cryogenic unit is the highest among the five studied technologies; similarly, amine scrubber needs huge amount of heat to operate.

Sensitivity analysis are done for the five upgrading units in order to find out the most impacting parameter in the process. To do so, changing electricity price and changing discount rates are assessed. Some of the upgrading technologies such as amine and cryogenic upgrading units are energy intensive in terms of specific electricity consumption and specific heat requirement in the process. Lowering the electricity price resulted in lower total annual costs for these technologies. Increasing electricity price results in an increasing life cycle costs (LCC) for all upgrading units, except for cryogenic technology. An increasing electricity price results in a decreasing LCC for the cryogenic upgrading unit, since the heat recovery is larger than energy need for the operation of the unit. Changes in the discount rates cause a proportional change in the present value for the annual cost. An increase in the discount rate, results in a decrease in LCC. The LCC for all upgrading plants decreases, when the discount rate is increased.

This chapter also investigated the production of biomethane from a specific landfill site by studying different scenarios. The raw biogas from the said landfill site contains more than 10-vol % nitrogen in the gas mixture. A 50-vol % CH_4 and a 200 Nm^3/h biogas flow rate are the characteristics of the biogas investigated in 3 scenarios on this landfill site. Knowing that the most of the upgrading

technologies cannot simultaneously remove nitrogen and carbon dioxide, secondary N_2-specific rejection system may be required at the end of the gas-upgrading unit to remove N_2 to achieve acceptable end use levels. Hence, three of the scenarios able to fully upgrade landfill biogas into biomethane are technically and economically investigated. These scenarios are Membrane + PSA, PSA+PSA and cryogenic upgrading unit. In case of Membrane +PSA or PSA+PSA, the two step biogas upgrading would have a lower methane recovery compare to cryogenic unit due to losses encountered during the process.

Total annual costs of these scenario were found by adding all the associated costs such as annual capital cost, energy cost, maintenance and operation costs in the process. Among the three scenarios investigated, cryogenic upgrading unit presented the least life cycle cost. The specific cost of biomethane production is calculated by dividing the total annual cost with annual biomethane production capacity of upgrading units. In case of cryogenic upgrading unit, heat recovery and its utilization showed an important contribution in the calculation of specific cost of biomethane production. Specific cost of biomethane production with cryogenic upgrading unit is calculated to be at 0.76 €/m^3 i.e. 70.6 €/MWh without heat recovery option. Nevertheless, the specific cost of biomethane production with cryogenic upgrading unit is calculated at 0.46 €/m^3 i.e. 42.2 €/MWh with heat recovery option. The cost of raw biogas is taken as zero given the fact that the said gas is generated in a landfill site.

Income through sales of upgraded biogas and payback period calculations were also performed for the specific landfill biogas upgrading scenarios. With the feed-in tariff for biomethane injected into natural gas grid, which guarantees and regulates purchase price for 15 years for biomethane producers, we have estimated the total sales of revenue. Moreover, knowing the total sales of revenue and total expenses i.e. total annual biomethane production costs, we have calculated the net income through sales of upgraded biogas. Lastly, the payback period and cumulative cash flow are estimated for cryogenic with heat recovery, cryogenic without heat recovery and Membrane +PSA scenarios. Given the fact that: increase in plant size decreases the unit production costs of biomethane, we have calculated payback periods for different biogas plant sizes i.e. raw biogas flow rates. One of the important findings in the calculations is, the shorter time required to return the total initial investment in case of higher biogas plant size. Knowing that the CH_4 vol % could rarely goes more than 55% in the raw landfill biogas mixture, the increase in biogas flow rate showed significant economic profitability in terms of shorter payback period of the investment and higher net income.

Similarly, economic analyses are carried out for a most-cost effective biogas upgrading unit i.e. water scrubbing. In this case vol % of nitrogen in the raw gas mixture is assumed at < 10% or in a range

that can be removed simultaneously with carbon dioxide removal in one step upgrading process. Hence there is no requirement of a specific nitrogen removal step. The source of such raw biogas is assumed anaerobic digestion tanks and two scenarios are studied: biogas cost at 0.2 €/m^3 and biogas cost at 0 €/m^3. From the calculations carried out, specific biomethane production costs at 0.6 and 0.3 €/m^3. Payback periods of 2 and 5 years were estimated at biogas cost 0 and 0.2 €/m^3.

One of the challenges of this study is that no data from actual plants or suppliers for the upgrading technologies were used. Meaning that all the calculations are based on data found in literature. Thus, it only allows for a general analysis of the technologies but not of a specific plant in a specific region. However, the data from literature used for the calculations is expected to be reliable and well within the values used at actual plants. Therefore, the calculations are thought to be reliable and accurately present a broad case for each of the upgrading technology. Moreover, to make the calculations more accurate and reliable, we have taken a specific case of landfill biogas source so that the implemented biogas upgrading technology could represent more realistic results. Energy costs, water costs and feed-in tariff supporting mechanisms corresponds to the case of France where the landfill site is located.

Furthermore, the raw biogas was assumed to only consist of methane, carbon dioxide, nitrogen and hydrogen sulfide. Any other impurities were omitted due to lack of data or simplicity of calculations. In order to get a complete picture of all the emissions, it is important to include all impurities in the raw biogas. Pre-treatment stage is integrated in the process of biogas upgrading that represent the elimination of hydrogen sulfide. Activated carbon consumption and its associated costs given that correspond to the operation of activated carbon filter to remove H_2S from the raw biogas.

Carbon dioxide is the second important element in the mixture of landfill biogas that represents 35-40 vol % mixture. To the best of knowledge, CO_2 could be separated and captured at the outlet of upgrading technologies such as PSA, membrane or cryogenic unit. Carbon dioxide could be used as a carbon source to produce synthetic methane in the methanation process via power-to-gas technology. In a landfill site if flow rate of biogas produced is lower, valorization of carbon dioxide content of such raw biogas into useful commodity such as synthetic natural gas (SNG) could increase the economic viability of such sites. In the next chapter the power-to-gas process is investigated with the help of first thermodynamic law and later kinetics of reactions.

4 Chapter 4: Methanation and Kinetics of Reaction

4.1 Introduction to the chapter

Bearing in mind the importance of synthetic methane production and its potential in the future to be a promising alternative renewable energy production, state of the art technologies in this domain are highlighted under a literature review [11], [58], [119]–[126]. Besides the importance of temperature control of the process in the exothermic reaction of synthetic methane production, the thermodynamic analysis, kinetics of reaction and selection of an appropriate catalyst play a vital rule in the optimization of this process and in achieving better CO_2 conversion rate.

A Thermodynamic analysis is carried out to highlight the influence of temperature, pressure, CO_2:H_2 ratio on the gas composition at steady state. A thermodynamic analysis presents the maximum CH_4 yield and CO_2 conversion achievable for each operating parameters. A perfect agreement is obtained between literature and the results derived with the simulations carried out on the thermodynamic analysis in this study.

Moreover, a detailed study of kinetics of methanation reaction is carried out. One of the mostly adopted kinetic model is the one from Xu & Froment [127]. This model is used and adopted in many methanation studies [122]–[124], [128], [129] and indicated excellent kinetic rates of reaction results. To perform a complete study of kinetics of reaction, firstly, we have carried out a parametric study with the objective to validate all the equations and parameters addressed from literature. This parametric study is carried out under a batch reactor using Matlab. Secondly, a plug flow reactor is chosen to perform a kinetic reaction study under the continuous steady state mode of reaction for the Xu & Froment model.

4.2 Kinetic analysis of methanation reaction

4.2.1 Kinetic models

Kinetic models applicable for the technical conditions are scarce; nonetheless, they are strongly needed for the reactor design and optimization and for a qualified comparison of catalyst systems. In the view of economic feasibility, Nickel (Ni) catalyst is mostly used because of being highly active and low in the cost, in addition to nickel, Rhodium (Rh), Ruthenium (Ru) and Palladium (Pd) have been reported to be catalytically active in the process of methanation. Nickel is expensive compared to few other available options such as Mn, Fe and Cu, but this is compensated by using a lower percentage of Ni in the catalyst. Ni based catalyst can withstand very high temperature (900°C-1000°C) and exhibits good mechanical performance.

The best mechanistic model for intrinsic kinetics for a nickel based catalyst has been presented by Weatherbee and Bartholomew for 3 wt.% Ni/SiO_2 [130]. More improvement regarding kinetics was realized by Kai et al.[131], who used both a differential and an integral reactor for kinetic studies at ambient pressure on an alumina supported Ni catalyst promoted by La_2O_3. By operating the integral reactor up to conversions of 90%, the influence of the products: water and methane on the kinetics was accessible in detail. Kinetics were described by a Langmuir–Hinshelwood rate equation based on the mechanism proposed by Weatherbee and Bartholomew [20], but assuming the hydrogenation of carbon instead of CO dissociation as rate determining step. It was found that measured conversions at integral operation were smaller than predicted by rate equations based on experiments run in differential mode. This was attributed to the adsorption of products on the catalyst surface. Consequently, the adsorption of water was accounted for in the Langmuir–Hinshelwood rate equation and an excellent fit of the data was obtained this way.

The first kinetic study of steam methane reforming was carried out in the temperature between (609-911) K, in this study the rate-determining step was the surface decomposition of methane [132]. In the later studies carried out, Kinetics of steam Methane Reforming (SMR) were carried out on 12% Ni/AL_2O_3 at a slightly higher temperature range (823 -953) K [133]. Xu and Froment [127] presented the most widely used kinetic model for SMR. In their model, they considered carbon dioxide (CO_2) as non-adsorbing gas on the surface of the catalyst. The reaction kinetics depends upon the partial pressure of the steam. According to Elnashaie et al. [133] the partial pressure of the steam has a negative influence on the rate of reaction. However, according to Elnashaie et al.'s different findings, partial pressure has also positive impact on the rate of reaction. Xu and Froment's model include both the positive and negative effect of the partial pressure of the steam. Xu and Froment's model performed on a typical steam reforming 15%Wt. $Ni/MgAl_2O_4$ catalyst is used for parameter estimation. Experimental conditions concerning the methanation experiments were temperatures between 300°C and 400°C and pressures between 3 and 8 bars, which are close to a technical implementation of CO_2 methanation.

Among the large number of reaction schemes, Xu and Froment came up with a scheme, which considered all the reactions taking place during SMR process and this reaction scheme helped in formulating the rate of reaction. The model comprises three reactions as given in Figure 4-2: the methanation of carbon dioxide (R_3) equation 4.1, the methanation of carbon monoxide (R_1) equation 4.2 and reverse-water-gas shift reaction (R_2) equation 4.3 . This schema of the reactions are presented in the Figure 4-1 as below.

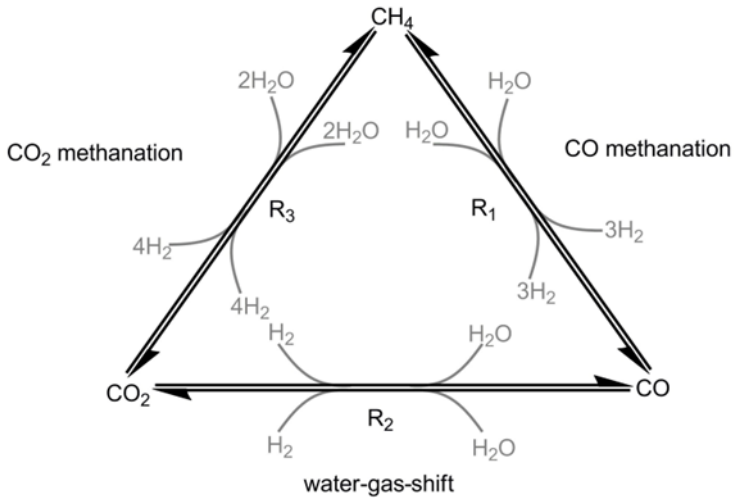

Figure 4-1:Reaction Schema according to Xu and Froment [127]

R3 $$CO_2 + 4H_2 \rightarrow CH_4 + 2H_2O \quad (4.1)$$

R1 $$CO + 3H_2 \rightarrow CH_4 + H_2O \quad (4.2)$$

R2 $$CO_2 + H_2 \rightarrow CO + H_2O \quad (4.3)$$

Concerning the methanation of CO_2, total pressures up to 10 bar and temperatures between 300 and 400 °C is in a technically relevant range. Excellent fits were obtained with the model covering also high hydrogen conversions at the investigated feed compositions with H_2/CO_2 = 1.0 and 0.5. All parameters are estimated significantly showing a small confidence interval and obey Arrhenius equation or van't Hoff's law, respectively. Both pre-factors and enthalpies are rated as thermodynamically consistent by the authors, though the adsorption enthalpy of water is estimated as positive [134].

The following equations are expressed in the sense of methanation of CO_2 and gives the rate of reactions of CO_2, CO and reverse water gas shift.

For equation R3 $$r_{CO_2} = -\frac{k_{CO2}}{P_{H2}^{3.5}}\left(P_{CH_4}P_{H_2O}^2 - \frac{P_{H2}^4 P_{co2}}{K_{eq,\,co_2}}\right)/(DEN)^2 \qquad \text{mol.}\, g^{-1}.h^{-1} \quad (4.4)$$

For equation R_2

$$r_{RWSG} = -\frac{\mathrm{k_{RWSG}}}{\mathrm{P_{H_2}}}(\mathrm{P_{co}P_{H_2O}} - \frac{\mathrm{P_{H2}P_{co2}}}{\mathrm{K_{eq,\,RWSG}}})/(\mathrm{DEN})^2 \quad \mathrm{mol}.\,g^{-1}.h^{-1} \tag{4.5}$$

For equation R_1

$$r_{co} = -\frac{\mathrm{k_{co}}}{p_{H2}^{2.5}}(\mathrm{P_{CH_4}}P_{H2O} - \frac{\mathrm{P_{H2}^3P_{co}}}{\mathrm{K_{eq,\,co}}})/(\mathrm{DEN})^2 \quad \mathrm{mol}.\,g^{-1}.h^{-1} \tag{4.6}$$

$$DEN = 1 + K_{co}P_{co} + K_{H_2}p_{H_2} + K_{CH_4}P_{CH_4} + K_{H_20}\,P_{H_2O}/p_{H_2} \tag{4.7}$$

Where,

$r_{CO_2}\ r_{RWSG}\ r_{co}$ = rates of reactions R_3, R_2 and R_1

$P_{H2}\ \mathrm{P_{CH_4}}\ \mathrm{P_{H_2O}}\ \mathrm{P_{co}}\ \mathrm{P_{co2}}$ = Partial pressure of H_2, CH_4, H_2O CO and CO_2

$\mathrm{k_{CO2}}\ \mathrm{k_{RWSG}}\ \mathrm{k_{co}}$ = rate coefficients of reactions R_3, R_2 and R_1

$\mathrm{K_{eq,\,RWSG}}$ = equilibrium constant of reaction R_2

$\mathrm{K_{eq,\,co}}$ = equilibrium constant of reaction R_1

$\mathrm{K_{eq,\,co_2}}$ = equilibrium constant of reaction R_3

$K_{co}\ K_{H_2}\ K_{H_20}\ K_{CH_4}$ = adsorption constants for CO, H_2, H_2O and CH_4

Xu and Froment model was used in several cases with several authors such as oliveira et al.(2011)[123] for the methane reforming study and in the context of methanation of CO_2 with Ducamp et al.(2016) [135] and with Zhang et al.(2013) [128]. Zhang et al particularly proposed a reduction of denominator pressure from two bar to one bar to correspond with the experimental results. Table 4-1 summarizes the kinetic parameters identified with different authors. In the comparison of the parameters identified, it is visible that the activation energy is close in all the cases, which indicate a coherency in the model proposed with Xu and Froment. However, the constants of kinetics are different because it depends on the type and quantity of catalyst used.

The numerically identified adsorption constants that is defined with the Arrhenius law is given as below where R is the gas constant and T is the temperature

$$K_{co} = 8.23 * 10^{-5} * \exp(\frac{70.65 * 10^3}{RT}) \tag{4.8}$$

$$K_{H2} = 6.12 * 10^{-9} * \exp(\frac{82.9 * 10^3}{RT}) \tag{4.9}$$

$$K_{CH4} = 6.65 * 10^{-4} * \exp(\frac{38.28 * 10^3}{RT}) \quad (4.10)$$

$$K_{H2O} = 1.77 * 10^5 * \exp(\frac{-88.68 * 10^3}{RT}) \quad (4.11)$$

Table 4-1: Kinetic parameters of Xu and Froment rate of reaction model identified with different publications

Parameters	Xu and Froment	E.L.G. Oliveira et al. (2010)	E.L.G. Oliveira et al. (2011)	M.V Navarro et al.	S.Z Abbas et al.	J.Zhang et al.
$K_{CO2,0}$ (mol.bar$^{0.5}$.kg^{-1}.s^{-1})	2.83*10^{14}	4.67*10^{13}	1.29*10^{13}	-	1.32*10^{10}	-
$K_{RWGS,0}$ (mol.bar^{-1}.kg^{-1}.s^{-1})	5.43*10^{5}	2.51*10^{14}	9.33*10^{5}	-	9.9*10^{3}	7.83*10^{6}
$K_{CO2,0}$ (mol.bar$^{0.5}$.kg^{-1}.s^{-1})	1.17*10^{15}	5.83*10^{11}	5.79*10^{12}	-	5.19*10^{9}	1.59*10^{17}
EA_{CO2} (KJ/mol)	243.9	236.85	215.84	248.2	236.7	-
EA_{RWGS} (KJ/mol)	67.13	73.52	68.2	61.3	89.23	62
EA_{CO} (KJ/mol)	240.1	218.55	217.02	252.2	257.01	248
Type of Catalyst	Ni/Mg Al_2O_4	Ni/AL_2O_3	Ni/AL_2O_3	Ni	NiO/AL_2O_3	Ni
Note: EA = Activation Energy						

4.2.2 Batch reactor simulation results

A batch reactor modeling has been carried out in Matlab to plot the rate of reaction, molar fraction of the components and normalized advancement of the reaction versus time. The obtained results are presented through Figures 4-2, 4-3 and 4-4. The objective was to test the kinetic model proposed with Xu and Froment (1989) [127] in the batch reactor model and validate the parameters found with Xu and Froment. In this parametric study, only one of the three-rate reactions that is methanation of CO_2 from Xu and Froment model has been considered. The operating conditions, explanation of the simulation model and the assumptions are given in the Table 4-2. Molar fractions of the consumed components and the products are in the good agreement and follow the same trend with the results obtained in the literature [136] hence this validated the parametric simulation carried out in this study.

Table 4-2: Presentation of the batch reactor model and operating conditions of the simulation

Presentation of the Batch reactor modeling	
Type of the gas law	Ideal gas law
Kinetic model	Xu and Froment with CO_2 Methanation
Type of reactor	Batch reactor with T and P constant

Numerical tools	Ode15 (Matlab Function)
Operating conditions of the simulation	
Temperature	450 °C = 723K
Pressure	1 atm = 1 bar
Stoichiometric Ration	CO_2 : H_2 = 1:4
Inlet Feed	
$x_0(H_2)$	0.8
$x_0(CO_2)$	0.2
Time	1000s

The total volume of the reactive mixture (V) is dependent on:

- The total pressure (P) and Temperature(T) applied to the system of reactive mixtures
- The total number of mole of the reactive mixture components

Since in a system of chemical mixture, the total number of moles of the mixture influences the volume of the reactive mixtures hence this volume variation has been taken into account. The equation of state for ideal gas in case of gas phase reaction is re-writen taking the advancement of reaction into account.

$$P.V = (n_0 + n_0.\vartheta.\varepsilon) * RT \quad (4.12)$$

Where ϑ is stoichiometric coefficient and ε is reaction advancement. The total quantithy of moles is given with the euqtion 4.13.

$$n_j = n_{j0} + \vartheta.n_0.\varepsilon \quad (4.13)$$

The advancement of the reaction is given in the relation below

$$\varepsilon = \frac{n_j - n_{j0}}{\vartheta.n_0} \quad (4.14)$$

The reaction considered for the simulation model is $CO_2 + 4H_2 \rightarrow CH_4 + 2H_2O$ (R_3) and volume change with advancment of the reaction for this reaction for each components are given as below :

Volume variation with respect to time $\frac{V(t)}{V_0} = \beta(1 + \alpha.\varepsilon)$, $V = \beta\, V_0(1 + \alpha.\varepsilon)$

Where $\beta = \frac{P_0.T}{T_0.P}$ physical dilatation factor and $\alpha = \sum_{i=1}^{\vartheta} \vartheta i \quad \alpha = -2$ and $\beta = 1$

The species-independent rate of reaction gives the variation of the advancement with time

$$r = \frac{1}{V}\frac{d\varepsilon}{dt} \tag{4.15}$$

Where r is the rate of reaction and V is the volume of mixture.

Advancement of the (R_3) with respect of volume change is given as below for the all components of the reaction

$$R_3 . V = \frac{d_{nCO2}}{dt} = \frac{d(n_{CO2} - n_0.\varepsilon)}{dt} = -n_0.\frac{d\varepsilon}{dt} \tag{4.16}$$

$$R_3.\beta\, V_0(1 + \alpha.\varepsilon) = n_0.\frac{d\varepsilon}{dt} \tag{4.16}$$

$$4.R_3 . V = \frac{d_{nH2O}}{dt} = \frac{d(n_{H2O} - 4n_0.\varepsilon)}{dt} \tag{4.17}$$

$$4.R_3.\beta . V_0(1 + \alpha.\varepsilon) = -4.n_0.\frac{d\varepsilon}{dt} \tag{4.18}$$

$$-R_3 . V = \frac{d_{nCH4}}{dt} = \frac{d(n_{CH4} + n_0.\varepsilon)}{dt} \tag{4.19}$$

$$-R_3.\beta.V_0(1 + \alpha.\varepsilon) = n_0.\frac{d\varepsilon}{dt} \tag{4.20}$$

$$-2.R_3 . V = \frac{d_{nH2O}}{dt} = \frac{d(n_{H2O} + 2.n_0.\varepsilon)}{dt} \tag{4.21}$$

$$-2.R_3.\beta.V_0(1 + \alpha.\varepsilon) = 2.n_0.\frac{d\varepsilon}{dt} \tag{4.22}$$

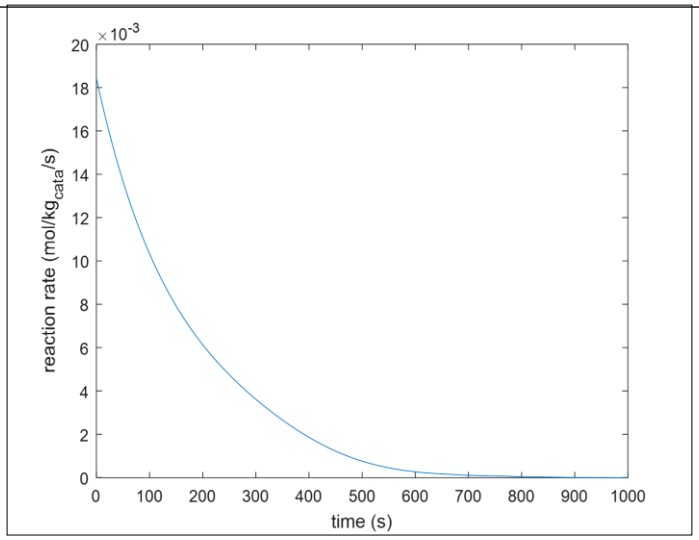

Figure 4-2: reaction rate versus time (s)

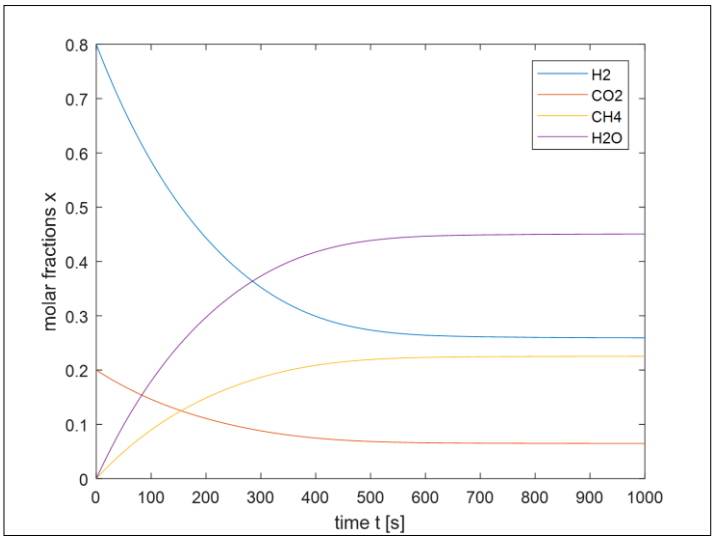

Figure 4-3 : Mole fraction versus time t (s)

4.3 Modelling and simulation of catalytic methanation reactor

A complete simulation and numeric modelling of methanation processes are rare in the literature. The only reference available so far in the literature is the one proposed by [137]. The authors although focused on the simulation of methanation of CO. The catalytic methanation hence fed with a mixture of ($CO+H_2$). The modeling and design of the reactor in the other hand, is diverse and many different works has been proposed with the literature [125], [136], [138], [139]. Moreover, many of them concentrated on CO methanation, the latter playing an important role in the reactions involved in the process of methanation.

The tool used in the present study to do the modelling and simulation of methanation is ProsimPlus. This software performs steady state material and energy balances of a large number of industrial processes such as petrochemicals, gas, pharmaceuticals etc. The used physical properties of the following components are already provided in the ProsimPlus: Hydrogen (H_2), carbon dioxide (CO_2), methane (CH_4), water (H_2O) and carbon monoxide (CO).

4.3.1 Gibbs reactor: thermodynamic analysis of methanation

To be able to represent the theoretical limits of the reaction and therefore to know the maximum performance of reactor being simulated, thermodynamic analysis of methanation is carried out at equilibrium. The equilibrium is determined using Gibb's free energy minimization method. This method calculates the final compositions at the outlet of reactor with respect to the mass balance while minimizing the Gibb's free energy of the system. The flow chart of the reactor is given by Figure 4-4. It is composed of feed gases, connected to the reactor with line 1, at the outlet of reactor the product gases are represented. The objective of this simulation is to validate the performance of a Gibb's reactor; this schematic presented here helps to obtain the required results in this study. The proposed thermodynamic model is Redlich-Kwong-Soave predictive equation of state (PSRK). This model is conventionally used to represent molecules in a non-polar gaseous state. The thermodynamic model chosen to represent the non-ideal behavior at equilibrium state. In the current presented thermodynamic model, the below parameters are considered as inputs:

- Temperature of the reactor or inlet feed gases
- Pressure of the reactor or inlet feed gases
- Inlet feed gases flow rate
- The constituents (molecules) involved in the reactions and their physical state.

It is important to note that there is no Kinetic model has included in the thermodynamic analysis and hence no need to include the chemical reactions but only the constituents take part in the analysis.

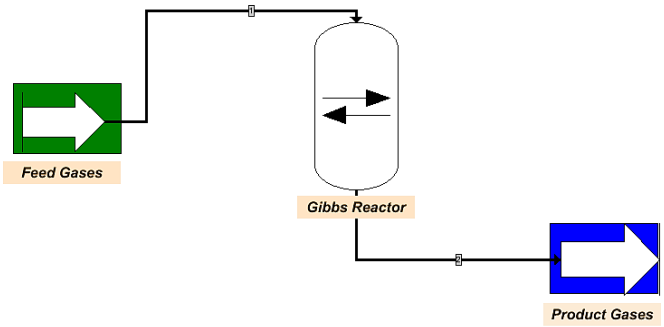

Figure 4-4: Schematic of the Gibbs reactor for thermodynamic analysis

4.3.2 Plug flow reactor: kinetic study of methanation

Among the various reactor module options, the one that improves the simulation of the process by making it more real is the Tubular Reactor. Indeed, this module allows to introduce additional information such as the kinetic model of the reaction, the dimensions of the reactor and catalytic bed and thermal parameters such as the overall coefficient of thermal exchange (U), among others. The variation of variables are only evaluated in one dimension (1-D dimensional). The reactor model is the core of a process and it requires that should be accurately configured. Kinetic model is the most sensitive parameter in the process since they couple both energy and mass balances and can be arranged in equations that can be slightly complex. In addition, the Kinect models depends on the properties of catalyst and the experimental conditions under which they were obtained.

Concerning the kinetics of reaction for the methanation of CO_2 over a nickel catalyst, they could behave a different level of complexity. For the current simulation, we have used the kinetics developed with Xu and Froment [127] given in the section 4.2.1. The reaction rates of Xu and Froment kinetic model is rewritten by a dynamic link library (dll) by coding it with FORTRAN and is connected to ProsimPlus through used-defined kinetic model. In order to validate the present simulation model, a comparison is made with a modeling and simulation work carried out by Abdulrazzaq S. Abdullah et al (2015) [139] where the same Xu and Froment kinetic of reactions has been used in their work. Subsequently a comparison is made between an experimental investigation on CO_2 Methanation process by Beatrice Castellani (2017) [61] with the present simulation model.

4.4 Results and discussion

4.4.1 Thermodynamic analysis

Simulation of thermodynamics of methanation reaction in a steady state helps to know the maximum quantity of products from reactants with different pressure, temperature and stoichiometric ratio. Gao et al [140] carried out a thermodynamic study of the methanation reaction, as well as secondary reactions, which can take place in a “real” reactor. These reactions are listed in Table 4-3.

We have carried out the simulation of the methanation reactions in the steady state at thermodynamic equilibrium. For this purpose, we used the Gibbs energy minimization method, implemented in the Gibbs reactor of the ProSimPlus simulation software. In order to validate the results obtained in this model, we have compared with Gao et coll [140] work and found an excellent agreement. The operating conditions used at the inlet of the Gibbs reactor are presented in Table 4-4.

Thanks to this simulation, we were able to validate our results and identify the most favorable operating conditions for the methanation reaction.

Table 4-3: Reactions involved in the simulation of thermodynamic analysis

CO_2 Methanation	$CO_2 + 4H_2 = CH_4 + 2H_2O$
Methane cracking	$CH_4 = 2H_2 + C$
Carbone dioxide reduction	$CO_2 + 2H_2 = C + 2H_2O$
CO Methanation	$CO + 3H_2 = CH_4 + H_2O$
Inverse CH_4 CO_2 Reforming	$2CO + 2H_2 = CH_4 + CO_2$
Boudouard reaction	$2CO = C + CO_2$
Water-gas shift	$CO + H_2O = CO_2 + H_2$
Carbone monoxide reduction	$CO + H_2 = C + H_2O$

Table 4-4: Operating conditions for the simulation of Gibbs reactor for the thermodynamic analysis

Operating Conditions at the inlet of the Gibbs reactor	
Temperature	250°C
Pressure	1 atm
Molar Flow rate	50 kmol/h
Stoichiometric Ratio	CO_2 /H_2 = 1:4
Compounds	CH_4, H_2O, CO, CO_2, H_2, C

From the simulations carried out and estimated rate of CO_2 conversion and CH_4 yield, we can conclude that, when the pressure is high, a better CO_2 conversion and higher CH_4 yield could be achieved. The influence of operating temperature is inversely proportional, with higher temperature the rate of conversion of CO_2 decreases. In addition, the formation of CO and CO_2 at the outlet of the reactor would increase. High temperatures favors carbon monoxide over methane, which is formed by the endothermic reverse water gas-shift reaction. In conclusion, the optimal operating conditions regarding the thermodynamic analysis are high pressure and low temperature. The conversion rate of carbon dioxide x_{CO_2} is calculated from the equation 4.23 given below where F is the fraction.

$$x_{CO_2} = \frac{F_{CO_2,in} - F_{CO_2,out}}{F_{CO_2,in}} \times 100 \quad (4.23)$$

It is evident that there is an excellent agreement between the results obtained from the simulations carried out in the current study and the literature [140]. Percentage mole fraction is drawn against a range of operating temperature (200-800°C) as given in Figure 4-5. With increase in

temperature, the mole fractions of products such as water and methane has reduced but in contrast, carbon monoxide, hydrogen and carbon dioxide have increased. The current simulation is carried out for 1 atm pressure and a stoichiometric ratio of 4:1 for H_2/CO_2. Figure 4-6 illustrates the conversion rate of carbon dioxide against different temperature. This result found to be in a good agreement with the work performed by Gao et coll [140]. The conversion rate of carbon dioxide decreases when temperature increases. The influence of pressure is low on conversion rate of carbon dioxide for lower temperature range. Higher pressure presented high conversion rate than lower pressures.

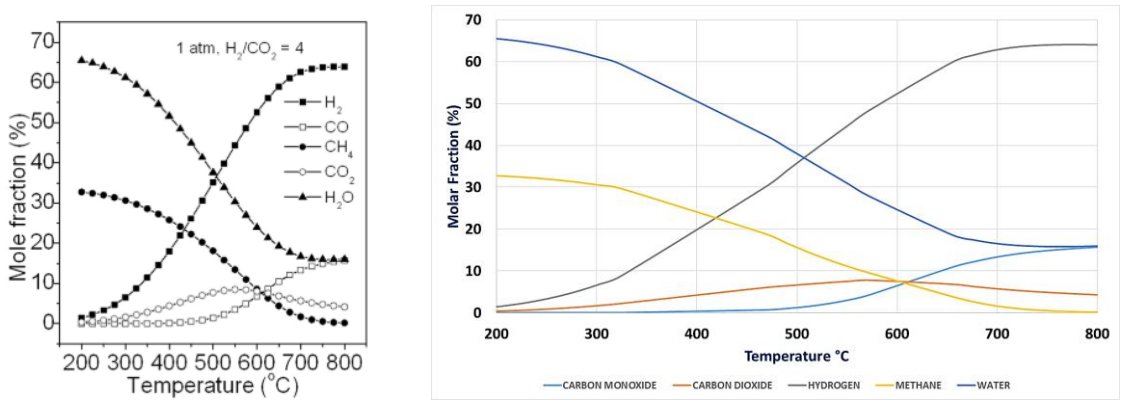

(A) : Gao et coll [140] **(B)** : Simulation in this work

Figure 4-5: Product fraction of CO_2 methanation- **(A)**: Gao et coll [140] and **(B)** :Present simulation results

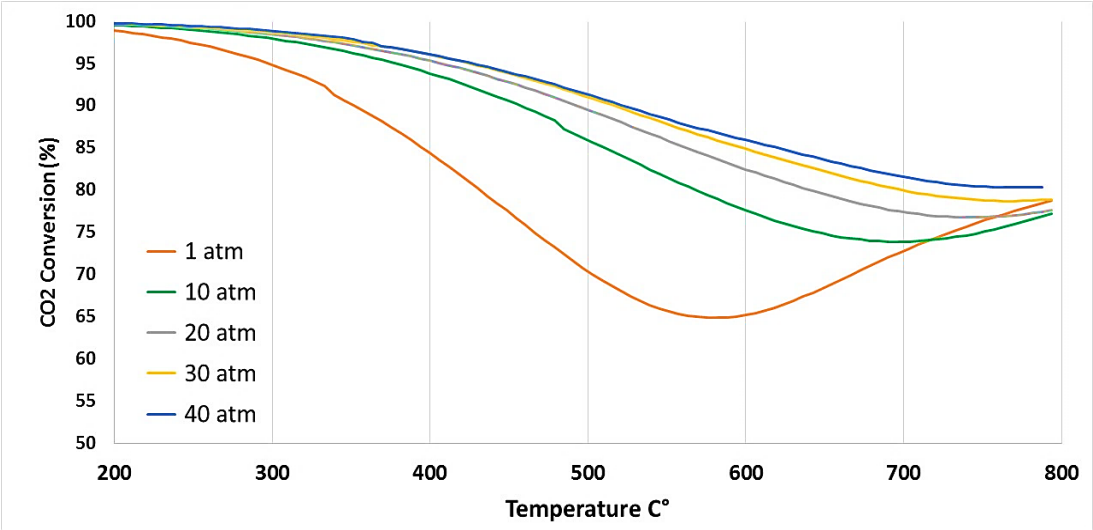

Figure 4-6: CO_2 Conversion with Different pressures versus Temperature-Present Simulation Results

4.4.2 Plug Flow reactor:

A plug flow reactor was modeled with ProsimPlus to validate the simulation work with literature. Xu & Froment kinetics model was taken into account in the simulation. To compare with

Abdulrazzaq S. Abdullah et al. work, two assumptions brought in the present simulation which are: the internal diameter of the reactor tube and density of the catalyst, because these data were missing in the reference. The input parameters and assumptions used in the current simulation model is given in Table 4-5.

Table 4-5: Input parameters and assumptions used in the plug flow reactor simulation model

Parameters	Values
Temperature (K)	580
Pressure(bar)	25.9
Length of the Reactor (L)	4
Density of the Nickel Catalyst (kg/m^3)	930 (Assumed)

The results obtained in the simulations carried out, are presented in the Table 4-6. To run the simulations in the ProsimPlus software, the reaction rates of Xu and Froment kinetic model is rewritten by a dynamic link library (dll) by coding it with FORTRAN and is connected to ProsimPlus through used-defined kinetic model as an external source. Moreover, the same parameters given in Table 4-5 are inserted in the software with the two assumptions made as described above. Since it was a continuous steady state simulation, in order to compare the results, input flow rate (Kmol/h) given as in the Table 4-6 are inserted into software for the simulation.

Table 4-6: comparison of present simulation results to literature data

Input flow rate (Kmol/h)		Output flow rate (Kmol/h)		
Component	Experimental [139]	Experimental [139]	Theoretical [139]	Present work (simulation results)
CH_4	16.7977	42.586	41.8534	43.49
H_2O	89.0564	110	119.172	120.47
H_2	3786.8	3704.32	3706.57	3701.64
CO	20.68	0	0	0
CO_2	5.06	0	5.74E-06	3.4E-04
N_2	1234.49	1236.49	1236.49	1236.47
Ar	14.71	14.71	14.71	14.71

The simulated model results are in an excellent agreement with the Abdulrazzaq S.Abdullah et al. work and the actual data used and compared in his work. Nevertheless, the internal diameter of the reactor tube used in the present simulation and its total number remains debatable for instance.

From the results obtained in the simulation, flow rates of CH_4 and H_2O increases and those of CO, H_2 and CO_2 decreases which proves that methane gas and water is being produced CO, H_2 and CO_2 are being consumed in the process.

A second simulation of plug flow reactor with ProsimPlus was carried out to compare the simulation results with experimental results from Beatrice Castellani (2017) [61]. In this simulation, reactor dimensions, catalyst specification, operating conditions and the concentration of the reactor input components adopted from [61] however, this reference literature does not include the kinetic model and corresponding parameters used in the model. Subsequently the same Xu & Froment kinetic model was taken in the current simulation model. Table 4-7 presents the data obtained from Beatrice Castellani (2017) [61]. The same data presented in the Table 4-7 was taken as input parameters and used in our simulation model to eventually compare the experimental results with simulation results,

Table 4-7: Input parameters and assumption considered in the simulation model

Parameters	Values
Length of the Reactor (mm)	300
Internal Diameter of the reactor(mm)	25.4
(GHSV(h^{-1})	414.4
Volume of the reactor V (m^3)	1.52×10^{-4}
Density of the Nickel Catalyst (kg/m^3)	930 (Assumed)

where GHSV is gas hourly space velocity and is given by the formula.

$$GHSV = \frac{Flow\ Rate}{Reactor\ Volume} \quad Flow\ Rate = 414.4 \times 1.52 \times 10^{-4} = 0.06\ {}^{m^3}/_{h} \qquad (1)$$

Again, the Xu and Froment kinetics model is used in the simulation. The Simulation is run in the continuous mode with CO_2: H_2 stoichiometric ratio (1:4) with several temperatures and pressures. The results presented in the experimental work carried out by Castellani [61] is questionable due to high range of temperatures and poor rate of CO_2 conversion. For a small range of temperature, a very high difference in the final % v/v of CH_4 and conversion efficiency (%). The present simulation carried out includes the assumed density of nickel catalyst at 930 (kg/m^3) an uncertainty that may encounter some disagreements in the comparison of experimental results with simulation results. Nevertheless, the sensitivity analysis carried out on the value of nickel catalyst density, did not highly impact the results obtained. Comparison of simulation results to experimental results is illustrated in the Table 4-8. From the results presented in the Table 4-8, for two out of four sets of simulations carried out, the results found to be coherent with the experimental one. From the simulations carried out at pressures

8 bar and 2 bar and at the temperatures 422 °C and 317°C, almost the same final % v/v for components as of experimental results were obtained. Nevertheless, simulations carried out at four bar and 490 °C shows higher final % v/v compare to experimental results. 46.79 % v/v compare to 19.47 % v/v for CH_4 in case of experimental results. In this way, a lower case was also noticed when the simulation test was run at 20 bar and 451 °C. This resulted in 79.28 % v/v of CH_4 compare to 97.24 % v/v of CH_4 in case of experimental one. This incoherency present between simulation results and experimental one implies the need of further improvement and enhancement in the entire process of simulation until it is fully validated or brought further modifications.

Table 4-8: Comparison of simulation results with the experimental data

		Experimental results by Castellani [61]			Present work (simulation results)		
Pressure(bar)	Temperature(°C)	Final % v/v			Final % v/v		
		H_2	CH_4	CO_2	H_2	CH_4	CO_2
8	422	24.58	64.75	10.67	24.86	68.91	6.21
20	451	1.74	97.24	1.02	3.2	79.28	17.5
4	490	72.61	19.47	7.92	42.56	46.79	10.64
2	317	15.53	37.80	46.68	9.98	35.54	54.47

4.5 Conclusions and perspectives

In this chapter, the study of kinetics of methanation reaction and its importance in the process of catalytic methanation of CO_2 and H_2 to produce synthetic methane was carried out. To begin with, a broad literature review was performed to highlight the different kinetic models and accordingly a parametric research was carried out for the mostly used Xu & Froment kinetic model. Prior to simulation done for a plug flow reactor by kinetic model, a thermodynamic analysis hence carried out in this chapter without any selected kinetic model. To perform a thermodynamic analysis, the set of reactions involved in the methanation of CO_2 were considered in a Gibb's reactor in ProsimPlus using Gibb's free energy minimization method.

The objective of carrying out a thermodynamic analysis was, to represent the theoretical limits of the reaction and therefore to know the maximum performance of the reactor being simulated. Results obtained through the thermodynamic analysis carried out in this chapter were in an excellent agreement when it was compared with literature data. From the simulations carried out and estimated rate of CO_2 conversion and CH_4 yield, we can conclude that, when the pressure is high, a better CO_2 conversion and higher CH_4 yield could be achieved. The influence of operating temperature is inversely proportional, with higher temperature the rate of conversion of CO_2 decreases. In addition, the

formation of CO and CO_2 at the outlet of the reactor would increase. High temperatures favor carbon monoxide over methane, which is formed by the endothermic reverse water gas-shift reaction. In conclusion, the optimal operating conditions regarding the thermodynamic analysis are high pressure and low temperature.

Thermodynamic analysis does not take into account the kinetics of reaction boundaries hence does not neither fully predict the maximum performance of a continuous steady state methanation reactor nor predict the evolution of consumption and production of inlet and outlet reactants involved in the reaction. Nevertheless, we have performed a steady state continuous plug flow reactor simulation combined with a catalytic methanation kinetic model by ProsimPlus. The results obtained from the simulations carried out in this chapter were in a good agreement with the literature data. We have presented a parametric study for the selected Xu & Froment kinetic model through a batch reactor through Matlab. The parametric study carried out through Matlab assured that the parameters used in the kinetic model were all valid and correct. The simulated ProsimPlus plug flow reactor model was compared with literature in two cases: The comparison is firstly made with a work carried in modeling and simulation of methanation catalytic reactor in ammonia plant. The input parameters and the same kinetic model were addressed from this work and finally the results of current simulated model were in a good agreement with the results obtained in the reference. Similarly, the comparison is secondly made with an experimental investigation on CO_2 methanation process for solar energy storage. Reactor geometry, inlet parameter such as temperature or pressure and volume flow rate were adopted from this work. For a second time, Xu & Froment model was taken into account in this simulation. When the similar test sets were run in the simulation models the results obtained were somehow not coherent. Out of four test sets were carried out, two of them represented the same results as of experimental work and two other were either low or high compare to experimental work.

The greatest challenge in validating these simulation model results is, the missing data in the literature. Each time when a literature study was carried out, we had at least some data missing such as dimensions of the reactor, operating conditions, input feed of the components or data on the kinetic model and its parameters. This lack of sufficient data necessitates customized laboratory scale tests to be performed so that an accurate kinetic model which is essential in the design of exothermal catalytic methanation reactor is validated and proposed.

5 Chapter 5: Power-to-Gas

5.1 Objective of the chapter

An ecologically sustainable energy supply that is economically viable and socially acceptable, is a high priority in European policy [53]. Production of carbon neutral gas and its injection into natural gas grid is a promising step to reduce greenhouse gases (GHG) emissions and lead towards zero carbon transition. The Law on Energy Transition for Green Growth (LTECV) fixes an objective of 10% renewable gas share in the French natural gas consumption for the horizon 2030 [22]. Synthetic methane production via two-step electrolysis of water and consequent methanation of CO_2 is a developed system and considered as an alternative way of producing green gas [2]. Established power-to-gas (PtG) technologies have proven their maturity and their versatility across all sectors.

It is evident that the use of fossil energy faces many challenges: decreasing reserves, emissions of GHG and dependence on importation. Renewable energy can play a vital role in minimizing the concerns associated in fossil energy and some of this renewable energy can be supplied by electricity from the sources such as photovoltaic panels and wind farms. Nevertheless, renewable electricity production faces two major drawbacks: first its intermittency and second its substitution to high energy density fuels, especially in transport and heat sectors [2]. Recent publication of the European Commission on energy production forecasts a large share of renewables in the energy mix 2050 [141], and scenarios developed by the ADEME [142]. The massive production of renewable energies will lead to overproduction periods, where produced renewable electricity would not be totally employed into grid and consequently there is a need to store this surplus electricity. PtG hence is the perfect and sophisticated technology to store the intermittent surplus renewable electricity and converts it into chemical gas energy. The obstacles that power-to-gas faces are no longer technical, but are principally, regulatory and economic [143].

Carbon dioxide sources from industries such as iron and steel require a CO_2 capture and upgrading units, hence reduces energy efficiency and increases the cost significantly, while PtG requires much smaller carbon sources such as biogas plants or even landfill sites [11]. Power-to-gas could utilize the carbon dioxide content of biogas as a novel upgrading system, offsetting significant costs of traditional upgrading with the additional benefits of utilizing the waste heat. HYCAUNAIS project [144] is an optimization of a nominal pilot power-to-gas unit in France launched in April 2019. The project is accompanied with French Environment and Energy Management Agency (ADEME) and one of the objectives of this pilot project, which lasts six years, is to study the adaptation of a biological methanation process into landfill biogas where the carbon dioxide is hydrogenated via methanation process into synthetic methane or synthetic natural gas (SNG).

The optimization of the PtG plant by means of intermediate storage of hydrogen and carbon dioxide shows that the methanation standby times can be reduced and thus the gas production costs are decreased. With the future expected development of CAPEX, OPEX, electricity prices, gas costs and efficiencies, an economic production of SNG for the years 2030, especially for 2050 should be feasible. In 2050, the gap between the market driven business models and economic feasibility is rather narrow [145].

The technical and economical parameters as well as electrolyzer and methanation efficiencies considered for the SNG production costs in this chapter are based on the expectations for 2030. The provision of electricity via a long-term contract is investigated in this study to estimate the production costs of SNG via PtG process. The power-to-gas system studied in this chapter is proposed to be installed into such a landfill site where the site is already equipped with an upgrading unit and supplies CO_2 separated and captured. As the production costs of SNG is reduced with the operation times of electrolyzer and methanation units, a flexible operating strategy case is also investigated. Source of CO_2 for the PtG in this study is considered from a landfill site at no extra cost. The selected landfill site i.e., La Poitevinière is in operation since 1990 and receives waste until 2032. The availability of biogas and percentage content of CO_2 from this landfill is estimated with the help of landfill biogas (LFG) mathematical modelling for the upcoming years presented in Chapter 2. The present study considered CO_2 is captured and supplied into PtG process at the outlet of an upgrading technology present in the site and if necessary, it is compressed to the required level of pressure before injecting into methanation reactor. The associated costs of CO_2 compression and an upgrading unit is not accounted in the model. Subsequently, specific costs of CO_2 supply are taken as zero for the current study despite the fact that it is not easy to define in general, because they strongly depend on the concentration in the source stream. Using landfill biogas as a source of carbon dioxide to produce synthetic natural gas is a novel study, which potentially shows the conversion of CO_2 into a useful commodity and avoids extra costs associated with the biogas upgrading stage.

5.2 METHODOLOGY

5.2.1 Power-to-gas system description

In the current study, power-to-gas (PtG) is stated as the combination of sub-systems such as electrolyzer to produce hydrogen, and methanation to produce synthetic methane, also referred as synthetic natural gas (SNG). In the envisioned system, the produced SNG is injected into the existing natural gas grid infrastructure. In many times, it may happen that methanation cannot follow the hydrogen generation profile of electrolyzer; consequently, the two sub-systems (electrolyzer and methanation) should be decoupled and operated independently if the electricity load profile fluctuates

strongly. Moreover, the maximum hydrogen processing rate of methanation reactor may be lower than the maximum hydrogen generation rate of electrolyzer. The operation of power-to-gas system may require a temporary hydrogen storage system that can help to maintain the load internal and load change rates that keep the gas quality constant during the operation of a power-to-gas plant.

An assumption is made that electrolyzer can function in a flexible load, with alternate switch on and off when required. The selected capacity of electrolyzer can respond to the production of sufficient amount of hydrogen so that the carbon dioxide content of biogas is consumed fully and the methanation unit is run at a continuous manner. For the optimization of sub-system methanation, the maximum demand is set to the maximum output of electrolyzer, and the minimum demand is set to process the produced hydrogen of 8500h of electrolyzer operation with 100% load of methanation over 8500h. Schematic of the proposed power-to-gas plant to produce hydrogen and SNG is given in Figure 5-1.

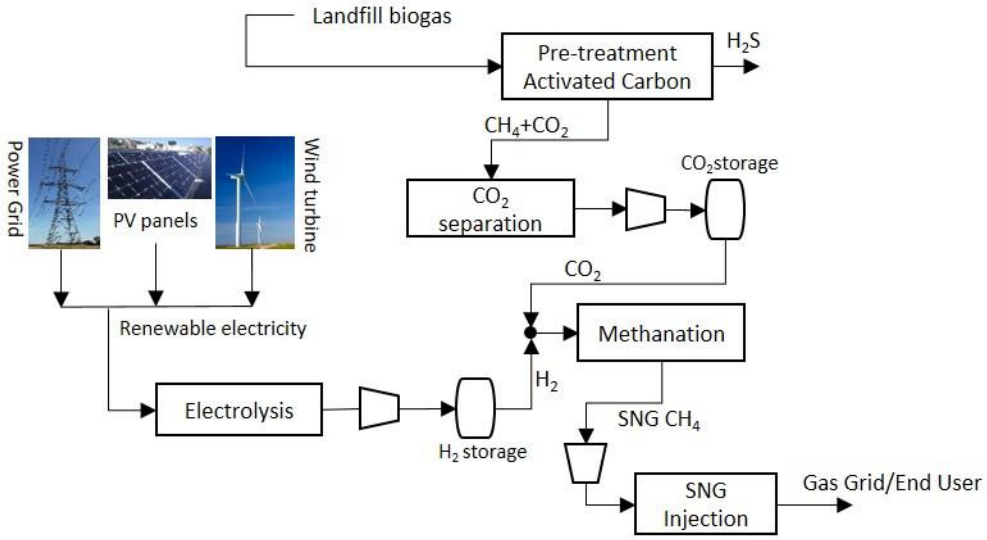

Figure 5-1: Schematic of the proposed PtG plant to produce synthetic methane. The proposed operating strategies are 1- Continuous (without H_2 storage) and 2- Flexible operation (with H_2 storage facility).

The objective of optimization is to reduce the gas production costs and to make sure that methanation can achieve the longest possible continuous operating times, to eventually reduce the number of shutdowns. The methanation load can vary between 40 and 100% depending on the level of hydrogen storage system. In a study carried out by [64], it is found that annual run hours would need to be high to minimize the gas production costs in a power-to-gas system. Thus, the high flexibility of biological methanation (BM) could be somehow canceled with higher efficiency of catalytic methanation (CM) being preferred.

The current study does not clearly distinguish between technologies while instead uses input parameters such as cost, efficiency, energy consumption of the parts. Due to further developments and research in electrolyzer technology, it is estimated that the efficiency of the process will increase from 60% and 64% (5.5-5.8 kW_{AC}/m^3) up to 75% (4.72 kW_{AC}/m^3) until 2030 and up to 78% [146] (4.54 kW_{AC}/m^3) in 2050. For the modeling of the PtG system in this chapter, an alkaline electrolyzer with a power input of 1 MW_{AC} and 30 bar operation pressure is assumed. A 100% degree of conversion for sub-system methanation unit is assumed and efficiency only referred to gaseous input and output. The theoretical efficiency of methanation is 78% based on the heating values of hydrogen and methane [146]. A 75% efficiency for electrolyzer and 78% efficiency for methanation unit are taken in this study for the further calculations to estimate the synthetic methane production costs.

Three power sources that are possible in the modeling of a PtG system are Wind, PV and control. In a study carried out by J.Gorre, et al. [143], the highest full load hour was reported for control compare to Wind and PV. In the interest of this study, a secondary control reserve was taken as a source of power in the PtG system to supply a stable and regular electricity to the electrolyzer unit to produce hydrogen. Hence the source of power is public electricity grid with the utilization of extra power produced by renewable sources. Another input-oriented operation of power-to-gas is in direct coupling with renewable energy sources (RES), and without connections to the public electricity grid [143]. Norway [147], Scotland [148], and Spain [149] tested direct coupling in demonstration projects. One advantage of direct coupling is that there is no need to pay network usage fees, and thus operating costs can be reduced. However, the resulting lower number of operating hours is a disadvantage. Control reserve is used to compensate for mismatches between production and consumption in the electricity grid that lead to deviations in the grid frequency. The aim of control reserve is to keep the frequency within a certain tolerance range (approximately 50 Hz), and to eliminate possible regional deviations of the power balance from its target value. Dynamic producers and consumers are necessary to provide control reserve. The control reserve is divided into primary, secondary, and tertiary control reserve according to dynamic and temporal requirements. Guinot et al. [150] investigated a case where the electrolysis process provided primary reserve to a French transmission system operator (TSO) [143].

5.2.2 Hydrogen storage

The fact that electrolyzer can be operated more dynamically than sub-system methanation reactor; there is a demand for a certain volume of hydrogen storage as a buffer. Smaller methanation reactor requires larger hydrogen storage facility. Suitable methods of storage include metal hybrid, cryogenic compressed liquid hydrogen tanks and compressed gas tanks. The integration of hydrogen storage facility helps to reduce the problems raised from operating a methanation plant intermittently and

eventually the number of shutdowns of methanation reactor will be decreased [64]. Until now, only gaseous storage at different pressure levels been used in large-scale PtG plants. According to internal offers from manufacturers, the prices vary between 375 €/kg (50 bar; 33 €/m^3) and 490 €/kg (200 bar; 44 €/m^3) [143]. In a study carried out with [54] a cost range of 20 - 100 €/kg is mentioned for hydrogen storage with no suggestion of maximum pressure level. A range between 100 - 3000 kg is thought practical for the hydrogen storage [143]. The cost of hydrogen storage has also been reported to be at 100 €/m^3H_2 for the year 2017, 75 €/m^3H_2 for the year 2030 and 50 €/m^3H_2 for the year 2050 [145].

5.2.3 Source of carbon dioxide

The certain source of carbon dioxide is irrelevant in terms of the overall conversion process however biological methanation is much more tolerant of impurities (such as H_2S) compared to catalytic methanation. The carbon dioxide needed for the synthesis of CH_4 can initiate from different sources, like ambient air, industrial point sources or raw biogas. Power-to-gas system could valorize the carbon dioxide content of biogas as a novel upgrading system, offsetting significant costs of traditional upgrading. The source of CO_2 focused in this study is, on the separation of CO_2 from landfill biogas. A carbon dioxide storage system is integrated in the model to assure a constant and sufficient supply of CO_2 into PtG process so that the unnecessary shutdowns of electrolyzer and methanation are avoided. No buffer storage for CO_2 was modeled as it would have introduced a new optimization parameter, and CO_2 was not considered as a focal point of this study. Carbon dioxide storage is less cost-intensive because four times less CO_2 is need as compared to H_2, and there are fewer materials requirements [143].

The present study supposed that CO_2 is separated and captured at the outlet of a biogas upgrading technology as a by-product and fed into PtG system. In addition, if necessary, it is compressed to the required level of pressure before injecting into methanation reactor. The associated costs of CO_2 compression and an upgrading unit is not accounted in the model. Subsequently, specific costs of CO_2 supply are taken as zero for the current study despite the fact that it is not easy to define in general, because they strongly depend on the concentration in the source stream.

5.2.4 Quality of SNG injected into natural gas grid.

A methane content of approximately 95% in the product gases could be achieved because of high selectivity of methanation process. Nevertheless, this still results in an energy content less than that of natural gas due to the lack of higher hydrocarbons [11]. When the quantity of SNG produced via power-to-gas technology is smaller, it can be compressed and injected easily into the transmission grid without any issues but in some instances the addition of propane may be required to meet the gas grid

specifications, particularly when injecting into the distribution network [60]. Yet the hydrogen could be injected directly into the gas gird, transmission or distribution grid but the hydrogen injection would rise many concerns because the gas grid is designed for natural gas.

Hydrogen injection into natural gas grid leads to more permeation and corrosion than injecting methane and hence for some safety reasons the maximum hydrogen content is limited to 10% by volume; depending on the specific country, limits up to 20% have been discussed [151]. The amount of hydrogen injected is also limited by gas quality regulations, as hydrogen has approximately one-third the volumetric energy content as compared to methane (12 vs. 36 MJ/m^3). Therefore, power-to-hydrogen for grid injection requires further work to define and standardize the allowable limits and is not feasible in the short-medium term in many regions [64].

5.3 Economics of power-to-gas system and operation

Auxiliary components such as water supply purification, pumps, and electronics are included for in the balance of plant (BoP). Several additional costs are not clearly included in the model, either because they were supposed to be specific to the certain sites, too uncertain, or already accounted for in (BoP). These excluded costs include for compression cost in the event of grid injection, the cost of CO_2 (site specific) and taxes and fees for gas grid connection [152]. Planning, wages, regulatory issues and breakdowns are not included [64]. The introduction of other costs increases uncertainty without additional accuracy. In order to validate the profitability of the PtG process, techno-economic analysis and feasibility studies of the power-to-gas plant are already done [153]–[155]. One of the validating approaches for the gas production costs is to calculate the present value of the total costs for the construction and operation of a plant over its economic life, divided into equal annual payments. Another approach is to estimate the levelized costs of energy (LCOE) [59] or as levelized cost of storage (LCOS) for energy storage application [156]. In the current study, the approach of LCOE is adopted to estimate the gas production costs (GPC) of SNG see Equation (5-1).

$$\mathbf{GPC} = \frac{\sum_{\mathbf{t=1}}^{\mathbf{n}} \frac{\mathbf{CAPEX_t + OPEX_t + Energy_t + Decommissioning_t}}{\mathbf{(1+r)^t}}}{\sum_{\mathbf{t=1}}^{\mathbf{n}} \frac{\mathbf{SNG_t}}{\mathbf{(1+r)^t}}} \qquad \text{5-1}$$

5.3.1 Capital Expenditure (CAPEX)

Today's capital expenditure (CAPEX) for PtG systems are high, but a decreasing trend due to size and experience is visible [146]. However, it is worth to mention that the development of the PtG technology

is subject to fundamental energy and climate policy decisions. If the PtG systems were manufactured in standardize sizes and series, the CAPEX of the technology is further decreased. In addition, technological developments will lead to better efficiencies. The expected CAPEX of the sub-system electrolyzer, methanation and further units of a PtG plant for the year 2030 is given in Table 5-1. With larger capacities of sub-system electrolyzer and methanation, their specific CAPEX is expected to decrease. The specific CAPEX presented in Table 5-1 are taken into account for the estimation of gas production cost in the this chapter.

Table 5-1: Specific CAPEX of the sub-system electrolyzer, methanation and further units of a PtG plant for the year 2030. Adopted from [146] [145]

	Electrical input of the electrolyzer ($MW_{el\ AC}$)	
	1	**10**
Electrolyzer system (€/kW_{el})	665	470
Methanation system (€/kW_{SNG})	530	375
Hydrogen storage (€/m^3 H_2)	75	75
CO_2 storage (€/m^3)	50	50
Gas grid injection station (k€)	75	75
SNG storage (€/m^3)	50	50
Additional costs for installation (% of CAPEX)	10%	10%
Additional costs for design, planning (k€)	100	140
Replacement costs (k€)	199.5	141

5.3.2 Operation expenditure (OPEX)

The operation expenditure of a power-to-gas plant could be grouped into two categories: fixed and variable OPEX [157]. Fixed OPEX of PtG system is independent of operation hours and they are expressed in €/year. While the variable OPEX of such system are concerned to the plant utilization and can be expressed in (€/kW*h). Fixed OPEX guarantee operational readiness, including personal costs, occupancy costs, and fees for maintenance agreements and insurance for the production facilities. These fixed OPEX can vary depending on the complexity and moving parts of each unit. The fixed OPEX of the methanation system also includes the costs of a catalyst change. Table 5-2 gives an overview of the fixed OPEX.

The variable OPEX depends on the operating state, the price and consumption of electricity, thermal energy, raw materials and auxiliaries. It includes the costs for the balance of plant (BoP), namely electricity for the operation of pumps, compressors, heat for the temperature control,

nitrogen, carbon dioxide and instrument air. Moreover, there is the disposal of continuously produced media such as condensate (wastewater) and, if necessary, the operation of a flare.

Table 5-2: Fixed OPEX in % of CAPEX adopted from [146], project experience from STORE&GO and other PtG projects.

	2030	
	Plant Size/ MW_{el}	
	1	**10**
Electrolyzer system (% of CAPEX)	3	3
Hydrogen storage (% of CAPEX)	1.5	1.5
Methanation system (% of CAPEX)	5	5
CO_2 storage (% of CAPEX)	1.5	1.5
Gas grid injection (% of CAPEX)	1	1
SNG storage (% of CAPEX)	1	1

The function of the two sub-systems electrolysis and methanation depend on application and certain limits. In general, the operation of both systems can be assigned to three states: cold standby (CS), hot standby (HS) and production (OP). The electrical consumption in operation is the same as in hot standby. The OPEX in normal operation are lower than in hot standby because there is no or less need to compensate heat losses. The overview of assumptions of the thermal and electrical energy demands are given in Table 5-3. The variable OPEX for PtG plants in 2030 depending on the electrical and thermal energy demand in each state are as listed in Table 5-4.

Like the electricity costs for electrolysis operation, the costs for water is also given. A water consumption of 200% of the stoichiometric at 0.9 liter/Nm^3 of hydrogen produced at a cost of 0.69 €/m^3 is assumed [158].

Table 5-3: Assumption of the thermal and electrical energy consumptions for a PtG plant in 2030.

	Energy demand/ kWh/(MW_{el}*h)		
	Cold standby	Hot standby	Production
Electrolysis system			
• Thermal	0	20	0
• Electrical	2	20	20*

Methanation			
• Thermal	0	50	0
• Electrical	2	20	25

Note: The energies are defined as kWh per operation hour and per installed MW_{el}.

*The electricity consumption of the electrolyzer is depending on the application, operation concept, conditions of purchase, and is therefore excluded in Table 5-3.

Table 5-4: Variable OPEX in 2030 for the sub-system electrolysis and methanation.

	Variable OPEX €/(MW_{el}*h)		
	Cold standby	Hot standby	Production
Electrolysis system 2030	0.05	1.50	0.50
Methanation system 2030	0.05	3.13	0.63

5.4 RESULTS AND DISCUSSION

The estimated gas production costs (GPC) presented in this section include all the costs over the lifetime of the plant, including CAPEX, yearly fixed and variable OPEX, electricity need of electrolyzer, which strongly depend on the operating mode and full load hours (FLH). Two operating strategies were considered to show the gas production costs (GPC) calculations. Continuous operating strategy and flexible operating strategies.

5.4.1 Continuous Operation

This operating strategy assumes a continuous operation of the plant i.e., sub-systems electrolyzer and methanation unit over a year at 97% availability-stream factor (8500 FLH) with an average electricity price. The synthetic methane gas in this operating strategy is produced and sold into natural gas grid with a constant price over a year through long-term contract. SNG storage costs could be offset since the plant run in continuous operation and there is no need to store SNG before it is injected into natural gas grid. In this strategy, there is no need for hydrogen and methane to store on-site since both sub-systems electrolyzer and methanation unit operate in the continuous mode hence, this strategy offsets the costs associated with the hydrogen storage and SNG storage on-site. In this strategy, it is assumed that the long-term electricity contract has the same purchase price as the yearly average day-ahead market price.

The gas production costs for different electricity prices and for different countries is given in Table 5-5 for the years 2016-2017 [145]. The power prices presented in Table 5-5 are based on a long-term contract that has the same price as the yearly average day-ahead market price. As can be seen

from Table 5-5, the methane production costs vary between 120.21 €/MWh and 161.28 €/MWh, depending on the electricity prices from 22.90 €/MWh to 44.7 €/MWh. To recover these costs, the plant must sell the methane i.e., SNG for at least the production prices.

Table 5-5: Total SNG production costs for different electricity prices [145]

Day-ahead market	Power price (€/MWh)	SNG costs (€/MWh)
Denmark (DK1) 2015	22.90	120.21
Germany 2016	28.98	131.53
Netherlands 2016	32.24	137.59
France 2017	44.7	161.28

The methane production costs in this chapter were estimated with the same power prices and continuous operating strategy for the year 2030 with reduced CAPEX, OPEX and enhanced efficiency; as a result, it is found to be lower than the methane production costs presented in Table 5-5. The assumption made here is, the future predicted power prices for 2030 is taken similar as the power prices given in the Table 5-5 above. These power prices presented in Table below were considered for the estimation of hydrogen production with electrolyzer. Similarly, the methane costs are calculated based on the continuous operation strategy in these cases .Yet they are volatile and subject to vary due to high proportion of fluctuating generation capacities. A comparison is made between the 2016, 2017 cases with 2030 case and is illustrated in Figure 5-2. Taking the France case as an example, where PtG processes are not expected to be feasible before 2030, with an average electricity price about 45 €/MWh, the SNG production costs are estimated at 100 €/MWh. This SNG production costs are higher than the expected revenue from SNG in the year 2030.

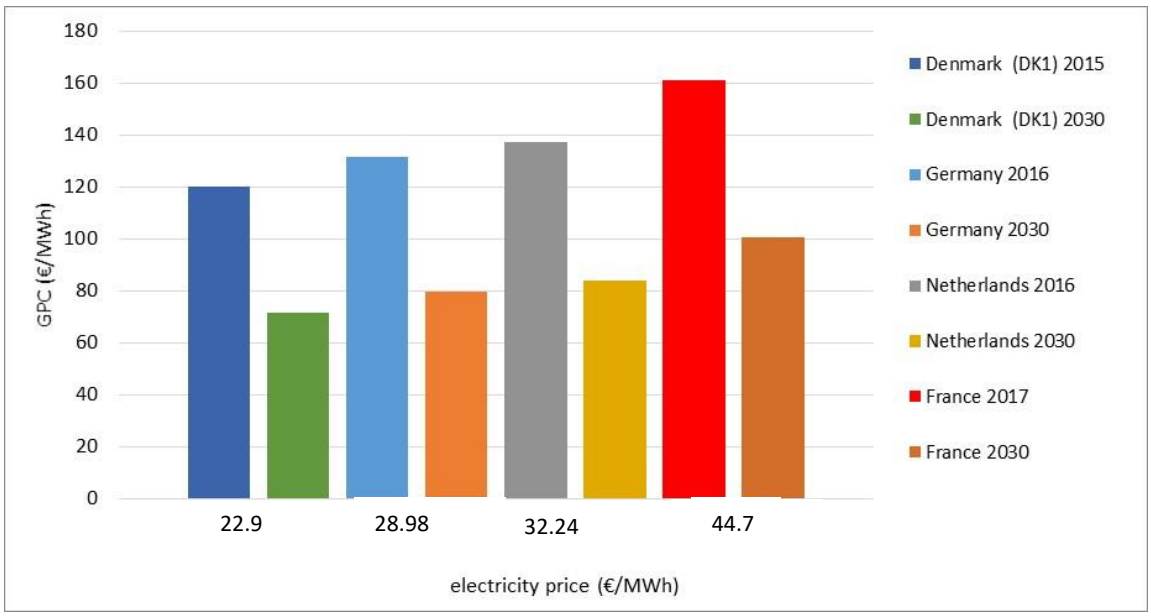

Figure 5-2: Comparison of SNG production costs for different electricity prices and different countries based on the long-term contract and continuous operating strategy.

Figure 5-3 illustrates the calculated methane production costs for different electricity prices for the year 2030. According to Figure 5-3, the methane production costs in 2030 are in the range of 47.5 €/MWh for an electricity price of 5 €/MWh and 100.8 €/MWh for an electricity price of 45 €/MWh. Percentage share of CAPEX, OPEX and electricity price are also illustrated with the same Figure 5-3. The higher the power price, the higher the percentage share of it and therefore the gas production (GPC) is higher too.

The maximum revenue from SNG in 2030 was indicated to be about 75 €/MWh [159], which is enough to cover the total costs of continuously operating a PtG methanation plant [146]. While, with higher electricity prices, an operation of a PtG to produce SNG is not profitable since the total costs exceed the revenue expected from selling SNG. Figure 5-3 illustrates that, for power price lower than 25 €/MWh, the GPC is 74.2 €/MWh. This indicates that a continuously running PtG system at electricity price equal to or lower than 25 €/MWh with an electrical input capacity of electrolyzer at 10 MW_{el} would be profitable since the total costs does not exceed the revenue expected from selling SNG.

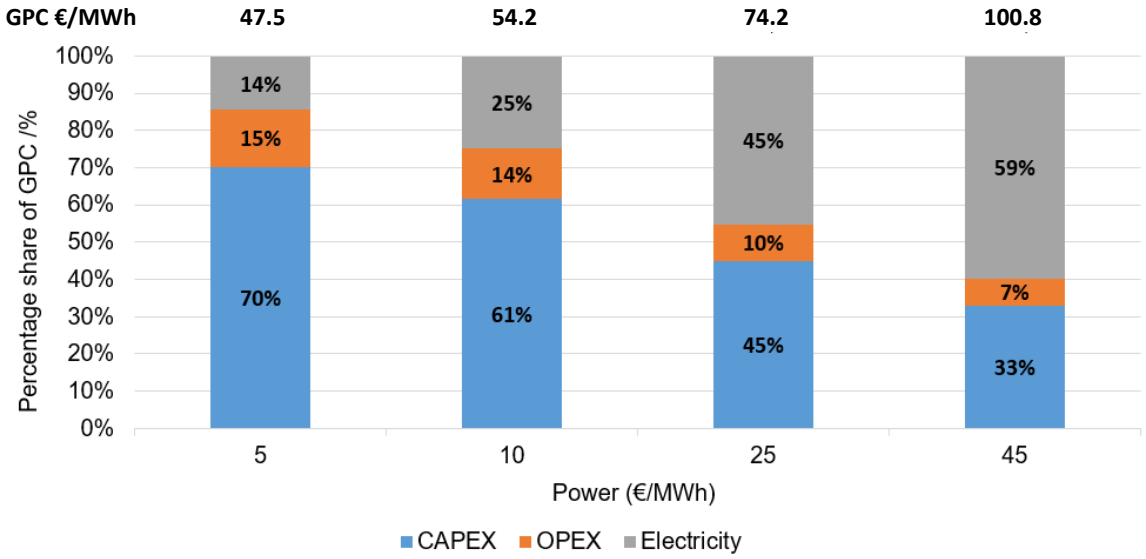

Figure 5-3: Percentage share of CAPEX, OPEX price and electricity of the gas production price (GPC) of a 10 MWel PtG plant with perspective cost parameters for 2030 and different power prices from 5 to 45 €/MWh

Results obtained from figures 5-2 and 5-3 clearly show that the 2030 scenario presented lower gas production costs compared to today's scenario or compared to 2016-2017 scenarios as given in Table 5-5 above. The reduction in GPC is certainly due to lower CAPEX and OPEX of sub-systems electrolyzer and methanation unit as well as due to higher efficiencies of electrolyzer for the year 2030. As mentioned previously above that, power-to-gas scenarios will not be feasible in France in next 10 years, this also justifies that the reason why the 2030 scenario has been selected for the current study.

Given the fact that the reference landfill case in this study produces around 180 Nm^3/h of biogas for the upcoming years and that, the produced gas contains 35-vol% carbon dioxide, the valorization of CO_2 content of such biogas through the power-to-gas system would eventually enhance the methane production potential of landfill site. GPC henceforth recalculated for a smaller size of power-to-gas system that is equivalence to consume the carbon dioxide available from the raw landfill biogas. Fixing the methanation unit capacity at 0.585 MW_{SNG} for one MW_{el} electrolyzer capacity, the methanation unit can produce up to 53 Nm^3/h of SNG. Hydrogen up to 212 Nm^3/h i.e., 4 times inlet CO_2 should be fed into methanation unit to have a full load continuous operation of sub-system methanation unit. This way, one MW_{el} electrolyzer capacity can produce up to 210 Nm^3/h at 75% efficiency and 3.54 KWh/Nm^3 hydrogen production. One MW_{el} electrolyzer and 0.585 MW_{SNG} methanation unit can process up to 90% of the carbon dioxide available in the La Poitevinière landfill site. Specific CAPEX, fixed and variable OPEX for one MW_{el} electrolyzer capacity for the year 2030 is presented in the Tables 5-1, 5-2 and 5-4 above. These data are used to estimate the gas production costs and is presented in Table 5-6 in view of different electricity prices.

GPC is estimated to be about 81 €/MWh for an electricity price of 25 €/MWh for 1 MW_{el} electrical input of electrolyzer. This GPC though is higher than the GPC estimated for 10 MW_{el} electrical input of electrolyzer for the same electricity price at 25 €/MWh which is because the specific CAPEX of the sub-systems electrolyzer and methanation unit decreases by higher input electrical capacity of electrolyzer and methanation unit. The operation of such plant would be profitable at the electricity purchase price equal to or lower than 20 €/MWh because at this electricity price and size of PtG plant, the total costs does not exceed the revenue expected from selling SNG i.e., 75 €/MWh.

Table 5-6: Methane production costs (€/MWh $_{SNG}$) for 1 MW_{el} electrical input of electrolyzer at different electricity prices

	Electricity Prices						
	5 €/MWh	10 €/MWh	15 €/MWh	20 €/MWh	25 €/MWh	35 €/MWh	45 €/MWh
SNG MWh/year	4972.5	4972.5	4972.5	4972.5	4972.5	4972.5	4972.5
GPC (€/MWh)	**47.0**	**55.6**	**64.1**	**72.7**	**81.2**	**98.3**	**115.4**
	Percentage share of GPC (%)						
CAPEX	66	56	48	43	38	31	27
OPEX	16	13	11	10	9	7	6
Electricity	18	31	40	47	53	61	67
Water	0.07	0.06	0.05	0.04	0.03	0.03	0.02

As can be seen from the Table 5-6, the percentage share GPC (%) of electricity purchase price goes up to 67% at only 45 €/MWh and hence increases the GPC correspondingly. Gas production costs presented in Table 5-6 is the result of continuous operation of both sub-systems electrolyzer and methanation unit taking into account.

5.4.2 Flexible Operation

The SNG production costs strongly differ on the electricity purchase price which is seen in the continuous operation section 5.4.1 Table 5-6 and also the operating time of the electrolyzer and methanation units. In the calculations for flexible operation, the operating hours of electrolyzer are supposed to be regularly distributed over the entire year. This could be correlated either with the higher willingness to pay for electricity price or the low electricity price periods. In the case where no electricity is available, the operation of electrolyzer is maintained in hot standby mode where in this case no gas is expected to be produced.

Table 5-7 is presented below to show the SNG production costs when operating PtG plant based on flexible operation. For each electricity price between 5 and 45 €/MWh, five different dwell

times in production mode of electrolyzer and methanation unit are estimated on a basis of 1 MW_{el} PtG plant. The results obtained from this estimation show that the full load hours (FLH) have a robust effect on the economic viability of SNG production via a PtG plant and eventual reduction in the gas production costs. The higher the operating hours, the larger the SNG product volume and the fixed costs are distributed and hence the gas production costs are reduced. This way with higher operating hours, the gas production costs are lower compare to gas costs estimated at lower operating hours see Table 5-7.

Table 5-7: Methane production costs for flexible operating strategy based on a PtG plant size of 1 MW_{el}.

	SNG Production costs (€/MWh $_{SNG}$)					
	Electricity prices					
FLH	**5 €/MWh**	**10 €/MWh**	**15 €/MWh**	**25 €/MWh**	**35 €/MWh**	**45 €/MWh**
1000	334.1	342.6	351.2	368.3	385.4	402.5
2000	171.4	180.0	188.5	205.6	222.7	239.8
3000	117.2	125.8	134.3	151.4	168.5	185.6
4000	90.1	98.7	107.2	124.3	141.4	158.5
6000	63.0	71.5	80.1	97.2	114.3	131.4
8500	47.0	55.6	64.1	81.2	98.3	115.4

It can be seen from Table 5-7 that, the gas production costs are very strongly connected with both full load hours and electricity prices which are two main influencing parameters in a power-to-gas system. For the same electricity price, the gas production costs vary between 240 €/MWh and 115 €/MWh at 2000 and 8500 FLH. This illustrates that intermittency in the operation of power-to-gas processes potentially increases the overall gas production costs. The other way around, gas production costs fluctuate between 47 €/MWh and 115 €/MWh for the same FLH at 8500 between electricity prices at 5 €/MWh and 45 €/MWh. In some of the cases, installation of hydrogen storage facility as an intermediate step could help to store hydrogen and feed in a continuous manner into methanation reactor. Nevertheless, it is worth to mention that the costs associated with the integration of intermediate hydrogen storage would be accounted in the PtG plant and in the gas production costs as well.

Integration of a hydrogen storage system could separate the electrolyzer from methanation unit which is eventually to compensate for the different rates of load changes of both sub-systems. The number of FLH of electrolyzer could be regulated to the fact that it corresponds to the low electricity price periods. Integration of an intermediate hydrogen storage facility into power-to-gas system provides a continuous supply of hydrogen and results for the continuous production of synthetic

methane with sub-system methanation unit respectively. A bigger capacity electrolyzer could be selected with H_2 production capacities higher than the necessary amount in methanation unit. Methanation is feed with either H_2 which is produced with electrolyzer during the time it is running or from the H_2 storage facility when extra amount of H_2 was stored during the operation of electrolyzer.

In the approach presented in this chapter, a fixed methanation capacity is chosen to illustrate the optimization of hydrogen storage as well as full load hour operation of electrolyzer system. The objective is to keep the methanation unit running continuously at 8500 FLH per year at full load capacity and supply the required amount of hydrogen in a continuous manner. Different electrolyzer capacities are selected for a 0.585 MW_{SNG} methanation unit to supply the sufficient amount of hydrogen regularly and constantly. From 1 to 6 MW_{el} electrolyzer capacities were illustrated aiming a full conversion of H_2 into SNG so that no H_2 is discarded. The different chosen sizes of electrolyzer determine at what capacity H_2 should be stored as well as at what FLH should the electrolyzer technology run. Hence, the optimization variables in the focus of this study were: hydrogen storage size and full load hour operation of electrolyzer technology. A key aspect in this scheme is that an intermittent source of power i.e., electricity can be used; this way it helps to reduce the amount of electricity curtailment from renewable energy generation. The flexible operating hours of electrolyzer could be adjusted according to the overproduction periods of renewable source of electricity, i.e., difference between supply and demand sides. Frequent shut downs could be possible for electrolyzer system since it reacts to changes in electrical input energy within seconds, while methanation unit takes several minutes to adjust the production rate maintaining the SNG quality.

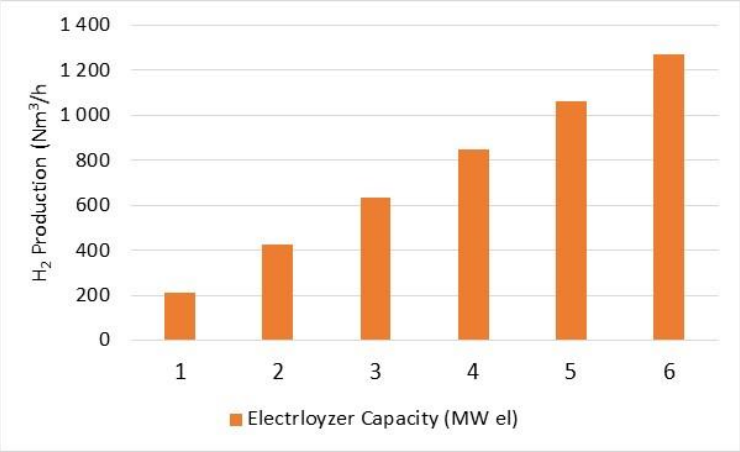

Figure 5-4: H_2 production of electrolyzer at different input electrical capacity

Figure 5-4 presents the H_2 production in Nm^3/h for the different selected electrical input (MW_{el}) capacity of electrolyzer. The H_2 production varies between 212 Nm^3/h and 1270 Nm^3/h for the Electrolyzer capacities from 1 to 6 MW_{el}. A 1 MW_{el} electrical input capacity electrolyzer has to run continuously throughout the year to supply the needed quantity of H_2 into methanation unit to

guarantee a continuous operation of methanation unit. Electricity has to be supplied constantly in a regular manner into electrolyzer with an average daily purchase price. A daily purchase price of electricity in such case would be high because of the peak load hours. A larger capacity electrolyzer than 1 MW_{el} electrical input does not need to run continuously throughout the year and eventually FLH of electrolyzer decreases but in contrast it requires an intermediate hydrogen storage integrated between the sub-systems electrolyzer and methanation unit. Given the fact that the electrolyzer runs flexibly, the power supply from the grid or surplus renewable source can be set in such period that the purchase price is the lowest possible within the year. Daily and yearly H_2 production at different electrical input capacity is presented in Table 5-8.

Table 5-8: H_2 production capacity of electrolyzer at the chosen electrical input capacity

	H_2 production capacity of electrolyzer at the chosen electrical input capacity	
Electrloyzer Capacity (MW_{el})	Nm^3/day	Nm^3/year @ 8500h
1	5 085	1 800 000
2	10 169	3 600 000
3	15 254	5 400 000
4	20 339	7 200 000
5	25 424	9 000 000
6	30 508	10 800 000

The higher the electrolyzer capacity the larger would be hydrogen storage size but the full load hour operation of electrolyzer would be lower inversely due to a fixed methanation unit size. Electrolyzer at 1 MW_{el} capacity runs 24 hours per day or 8500h per year while electrolyzer capacity at 4 MW_{el} runs only 6 hours per day or 2100h per year which is 75% lower than the 1 MW_{el} operation time. A crucial aspect in this argument is the lower specific CAPEX due to larger electrolyzer capacity would be taken into account. Higher costs due to larger hydrogen storage which in fact it is because of larger capacity of electrolyzer would be compensated by lower electricity purchase price operating electrolyzer flexibly at very low full load operation hours. Data on the hourly fluctuating price of electricity due to integration of surplus renewable source for the moment is not available, which restrain to compare the impact on the gas production costs with continuous operation with no intermediate hydrogen storage system. The full load hour operation of electrolyzer and its corresponding operation time per year is presented in Table 5-9 which keeps the methanation unit running continuously at a regular and constant supply of hydrogen.

Table 5-9: Electrolyzer full load hour operation required corresponding to the input electrical capacity

	H_2 production capacity of electrolyzer at the chosen electrical input capacity	
Electrolyzer Capacity (MW_{el})	FLH/day	FLH/year @ 8500h
1	24	8 500
2	12	4 213
3	8	2 808
4	6	2 106
5	5	1 685
6	4	1 404

Table 5-10 presents the hydrogen storage capacity in Nm^3 and its associated costs respectively. Up to 280 000 € at 4 MW_{el} (3790 Nm^3) and 315 000 € at 6 MW_{el} (4200 Nm^3) extra cost can be encountered when an intermediate hydrogen storage facility is integrated into PtG system. For a gas production cost optimization, these extra hydrogen storage costs could be compensated with the lower specific CAPEX for electrolyzer and methanation unit and also with the lower electricity purchase prices.

Table 5-10: Required size of hydrogen storage in Nm^3 and associated costs for different electrical capacity of electrolyzer system from 1 MW_{el} to 6MW_{el}

			Cost of storage @ 75 €/Nm^3 H_2
Electrolyzer Capacity (MW_{el})	Nm^3	m^3 @ 30 bar	€
1	0	0	0
2	2 542	85	190 663
3	3 375	112	253 109
4	3 791	126	284 332
5	4 041	135	303 065
6	4 207	140	315 554

5.5 Discussion

Since the revenue of gas is known in advance, the determination of willingness to pay (WTP) for electricity is possible. In the methodology presented byV. Van Leeuwen et al. [160], the authors presented that there are currently (@2018) not enough hours with sufficiently low electricity prices to be profitable. Nevertheless, for optimistic future scenarios it is shown, that power-to-gas plants can become profitable with higher revenues and lower costs. The WTP for electricity is dependent on the revenue of the methane. In the case where revenue of gas is based only on wholesale natural gas market, the WTP for electricity is very low with only 5.32 €/MWh. With very strong governmental

support schemes such as in Italy or Germany for biogas, the WTP can increase up to almost 40 €/MWh and 84 €/MWh respectively [145].

Due to high proportion of fluctuating generation capacities, electricity prices are becoming more volatile. Moreover, extremely high and extremely low prices arise on the electricity exchange. Extreme prices are equal to or less than 0 €/MWh and more than 100 €/MWh [146]. Extreme prices expected to rise sharply in Europe from 2026 onwards. In 2030, number of extreme prices are between 500 and 1000 hours and this trend is increasing and reaching 2500 hours in 2050 [145]. This illustrates that the relation between two extreme prices bring market opportunities for new market technologies such as storage systems.

A detailed study illustrating the percentage reduction of GPC due to integration of intermediate hydrogen storage system is not included in the scope of current study. However the studies carried out with [146] and [143] show a reduction of 5 to 8% GPC by integrating hydrogen storage. In the calculation to account for the reduction of GPC due to hydrogen storage system and seeking cost benefits of optimizing hydrogen storage, the associated CAPEX, OPEX of hydrogen storage are unavoidable. A bigger hydrogen storage capacity separates two sub-systems and guarantees that SNG is supplied constantly over 8500 h in a year. This manner, the produced and stored hydrogen is fully processed with methanation unit. With an optimized size of the hydrogen storage and the methanation is used, the fluctuated load of the electrolyzer can be flattened and longer continuous operation of the methanation is possible. A suitable size of hydrogen storage depends on the profile of the electrical input of electrolyzer as well as the methanation capacity. Well-balanced hydrogen storage and methanation capacities increase the annual full-load and decrease SNG production costs.

5.6 CONCLUSIONS AND PERSPECTIVES

This chapter focused on the estimation of synthetic methane production costs based on two operating strategies: continuous and flexible. The proposed power-to-gas system in this chapter is installed on a landfill site which has already an upgrading unit. A continuous operating strategy accounted for a continuous operation of both sub-systems electrolyzer and methanation unit while a flexible operating strategy accounted for a variable operation of electrolyzer keeping the methanation unit running constantly. Carbon dioxide is supplied to the power-to-gas system from a landfill site hence offsetting the cost of CO_2 capture from industrial waste gases ranging from 25 to 125 €/t_{CO2}. Due to current lack of some governmental support schemas and subsidies to promote PtG, a business case of 2030 has been selected to carry out the calculations to gas production costs. Compared to current CAPEX, OPEX and share of renewables and efficiencies of PtG units, in the near future 2030, PtG will witness economic efficiency, feasibility and more adaptability and as a result, the estimated synthetic methane

production costs will be reduced.

The SNG production costs strongly depend on the electricity price due to the presence of electrolyzer to produce enough hydrogen and on the operating time of the electrolyzer and methanation unit. Integration of an intermediate hydrogen storage tank moreover could help to operate the sub-systems independently and offers the potential for improvement of the PtG economics. For a 1 MW_{el} electrical input capacity of electrolyzer and 0.585 MW_{SNG} methanation unit capacity, synthetic methane gas production cost was estimated to be about 72.7 €/MWh for an electricity/power purchase price at 20 €/MWh. The operation of such plant would be profitable at the electricity purchase price equal to or lower than 20 €/MWh because at this electricity price, the total costs of gas production does not exceed the revenue expected from selling SNG i.e., 75 €/MWh at the year 2030.

Some strategies such as direct coupling of the PtG plant with a renewable energy source and the seasonal use of surplus energy from renewables are considered as future opportunities for PtG application soon for the near future 2030-2050. One of the advantages of direct coupling is that there is no need to pay network usage fees, and thus operating costs can be reduced. However, the resulting lower number of operating hours is a disadvantage. The future availability of appropriate incentives or governmental support schemes for these strategies i.e. Direct coupling of PtG plant and seasonal use of surplus energy can have a positive effect on the economic efficiency of PtG plant and a potential reduction of production costs.

In the continuous operating strategy, electricity is bought based on the long-term contract and gas is sold continuously into natural gas grid with a fixed price. Another possible way is; gas is stored and sold based on short-term contract at peak price periods. The associated SNG storage costs in this case must be considered. In the flexible operating strategy, electricity is purchased on the short-term market and gas is sold either based on short-term market or long-term market. The willingness to pay (WTP) in case of short-term electricity purchase contract can be determined and based on the trend in the electricity price.

The aim is to achieve a long and continuous full-load operation of methanation. In the future, methanation will also have to be more flexible due to new fields of application. The gas composition of the product of chemical methanation changes if the temperature and pressure in the reactor system are changed too quickly. These changes must be so slow that they have no effect on gas quality. Therefore, it makes sense to add a hydrogen puffer tank in between the chemical methanation and the electrolyzer technology. The methanation unit can then be designed independent in terms of

possible load change rates from the electrolyzer sub-system. Ideally, cost-intensive standby can be avoided by operating as much as possible, at full or partial load.

General conclusion and perspectives

This thesis was an approach to study and research on how to valorize landfill biogas into biomethane in an innovative way. A deep insight is given in this thesis regarding the different aspects of producing biomethane from a raw landfill biogas containing nitrogen in the gas mixture. State of the art technologies are broadly studied to select the cost-effective and energy efficient upgrading unit for the treatment and upgrading of landfill biogas. Moreover, the presence of nitrogen is also taken into account while selecting an appropriate upgrading technology. A brief study is also integrated in this dissertation to show how to enhance the decomposition of organic material to boost biogas production from a landfill site with the help of leachate recirculation.

In the first part of this dissertation, a global review of biomethane production from biogas through a literature review was given. The literature review was focused on the comprehensive study of different biogas upgrading technologies, leachate recirculation to enhance biogas production from landfill site and power-to-gas technology to valorize the carbon dioxide content of landfill biogas. The findings from different upgrading technologies showed that there is no optimal upgrading unit considering all the technical features. In addition to conventional biogas upgrading technologies, emerging biogas upgrading technologies exist too. These technologies such as cryogenic, in situ methane enrichment and hybrid are still under research and development and could possibly replace the conventional biogas upgrading in the future. The methods, that are used to purify and upgrade, are mainly distinguished based on their consistency, methane purity at outlet and methane loss during the process of operation. The lower the plant consumes energy, the higher the net energy be saved and makes it more suitable in commercial and industrial skills.

In the second part of this thesis, four different first order landfill gas (LFG) mathematical models were used to estimate the production of biogas for the landfill site considered in this thesis. Two of the important input parameters for the models that are: methane potential generation of landfilled waste and methane generation rate constant were found with two different approaches from the given waste composition and conditions of landfill site. To estimate methane generation potential, guidelines by Conestoga-Rovers & Associates (CRA) prepared for British Colombia Ministry of Environment was used. In addition, the Guidelines given by EPA US method is also used to estimate methane generation potential. Yearly waste disposed into landfill and corresponding compositions were provided with Groupe Brangeon, the owner and operator of Landfill site, La Poitevinière. The models used in this thesis to estimate the biogas production from La Poitevinière landfill site are TNO model, Multiphase Afvalzorg model, LandGEM model and Tabasaran & Rettenberger model. Output of the model LFG estimates were calculated with CRA and EPA methods taking into consideration the annual waste disposal from 1990 to 2032. Methane generation potential as well as LFG were estimated

for different sets of years such as 2010-2020, 2021-2032 and 2033-2060. Year 2032 is the closure year of landfill site, beyond that period the site will not receive any further waste. The year 2060 is considered the end of landfill gas production since beyond this year the estimated LFG is almost negligible. Model outputs were compared in terms of annual volume of biogas produced to site data for the period 2010-2020, and consequently TNO model showed better agreement than other LFG models. LFG model estimations in (Nm^3/h) for the studied landfill site is proposed between 2020-2060 with TNO model at different methane generation rate constant (k) value. The range of estimated biogas flow rate is between 300 to 50 Nm^3/h. The actual biogas flow rate recorded in the landfill site is 200 Nm^3/h for the current period.

In the third part of this thesis, biomethane production from the estimated landfill biogas and its associated costs of production is comprehensively studied. Since the source of raw biogas comes from a landfill site with more than 10 vol% N_2, hence a definite landfill biogas upgrading into biomethane process is studied in this part of thesis taking into account nitrogen removal from the raw biogas to produce a methane gas that meets the standards of natural gas injection. Meanwhile, simultaneous removal of N_2 is not possible due to higher N_2 vol% present in the gas mixture, two separate scenarios were broadly studied to estimate the cost of biomethane production in €/Nm^3 as well as in €/MWh. The considered scenarios hence are Membrane+PSA and cryogenic distillation. Specific costs of biomethane were calculated at 42.2 €/MWh and 70.6 €/MWh in case of cryogenic technology with and without heat recovery and 56.1 €/MWh in case of Membrane+PSA. Meanwhile, the impact of increase of plant size (biogas flow rate in Nm^3/h) on the specific cost of biomethane also has been presented. Increasing the plant size from 200 Nm^3/h to 400 Nm^3/h presented 40 to 50% reduction in specific cost of biomethane production. Bearing in mind the lower biogas flow rate estimated from the studied landfill site through LFG models, valorization of carbon dioxide content of biogas in power-to-gas process to enhance the methane generation potential of the site has been deeply studied in the fourth and fifth part of this thesis.

In the fourth part of this dissertation, catalytic methanation and kinetics of reaction have been broadly studied. A thermodynamic analysis as well as simulation of kinetics of methanation reaction have been conducted in this part of thesis. For the thermodynamic analysis part, a Gibb's energy minimization method with a Gibb's reactor by the help of ProsimPlus steady state simulation software was considered. The results obtained through this simulation were promising and presented a good agreement when compared with literature. When the pressure is high, a better CO_2 conversion is achieved but the influence of operating temperature is inversely proportional; with higher temperature, the rate of conversion of CO_2 is decreased. In addition, the formation of CO and CO_2 at the outlet of reactor would increase by increasing temperature. Hence, the optimal operating

conditions in the boundary of thermodynamic analysis are high pressure and low temperature. Thermodynamic analysis lack in taking into account the kinetic of reaction boundaries hence would not be enough in optimizing the process, which is why a simulation of kinetics of reaction also conducted in this thesis. A plug flow reactor was modeled with ProsimPlus software to validate the simulated steady state continuous plug flow reactor integrated with an externally linked user defined kinetic model. Kinetic model taken into account in this simulation is the model proposed with Xu & Froment. This model is first subjected to a broad parametric study and later coded in visual studio with FORTRAN coding language and linked into ProsimPlus through dynamic library link (dll). An excellent agreement was found with comparing the results of simulation model with the literature. The presence of a kinetic model helped to evaluate the evolution of input reactants and output products in molar and mass fraction in the process.

In the last part of this thesis, power-to-gas process with an interest in using carbon dioxide generated from the same landfill site to produce synthetic methane or synthetic natural gas (SNG) was widely studied. One MW_{el} electrical input capacity of alkaline electrolysis technology and a catalytic methanation with 75% and 78% efficiencies were considered correspondingly. In to the two-step hydrogen production with electrolysis technology and SNG with methanation unit, source of electricity is provided to the system by power grid. It is assumed for the calculations that the produced SNG is injected into natural gas gird. The production cost of SNG is estimated in this part of thesis in €/MWh taking into account all the CAPEX and OPEX data from literature. Two operating strategies were considered for the power-to-gas process with an objective in producing a continuous SNG from the methanation unit. The most influencing parameters in the system are electricity purchase price to supply green hydrogen and operating hours of sub-systems electrolyzer and methanation. The lower the electricity purchase price, the lower the SNG production cost and the other way around. In contrast, the lower the operating hours, the higher would the SNG production costs be and contrariwise. For a one MW_{el} electrical input capacity of electrolyzer, SNG production cost was estimated to be about 72.7 €/MWh for an electricity purchase price at 20 €/MWh.

Perspectives:

Beside the results presented in the general conclusion of this thesis, few perspectives could be proposed as future tasks in further enhancing the overall landfill biogas into biomethane transformation process. The future perspectives are detailed as below for the each separate part of this thesis.

Chapter 2: Mathematical modeling of landfill biogas production

The entire landfill site in this thesis is considered as a one landfill cell for the estimation of biogas production through mathematical modeling. The more accurate scenario would be to take into account each and individual landfill cell to run the mathematical modeling. At the end, biogas production from all the landfill cells could be accumulated to derive the entire capacity of landfill site. Further perspective in this section would be to take into account a more precise and relevant temperature of the landfill site or more precisely an average annual temperature of each landfill cells. In the LFG model, Tabasaran & Rettenberger, the presence of temperature term in the model can lead to a less degree of precision if the temperature data is not accurately selected.

Chapter 3: Biomethane production from landfill site

Selection of an appropriate upgrading technology to convert landfill biogas into biomethane is site specific and especially when larger nitrogen vol% is present in the gas mixture. As a future task in this part of this thesis, the valorization of separated nitrogen in the process could be taken into account in case of cryogenic distillation. The valorization of captured and separated nitrogen at the end of either pressure swing adsorption (PSA) or cryogenic distillation would be counted as a positive contribution into the process and hinder the specific cost of biomethane eventually lower. Moreover, reduction in the methane capture due to integration of nitrogen removal step should also need to be taken into account.

Power-to-Gas

Heat integration is something which is not integrated in the power-to-gas process studied in this thesis. The integration of waste heat at the outlet of an exothermic catalytic methanation reactor in the process would enhance the process and eventually helps reduce the specific cost of synthetic methane production. Moreover, the supply of electricity to produce hydrogen through electrolyzer and its associated purchase price plays a vital role in the power-to-gas. Cheaper electricity results in cheaper methane gas production. The below are the four factors proposed as future discussion and perspectives for the optimal time profile and operation of the power-to-gas system.

1- Market price of electricity and plant's willingness to pay (WTP) for electricity.
2- Market price of gas and plant's WTP for gas
3- Availability of CO_2
4- Availability of storage capacities for CO_2 and H_2

Objectif et structure de la thèse :

Cette thèse présente un travail sur la valorisation de déchets de décharge en vue de produire le biogaz et le méthane. L'objectif de cette étude s'inscrit dans une alternative énergétique de substitution et de remplacement de combustibles fossiles et de réduction des émissions de gaz à effet de serre. Différents modèles et méthodes ont été proposés et analysés dans le but d'améliorer ce processus de valorisation de déchets. Le site de La Poitevinière situé près de Nantes est considéré pour la plupart des expérimentations. Les résultats obtenus ont permis de dégager les limites de validité des modèles étudiés et aussi leur efficacité en termes de pourcentages de biogaz et de méthane récupérés. L'impact de nombreux paramètres physiques sur les résultats est mis en évidence par une analyse de sensibilité et par comparaison avec la bibliographie.

Le manuscrit composé d'une introduction générale, cinq chapitres d'importance équivalente, une conclusion et des perspectives, des références bibliographiques et trois annexes. Il comprend aussi une table de matières, des illustrations et des tableaux, et une nomenclature générale, ce qui représente une aide précieuse à la lecture de ce document.

Introduction Générale:

Le plus grand problème environnemental à l'heure actuelle est la combustion de combustibles fossiles tels que le charbon, le pétrole et le gaz naturel. En raison du développement et de la croissance de l'économie mondiale, les besoins énergétiques de plus en plus de pays augmentent énormément. Actuellement, les combustibles fossiles sont responsables des principales ressources énergétiques d'environ 80% de la demande mondiale pour une utilisation dans notre vie quotidienne, dans les activités économiques ou industrielles. Près de 80 % des émissions mondiales de CO_2 proviennent de la combustion de ces carburants [1]. L'utilisation de combustibles fossiles comporte de nombreux risques associés tels que la diminution des réserves, les émissions de gaz à effet de serre (GES) et aussi la dépendance à l'importation [2]. Pour résoudre ces graves problèmes, les traités internationaux comme le protocole de Kyoto et la COP21 mettent l'accent sur le développement et l'utilisation des sources d'énergie renouvelables [3]. Ainsi, en tant que solution encourageante, les sources d'énergie renouvelables, comme le biométhane, peuvent constituer des alternatives puissantes pour freiner l'utilisation des combustibles fossiles [4]. De plus, les membres de l'UE ont convenu d'atteindre dans le secteur du chauffage une augmentation annuelle de 1 % des énergies renouvelables et un objectif de 14 % des sources renouvelables dans le secteur des transports d'ici 2030. La projection est une décarburation à long terme jusqu'en 2050 [5].

Dans cette perspective, la décomposition des déchets et substrats biodégradables dans des conditions anaérobies telles que dans les ISDND est un processus bien établi pour la production de biogaz et la génération conséquente de biométhane. Les principaux pays producteurs de biogaz étaient l'Allemagne (46,7% du total de biogaz produit de l'UE), suivi du Royaume-Uni et de l'Italie en tant que deuxième et troisième principaux producteurs, avec respectivement 16,2 % et 11,3 % de la production totale de biogaz dans l'UE. Fin 2017, il y avait 17 783 installations de biogaz avec une tendance vers des installations de plus grandes capacités [5]. Dans environ 71% des installations, le biogaz est obtenu à partir de cultures et de résidus agricoles, dans environ 16% des boues d'épuration, dans 8% des décharges et dans les 5% restants d'autres substrats [4].

En tant que source d'énergie neutre en carbone, le biogaz gagne plus d'attraits pour faire partie des alternatives aux combustibles fossiles et dans la réduction des émissions de gaz à effet de serre. Le contenu énergétique du biogaz qui provient en fait du CH_4 est capté et utilisé dans de nombreux services différents tels que : la production d'électricité via des cogénérations, l'injection dans le réseau, ou utilisé comme biocarburant principalement [6]. Dans tous ces cas, le biogaz brut non traité doit être correctement purifié de toutes les impuretés et séparé du dioxyde de carbone pour générer du biométhane. La loi sur la transition énergétique et la croissance verte (LTECV) [1] a fixé un objectif de 10 % de la consommation totale de gaz qui devrait être représentée par du gaz vert d'ici fin 2030. Le biogaz correctement valorisé serait utilisé dans le secteur des transports ou alimenterait directement dans le réseau de gaz naturel atteignant les consommateurs finaux, les deux solutions ajoutant de la valeur au biogaz.

Dans ce contexte, cette thèse a porté sur la recherche et l'étude d'une solution innovante pour la transformation du biogaz de (ISDND) en biométhane. Pour le site d'enfouissement étudié, une modélisation mathématique a été réalisée pour prédire la production de biogaz pour les 20 prochaines années. Une analyse de l'état de l'art a été réalisée pour identifier les technologies de traitement du biogaz capables de valoriser le biogaz de l'ISDND en biométhane. Une analyse des coûts du cycle de vie a été réalisée pour cinq technologies afin d'identifier les paramètres les plus influents. Le coût spécifique de la production de biométhane a été estimé dans deux scénarios : Membrane+PSA et distillation cryogénique. Pour remédier au faible débit de biogaz, la valorisation de la fraction de dioxyde de carbone a été étudiée via le procédé Power-to-Gas. Dans le processus Power-to-Gas en deux étapes, la source du carbone dans l'unité de méthanisation a été considérée à partir de la capture du dioxyde de carbone et séparée à la sortie d'une technologie de traitement. La production d'hydrogène dans le processus a été étudiée en utilisant l'électricité renouvelable excédentaire intermittente via la technologie d'électrolyse. Deux modes opératoires ont été étudiés pour le procédé Power-to-Gas avec et sans stockage intermédiaire d'hydrogène : continu et flexible. Le coût spécifique

de la production de gaz naturel de synthèse (GNS) a été estimé en €/MWh pour deux stratégies opératoires. Une analyse de sensibilité a été réalisée pour présenter l'effet du prix d'achat de l'électricité ainsi que des heures de fonctionnement à pleine charge sur le coût de production de GNS.

Recherche bibliographique :

Le contenu de cette chapitre est consacré à mettre en évidence les données de pointe concernant la chaîne de production du biogaz au biométhane en décrivant les techniques de valorisation du biogaz telles que l'absorption physique et chimique, l'adsorption par variation de pression, la technologie membranaire ou encore la distillation cryogénique. Les caractéristiques techniques de cinq technologies de valorisation du biogaz sont aussi étudiées et comparées sur des critères de récupération du méthane, d'élimination de l'azote et de consommation spécifique en termes de chaleur et d'électricité. Une revue bibliographique supplémentaire sur l'importance de la recirculation et de traitement de décharge des lixiviat est également présentée.

La suite du chapitre est consacrée à une description des quatre phases de la décomposition bactérienne des déchets dans les sites de décharge, à savoir la phase de production de dioxyde de carbone suivi d'une phase de décomposition en acides acétiques, lactiques et formiques et en alcools tels que le méthanol et l'éthanol. Dans la phase 3, les bactéries productrices de méthane commencent à s'établir et à consommer le dioxyde de carbone et l'acétate jusqu'à ce que la composition et les taux de production du gaz de décharge restent relativement constants.

Le lixiviat de décharge figure aussi parmi les grands problèmes à traiter lors de la conception, de la construction et de la gestion d'un site de décharge. Il permet d'améliorer la qualité du gaz produit et d'accélérer les processus biochimiques et enfin de contrôler la teneur en humidité, des nutriments et de la migration des microbes dans la décharge. L'âge des sites de décharge, le type de déchets et les conditions météorologiques figurent parmi les facteurs les plus influents sur les caractéristiques du lixiviat de décharge.

Une description des technologies les plus utilisées pour éliminer le CO_2 donné dans ce chapitre à savoir l'absorption physique ou chimique (lavage à l'eau ou aux amines), l'adsorption par variation de pression et les membranes ainsi que d'autres techniques émergentes. De cette description, on peut retenir que le lavage à l'eau est la technologie de valorisation du biogaz la plus largement utilisée.

L'eau est utilisée dans ce processus comme solvant pour éliminer le H_2S et le CO_2 du biogaz et pour obtenir un méthane riche à la sortie du lavage à l'eau. Les autres technologies présentent des particularités spécifiques sur le mécanisme d'absorption physique ou chimique du solvant. Un tableau dresse une comparaison des différentes technologies de valorisation du biogaz. Parmi les technologies

émergentes, la distillation cryogénique figure parmi les technologies les plus gourmandes en consommation d'électricité. Un état de l'art sur la technologie Power-to Gas (PtG) comme une alternative de développement et de conversion de dioxyde de carbone des sites de décharge en méthane synthétique a été réalisé dans ce chapitre. On peut utiliser des sources d'énergie renouvelables intermittentes pour produire de l'hydrogène grâce à des techniques de méthanisation, d'électrolyse de l'eau et des électrolyseurs de type PEM ou SOE.

Chapitre 2 : Prédiction de la production du biogaz ISDND avec les modèles mathématique

Dans la deuxième partie de cette thèse, quatre modèles mathématiques de premier ordre (LFG) ont été utilisés pour estimer la production de biogaz pour la décharge considérée dans cette thèse. Deux des paramètres d'entrée importants pour les modèles, à savoir : le potentiel de production de méthane des déchets mis en décharge et la constante du taux de génération de méthane ont été trouvés avec deux approches différentes à partir de la composition des déchets et des conditions données du site d'enfouissement. Pour estimer le potentiel de production de méthane, les guidelines de Conestoga-Rovers & Associates (CRA) préparées pour le ministère de l'Environnement de la Colombie-Britannique ont été utilisées. De plus, les directives données par la méthode EPA US sont également utilisées pour estimer le potentiel de génération de méthane. Les déchets annuels mis en décharge et les compositions correspondantes ont été fournis par le Groupe Brangeon, propriétaire et exploitant du site d'ISDND de La Poitevinière. Les modèles utilisés dans cette thèse pour estimer la production de biogaz de la décharge de La Poitevinière sont le modèle TNO, le modèle Multi phase Afvalzorg, le modèle LandGEM et le modèle Tabasaran & Rettenberger.

Les résultats des estimations du modèle LFG ont été calculés avec les méthodes CRA et EPA en tenant compte d'admission annuelle des déchets de 1990 à 2032. Le potentiel de production de méthane ainsi que le biogaz ont été estimés pour différents ensembles d'années telles que 2010-2020, 2021-2032 et 2033-2060. L'année 2032 est l'année de fermeture du site d'ISDND, au-delà de cette période, le site ne recevra plus de déchets. L'année 2060 est considérée comme la fin de la production de gaz de décharge puisqu'au-delà de cette année le biogaz estimé est presque négligeable. Les sorties du modèle ont été comparées en termes de volume annuel de biogaz produit aux données du site pour la période 2010-2020, et par conséquent le modèle TNO a montré une meilleure concordance que les autres modèles LFG. Les estimations du modèle en (Nm^3/h) pour le site d'ISDND étudié sont proposées entre 2020-2060 avec le modèle TNO à différentes valeurs de constante de taux de génération de méthane (*k*). La plage de débit de biogaz estimé est comprise entre 300 et 500 Nm^3/h. Le débit réel de biogaz enregistré dans la décharge est de 200 Nm^3/h pour la période actuelle 2021.

Chapitre 3 : La production de biométhane à partir de biogaz brut.

Dans la troisième partie de cette thèse, la production de biométhane à partir du biogaz estimé de décharge et ses coûts de production associés sont étudiés de manière approfondie. Étant donné que la source de biogaz brut provient d'un site d'ISDND avec plus de 10 % en volume de N_2, un processus défini de valorisation du biogaz de décharge en biométhane est donc étudié dans cette partie de la thèse en tenant compte de l'élimination de l'azote du biogaz brut pour produire un gaz méthane qui répond aux normes d'injection de gaz naturel. Le premier objectif de ce chapitre est d'évaluer les cinq technologies de valorisation du biogaz mentionnées, indépendamment de la source de biogaz. Une évaluation du coût du cycle de vie tenant compte de toutes les caractéristiques techniques et économiques des technologies est effectuée pour découvrir la technologie la plus économique et la plus économe en énergie. De plus, une analyse de sensibilité est également effectuée dans le but de trouver le paramètre le plus important de la technologie et son impact sur l'évaluation du coût total du cycle de vie. L'évaluation du coût du cycle de vie avec et sans récupération de chaleur est également évaluée pour déterminer l'influence de la récupération de chaleur dans certaines technologies. L'évaluation de ces cinq technologies est réalisée à partir des données de la littérature. En plus de cela, certaines hypothèses sont formulées et plusieurs données sont incluses pour rendre les évaluations plus réalistes et spécifiques à un site particulier.

Le deuxième objectif de ce chapitre est d'évaluer les technologies existantes de valorisation du biogaz qui pourraient être adoptées et sélectionnées pour une décharge spécifique à un site. Certaines technologies peuvent ne pas être facilement proposées pour les sites de décharge, soit elles ne sont pas capables d'éliminer simultanément l'azote et le dioxyde de carbone, soit elles sont trop coûteuses. Le site de décharge choisi pour cette étude contient plus de 10 % en volume d'azote dans le mélange de biogaz brut. Pendant ce temps, l'élimination simultanée de N_2 n'est pas possible en raison du pourcentage plus élevé de N_2 en volume présent dans le mélange gazeux. Deux scénarios distincts ont été largement étudiés pour estimer le coût de production de biométhane en €/Nm^3 ainsi qu'en €/MWh. Les scénarios envisagés sont donc Membrane+PSA et la distillation cryogénique. Les coûts spécifiques du biométhane ont été calculés à 42,2 €/MWh et 70,6 €/MWh en cas de technologie cryogénique avec et sans récupération de chaleur et 56,1 €/MWh en cas de Membrane+PSA. Parallèlement, l'impact de l'augmentation de la taille de l'installation (débit de biogaz en Nm^3/h) sur le coût spécifique du biométhane a également été présenté. L'augmentation du débit de 200 Nm^3/h à 400 Nm^3/h a entraîné une réduction de 40 à 50 % du coût spécifique de production de biométhane. Compte tenu du débit de biogaz plus faible estimé à partir du site d'enfouissement étudié grâce aux modèles, la valorisation de la teneur en dioxyde de carbone du biogaz dans le processus de conversion

au gaz pour améliorer le potentiel de génération de méthane du site a été profondément étudiée dans les quatrième et cinquième partie de cette thèse.

Chapitre 4 : étude sur la cinétique de la réaction de méthanisation catalytique pour produire du méthane synthétique

Dans la quatrième partie de cette thèse, la méthanation catalytique et la cinétique de réaction ont été largement étudiées. Une analyse thermodynamique ainsi qu'une simulation de cinétique de réaction de méthanation ont été menées dans cette partie de thèse. Pour la partie analyse thermodynamique, une méthode de minimisation d'énergie de Gibbs avec un réacteur de Gibbs à l'aide du logiciel de simulation en régime permanent ProsimPlus a été envisagée. Les résultats obtenus grâce à cette simulation étaient prometteurs et présentaient un bon accord par rapport à la littérature. Lorsque la pression est élevée, une meilleure conversion du CO_2 est obtenue mais l'influence de la température de fonctionnement est inversement proportionnelle ; avec une température plus élevée, le taux de conversion du CO_2 est diminué. De plus, la formation de CO et de CO_2 en sortie de réacteur augmenterait en augmentant la température. Par conséquent, les conditions de fonctionnement optimales dans la limite de l'analyse thermodynamique sont la haute pression et la basse température. L'analyse thermodynamique manque de prise en compte de la cinétique des frontières de réaction et ne serait donc pas suffisante pour optimiser le procédé, c'est pourquoi une simulation de cinétique de réaction également menée dans cette thèse. Un réacteur à écoulement piston a été modélisé avec le logiciel ProsimPlus pour valider le réacteur à écoulement continu en régime permanent. Le modèle cinétique pris en compte dans cette simulation est le modèle proposé avec Xu & Froment. Ce modèle est d'abord soumis à une vaste étude paramétrique, puis codé en Visual studio avec le langage de codage FORTRAN et implémenté sous ProsimPlus via un lien de bibliothèque dynamique (dll). Un excellent accord a été trouvé avec la comparaison des résultats du modèle de simulation avec la littérature. La présence d'un modèle cinétique a permis d'évaluer l'évolution des réactifs d'entrée et des produits de sortie en fraction molaire et massique dans le processus.

Chapitre 5 : étude technico-économique sur un système power-to-Gas (PtG)

Dans la dernière partie de cette thèse, le procédé power-to-Gas avec un intérêt à utiliser le dioxyde de carbone généré à partir du même site d'ISDND pour produire du méthane synthétique ou du gaz naturel synthétique (GNS) a été largement étudié. Une capacité d'entrée électrique d'un MW_{el} de la technologie d'électrolyse alcaline et une méthanation catalytique avec des rendements de 75 % et 78 % ont été considérées en conséquence. Dans la production d'hydrogène en deux étapes avec technologie d'électrolyse et GNS avec unité de méthanation, la source d'électricité est fournie au système par le réseau électrique. Il est supposé pour les calculs que le GNS produit est injecté dans le

réseau de gaz naturel. Le coût de production du GNS est estimé dans cette partie de la thèse en €/MWh en tenant compte de l'ensemble des données CAPEX et OPEX de la littérature.

Deux stratégies d'exploitation ont été envisagées pour le procédé Power-to-Gas avec pour objectif de produire un GNS en continu à partir de l'unité de méthanisation. Les paramètres les plus influents dans le système sont le prix d'achat de l'électricité pour fournir de l'hydrogène vert et les heures de fonctionnement des sous-systèmes électrolyseur et méthanation. Plus le prix d'achat de l'électricité est bas, plus le coût de production du GNS est bas et inversement. En revanche, plus les heures d'exploitation sont réduites, plus les coûts de production du GNS seront élevés et inversement. Les coûts de production du GNS dépendent fortement du prix de l'électricité du fait de la présence d'électrolyseur pour produire suffisamment d'hydrogène et de la durée de fonctionnement de l'électrolyseur et de l'unité de méthanisation. L'intégration d'un réservoir intermédiaire de stockage d'hydrogène pourrait en outre aider à faire fonctionner les sous-systèmes de manière autonome et offre un potentiel d'amélioration de l'économie du PtG.

Pour une capacité d'entrée électrique d'électrolyseur de 1 MW_{el} et une capacité d'unité de méthanisation de 0,585 MW_{SNG}, le coût de production de gaz méthane de synthèse a été estimé à environ 72,7 €/MWh pour un prix d'achat de l'électricité de 20 €/MWh. L'exploitation d'une telle centrale serait rentable au prix d'achat de l'électricité égal ou inférieur à 20 €/MWh car à ce prix de l'électricité, les coûts totaux de production de gaz n'excèdent pas le revenu attendu de la vente de GNS soit 75 €/MWh à l'année 2030. Certaines stratégies telles que le couplage direct de la centrale PtG avec une source d'énergie renouvelable et l'utilisation saisonnière de l'excédent d'énergie provenant d'énergies renouvelables sont considérées comme des opportunités futures pour l'application du PtG dans un avenir proche 2030-2050. L'un des avantages du couplage direct est qu'il n'est pas nécessaire de payer des frais d'utilisation du réseau, ce qui permet de réduire les coûts d'exploitation. Cependant, la diminution du nombre d'heures de fonctionnement qui en résulte est un inconvénient. La disponibilité future d'incitations appropriées ou de programmes de soutien gouvernementaux pour ces stratégies, c'est-à-dire le couplage direct de l'usine PtG et l'utilisation saisonnière de l'énergie excédentaire, peut avoir un effet positif sur l'efficacité économique de l'usine PtG et une réduction potentielle des coûts de production.

En plus des résultats présentés au-dessus, quelques perspectives pourrait être proposées comme tâches futures pour améliorer davantage le processus de transformation global du biogaz de décharge en biométhane.

- L'ensemble du site de décharge dans cette thèse est considéré comme un seul cassier pour l'estimation de la production de biogaz par modélisation mathématique. Le scénario le plus

précis serait de prendre en compte chaque cassier de décharge individuel pour exécuter la modélisation mathématique. À la fin, la production de biogaz de tous les cassiers de décharge pourrait être accumulée pour dériver la totalité de la capacité du site de décharge.

- Le choix d'une technologie de valorisation pour convertir le biogaz de décharge en biométhane est spécifique au site et en particulier lorsqu'un pourcentage en volume d'azote plus important est présent dans le mélange gazeux. Comme perspective, la valorisation de l'azote séparé dans le procédé pourrait être prise en compte en cas de distillation cryogénique. La valorisation de l'azote capté et séparé à l'issue soit de (PSA) soit de la distillation cryogénique serait considérée comme une contribution positive dans le procédé et entraverait le coût spécifique du biométhane éventuellement inférieur.
- La récupération de la chaleur n'est pas intégré dans le procédé Power-to-Gas étudié dans cette thèse. L'intégration de la chaleur résiduelle à la sortie d'un réacteur de méthanation catalytique exothermique dans le procédé améliorerait le procédé et contribuerait à terme à réduire le coût spécifique de la production de méthane de synthèse. De plus, la fourniture d'électricité pour produire de l'hydrogène par électrolyseur et son prix d'achat associé joue un rôle essentiel dans le Power-to-Gas.

References

[1] K. Zhou, S. Chaemchuen, and F. Verpoort, “Alternative materials in technologies for Biogas upgrading via CO2 capture,” *Renew. Sustain. Energy Rev.*, vol. 79, no. June, pp. 1414–1441, 2017, doi: 10.1016/j.rser.2017.05.198.

[2] P. Collet *et al.*, “Techno-economic and Life Cycle Assessment of methane production via biogas upgrading and power to gas technology,” *Appl. Energy*, vol. 192, pp. 282–295, 2017, doi: 10.1016/j.apenergy.2016.08.181.

[3] S. Sahota *et al.*, “Review of trends in biogas upgradation technologies and future perspectives,” *Bioresour. Technol. Reports*, vol. 1, pp. 79–88, 2018, doi: 10.1016/j.biteb.2018.01.002.

[4] A. M. Yousef, W. M. El-Maghlany, Y. A. Eldrainy, and A. Attia, “Upgrading biogas to biomethane and liquid CO2: A novel cryogenic process,” *Fuel*, vol. 251, no. August 2018, pp. 611–628, 2019, doi: 10.1016/j.fuel.2019.03.127.

[5] L. Lombardi and G. Francini, “Techno-economic and environmental assessment of the main biogas upgrading technologies,” *Renew. Energy*, vol. 156, pp. 440–458, 2020, doi: 10.1016/j.renene.2020.04.083.

[6] Gaz Réseau Distribution France, “Renewable Gas French Panorama 2017,” p. 36, 2017, [Online]. Available: http://www.grtgaz.com/fileadmin/plaquettes/en/2018/Overview-Renewable-Gas-2017.pdf.

[7] I. Rocamora, S. T. Wagland, R. Villa, E. W. Simpson, O. Fernández, and Y. Bajón-Fernández, “Dry anaerobic digestion of organic waste: A review of operational parameters and their impact on process performance,” *Bioresour. Technol.*, vol. 299, no. December 2019, 2020, doi: 10.1016/j.biortech.2019.122681.

[8] Q. Sun, H. Li, J. Yan, L. Liu, Z. Yu, and X. Yu, “Selection of appropriate biogas upgrading technology-a review of biogas cleaning, upgrading and utilisation,” *Renew. Sustain. Energy Rev.*, vol. 51, pp. 521–532, 2015, doi: 10.1016/j.rser.2015.06.029.

[9] R. Kadam and N. L. Panwar, “Recent advancement in biogas enrichment and its applications,” *Renew. Sustain. Energy Rev.*, vol. 73, no. September 2016, pp. 892–903, 2017, doi: 10.1016/j.rser.2017.01.167.

[10] M. Pöschl, S. Ward, and P. Owende, “Evaluation of energy efficiency of various biogas production and utilization pathways,” *Appl. Energy*, vol. 87, no. 11, pp. 3305–3321, 2010, doi:

10.1016/j.apenergy.2010.05.011.

[11] M. Götz *et al.*, "Renewable Power-to-Gas: A technological and economic review," *Renew. Energy*, vol. 85, pp. 1371–1390, 2016, doi: 10.1016/j.renene.2015.07.066.

[12] M. Marchese, E. Giglio, M. Santarelli, and A. Lanzini, "Energy performance of Power-to-Liquid applications integrating biogas upgrading, reverse water gas shift, solid oxide electrolysis and Fischer-Tropsch technologies," *Energy Convers. Manag. X*, vol. 6, no. April, p. 100041, 2020, doi: 10.1016/j.ecmx.2020.100041.

[13] T. Schaaf, J. Grünig, M. R. Schuster, T. Rothenfluh, and A. Orth, "Methanation of CO2 - storage of renewable energy in a gas distribution system," *Energy. Sustain. Soc.*, vol. 4, no. 1, pp. 1–14, 2014, doi: 10.1186/s13705-014-0029-1.

[14] H. L. Huynh, W. M. Tucho, X. Yu, and Z. Yu, "Synthetic natural gas production from CO2 and renewable H2: Towards large-scale production of Ni–Fe alloy catalysts for commercialization," *J. Clean. Prod.*, vol. 264, p. 121720, 2020, doi: 10.1016/j.jclepro.2020.121720.

[15] G. Iaquaniello, S. Setini, A. Salladini, and M. De Falco, "CO2 valorization through direct methanation of flue gas and renewable hydrogen: A technical and economic assessment," *Int. J. Hydrogen Energy*, vol. 43, no. 36, pp. 17069–17081, 2018, doi: 10.1016/j.ijhydene.2018.07.099.

[16] A. Alarcón, J. Guilera, and T. Andreu, "CO2 conversion to synthetic natural gas: Reactor design over Ni–Ce/Al2O3 catalyst," *Chem. Eng. Res. Des.*, vol. 140, pp. 155–165, 2018, doi: 10.1016/j.cherd.2018.10.017.

[17] M. Thema, F. Bauer, and M. Sterner, "Power-to-Gas: Electrolysis and methanation status review," *Renew. Sustain. Energy Rev.*, vol. 112, no. May, pp. 775–787, 2019, doi: 10.1016/j.rser.2019.06.030.

[18] M. Gruber *et al.*, "Power-to-Gas through thermal integration of high-temperature steam electrolysis and carbon dioxide methanation - Experimental results," *Fuel Process. Technol.*, vol. 181, no. September, pp. 61–74, 2018, doi: 10.1016/j.fuproc.2018.09.003.

[19] E. B. Association, https://www.europeanbiogas.eu/the-european-biomethane-map-2020-shows-a-51-increase-of-biomethane-plants-in-europe-in-two-years/ (accessed May 06, 2021).

[20] PANORAMA DU GAZ RENOUVELABLE EN 2020

[21] I. Ullah Khan *et al.*, "Biogas as a renewable energy fuel – A review of biogas upgrading,

utilisation and storage," *Energy Convers. Manag.*, vol. 150, no. May, pp. 277–294, 2017, doi: 10.1016/j.enconman.2017.08.035.

[22] L. Maggioni and C. Pieroni, "Report on the biomethane injection into national gas grid," *Rep. Ital. Eur. Regul. Framew. biomethane Inject. into Natl. gas grid*, pp. 1–44, 2016, [Online]. Available: http://www.isaac-project.it/wp-content/uploads/2017/07/D5.2-Report-on-the-biomethane-injection-into-national-gas-grid.pdf.

[23] Atsdr, "Landfill Gas Basics," *Landfill Gas Prim. An Overv. Environ. Heal. Prof.*, pp. 3–14, 2001.

[24] L. Aleya, E. Grisey, M. Bourioug, P. Bourgeade, and S. G. Bungau, "Proposed changes for post-closure monitoring of Etueffont landfill (France) from a 9-year survey," *Sci. Total Environ.*, vol. 656, pp. 634–644, 2019, doi: 10.1016/j.scitotenv.2018.11.406.

[25] P. S. Calabrò, S. Sbaffoni, S. Orsi, E. Gentili, and C. Meoni, "The landfill reinjection of concentrated leachate: Findings from a monitoring study at an Italian site," *J. Hazard. Mater.*, vol. 181, no. 1–3, pp. 962–968, 2010, doi: 10.1016/j.jhazmat.2010.05.107.

[26] H. Luo, Y. Zeng, Y. Cheng, D. He, and X. Pan, "Recent advances in municipal landfill leachate: A review focusing on its characteristics, treatment, and toxicity assessment," *Sci. Total Environ.*, vol. 703, p. 135468, 2020, doi: 10.1016/j.scitotenv.2019.135468.

[27] T. A. Kurniawan, W. H. Lo, and G. Y. S. Chan, "Physico-chemical treatments for removal of recalcitrant contaminants from landfill leachate," *J. Hazard. Mater.*, vol. 129, no. 1–3, pp. 80–100, 2006, doi: 10.1016/j.jhazmat.2005.08.010.

[28] "Colombo, A., Módenes, A.N., Góes Trigueros, D.E., Giordani da Costa, S.I., Borba, F.H., Espinoza-Quiñones, F.R., 2019. Treatment of sanitary landfill leachate by the combi- nation of photo-Fenton and biological processes. J. Clean. Prod. 214, 145–153."

[29] "Torretta, V., Ferronato, N., Katsoyiannis, I., Tolkou, A., Airoldi, M., 2017. Novel and conventional technologies for landfill leachates treatment: a review. Sustainability 9, 9."

[30] L. Morello, R. Cossu, R. Raga, A. Pivato, and M. C. Lavagnolo, "Recirculation of reverse osmosis concentrate in lab-scale anaerobic and aerobic landfill simulation reactors," *Waste Manag.*, vol. 56, pp. 262–270, 2016, doi: 10.1016/j.wasman.2016.07.030.

[31] "Biogaz issu de la mise en décharge : comment optimiser son captage ?," 2007, www.ademe.fr / Médiathèque / Documents en téléchargement.

[32] N. Sanphoti, S. Towprayoon, P. Chaiprasert, and A. Nopharatana, "The effects of leachate

recirculation with supplemental water addition on methane production and waste decomposition in a simulated tropical landfill," *J. Environ. Manage.*, vol. 81, no. 1, pp. 27–35, 2006, doi: 10.1016/j.jenvman.2005.10.015.

[33] A. Błałowiec, M. Siudak, B. Jakubowski, and D. Wisniewski, "The influence of leachate recirculation on biogas production in a landfill bioreactor," *Environ. Prot. Eng.*, vol. 43, no. 1, pp. 113–120, 2017, doi: 10.5277/epe170109.

[34] "TOWNSEND T., KUMAR D., KO J., Bioreactor Landfill Operation. A Guide for Development, Implementation and Monitoring, Hinkley Center for Solid and Hazardous Waste Management, Gainesville, FL, 2008."

[35] IRENA and IEA, *Biogas for road vehicles*, no. March. 2017.

[36] G. Ruiling, C. Shikun, and L. Zifu, "Research progress of siloxane removal from biogas," *Int. J. Agric. Biol. Eng.*, vol. 10, no. 1, pp. 30–39, 2017, doi: 10.3965/j.ijabe.20171001.3043.

[37] L. A. Pellegrini, G. De Guido, S. Consonni, G. Bortoluzzib, and M. Gatti, "From biogas to biomethane: How the biogas source influences the purification costs," *Chem. Eng. Trans.*, vol. 43, no. January, pp. 409–414, 2015, doi: 10.3303/CET1543069.

[38] K. Hoyer, C. Hulteberg, M. Svensson, J. Jenberg, and Ø. NØrregård, *Biogas upgrading: a technical review. REPORT 2016:275, Energiforsk AB*. 2016.

[39] Hanne Wasmuth Brendeløkken, "Upgrading Technologies for Biogas Production Plants Overview and life cycle cost analysis of available technologies," June, 2016,..

[40] A. I. Adnan, M. Y. Ong, S. Nomanbhay, K. W. Chew, and P. L. Show, "Technologies for biogas upgrading to biomethane: A review," *Bioengineering*, vol. 6, no. 4, pp. 1–23, 2019, doi: 10.3390/bioengineering6040092.

[41] S. Cavenati, C. A. Grande, and A. E. Rodrigues, "Upgrade of methane from landfill gas by pressure swing adsorption," *Energy and Fuels*, vol. 19, no. 6, pp. 2545–2555, 2005, doi: 10.1021/ef050072h.

[42] C. A. Grande, "Advances in Pressure Swing Adsorption for Gas Separation," *ISRN Chem. Eng.*, vol. 2012, pp. 1–13, 2012, doi: 10.5402/2012/982934.

[43] K. Hjuler and N. Aryal, *Review on Biogas Upgrading*, no. September. 2016.

[44] I. Angelidaki *et al.*, "Biogas upgrading and utilization: Current status and perspectives," *Biotechnol. Adv.*, vol. 36, no. 2, pp. 452–466, 2018, doi: 10.1016/j.biotechadv.2018.01.011.

[45] S. Singhal, S. Agarwal, S. Arora, P. Sharma, and N. Singhal, “Upgrading techniques for transformation of biogas to bio-CNG: a review,” *Int. J. Energy Res.*, vol. 41, no. 12, pp. 1657–1669, 2017, doi: 10.1002/er.3719.

[46] R. Augelletti, M. Conti, and M. C. Annesini, “Pressure swing adsorption for biogas upgrading. A new process configuration for the separation of biomethane and carbon dioxide,” *J. Clean. Prod.*, vol. 140, pp. 1390–1398, 2017, doi: 10.1016/j.jclepro.2016.10.013.

[47] K. Friess *et al.*, “CO2/CH4 separation performance of ionic-liquid-based epoxy-amine ion gel membranes under mixed feed conditions relevant to biogas processing,” *J. Memb. Sci.*, vol. 528, no. January, pp. 64–71, 2017, doi: 10.1016/j.memsci.2017.01.016.

[48] A. Park *et al.*, “Biogas upgrading using membrane contactor process: Pressure-cascaded stripping configuration,” *Sep. Purif. Technol.*, vol. 183, pp. 358–365, 2017, doi: 10.1016/j.seppur.2017.03.006.

[49] T. D. Hayes, H. R. Isaacson, J. T. Pfeffer, and Y. M. Liu, “In situ methane enrichment in anaerobic digestion,” *Biotechnol. Bioeng.*, vol. 35, no. 1, pp. 73–86, 1990, doi: 10.1002/bit.260350111.

[50] B. K. Richards, F. G. Herndon, W. J. Jewell, R. J. Cummings, and T. E. White, “In situ methane enrichment in methanogenic energy crop digesters,” *Biomass and Bioenergy*, vol. 6, no. 4, pp. 275–282, 1994, doi: 10.1016/0961-9534(94)90067-1.

[51] A. Lindberg and Å. C. Rasmuson, “Selective desorption of carbon dioxide from sewage sludge for in situ methane enrichment - Part II: Modelling and evaluation of experiments,” *Biotechnol. Bioeng.*, vol. 97, no. 5, pp. 1039–1052, 2007, doi: 10.1002/bit.21328.

[52] A. F. Peterson and G. D. Durgin, “Transient signals on transmission lines: An introduction to non-ideal effects and signal integrity issues in electrical systems,” *Synth. Lect. Comput. Electromagn.*, vol. 24, no. 2009, pp. 1–151, 2008, doi: 10.2200/S00155ED1V01Y200812CEM024.

[53] E. Union, “This project has received funding from the European Union’s Horizon 2020 research and innovation programme under grant agreement No 649436,” no. 649436, pp. 1–2, 2015.

[54] C. van Leeuwen and M. Mulder, “Power-to-gas in electricity markets dominated by renewables,” *Appl. Energy*, vol. 232, no. September, pp. 258–272, 2018, doi: 10.1016/j.apenergy.2018.09.217.

[55] H. Karjunen, T. Tynjälä, and T. Hyppänen, “A method for assessing infrastructure for CO2 utilization: A case study of Finland,” *Appl. Energy*, vol. 205, no. May, pp. 33–43, 2017, doi: 10.1016/j.apenergy.2017.07.111.

[56] E&E consultant, HESPUL, and Solagro, “Etude portant sur l’hydrogène et la méthanation comme procédé de valorisation de l’électricité excédentaire,” p. 238, 2014, [Online]. Available: http://www.grtgaz.com/fileadmin/engagements/documents/fr/Power-to-Gas-etude-ADEME-GRTgaz-GrDF-complete.pdf.

[57] “Juipter1000-First Industrail demonstrator of POWER-To-GAS in France.” https://www.jupiter1000.eu/english (accessed Sep. 01, 2021).

[58] M. Götz, A. M. D. Koch, and F. Graf, “State of the art and perspectives of CO2 methanation process concepts for power-to-gas applications,” *Int. Gas Res. Conf. Proc.*, vol. 1, no. January, pp. 314–327, 2014.

[59] S. McDonagh, R. O’Shea, D. M. Wall, J. P. Deane, and J. D. Murphy, “Modelling of a power-to-gas system to predict the levelised cost of energy of an advanced renewable gaseous transport fuel,” *Appl. Energy*, vol. 215, no. February 2018, pp. 444–456, 2018, doi: 10.1016/j.apenergy.2018.02.019.

[60] ENEA Consulting, “The Potential of Power-To-Gas,” vol. 33, no. 0, p. 51, 2016.

[61] B. Castellani *et al.*, “Experimental investigation on CO2 methanation process for solar energy storage compared to CO2-based methanol synthesis,” *Energies*, vol. 10, no. 7, pp. 1–13, 2017, doi: 10.3390/en10070855.

[62] “Graf F, Götz M, Henel M, Schaaf T, Tichler R. Technoökonomische Studie von Power-to-Gas-Konzepten; 2014.”

[63] K. Müller, M. Fleige, F. Rachow, and D. Schmeißer, “Sabatier based CO2-methanation of flue gas emitted by conventional power plants,” *Energy Procedia*, vol. 40, pp. 240–248, 2013, doi: 10.1016/j.egypro.2013.08.028.

[64] S. McDonagh, R. O’Shea, D. M. Wall, J. P. Deane, and J. D. Murphy, “Modelling of a power-to-gas system to predict the levelised cost of energy of an advanced renewable gaseous transport fuel,” *Appl. Energy*, vol. 215, no. January 2018, pp. 444–456, 2018, doi: 10.1016/j.apenergy.2018.02.019.

[65] A. Ursúa, L. M. Gandía, and P. Sanchis, “Hydrogen production from water electrolysis: Current status and future trends,” *Proc. IEEE*, vol. 100, no. 2, pp. 410–426, 2012, doi:

10.1109/JPROC.2011.2156750.

[66] A. Kovač, D. Marciuš, and L. Budin, “Solar hydrogen production via alkaline water electrolysis,” *Int. J. Hydrogen Energy*, vol. 44, no. 20, pp. 9841–9848, 2019, doi: 10.1016/j.ijhydene.2018.11.007.

[67] F. Moradi Nafchi, E. Baniasadi, E. Afshari, and N. Javani, “Performance assessment of a solar hydrogen and electricity production plant using high temperature PEM electrolyzer and energy storage,” *Int. J. Hydrogen Energy*, vol. 43, no. 11, pp. 5820–5831, 2018, doi: 10.1016/j.ijhydene.2017.09.058.

[68] ProtonOnsite.com, “Proton OnSite,”. February. 2015, [Online]. Available: protononsite.com.

[69] Ö. F. Selamet, F. Becerikli, M. D. Mat, and Y. Kaplan, “Development and testing of a highly efficient proton exchange membrane (PEM) electrolyzer stack,” Int. J. Hydrogen Energy, vol. 36, no. 17, pp. 11480–11487, 2011, doi: 10.1016/j.ijhydene.2011.01.129.

[70] F. Barbir, “PEM electrolysis for production of hydrogen from renewable energy sources,” *Sol. Energy*, vol. 78, no. 5, pp. 661–669, 2005, doi: 10.1016/j.solener.2004.09.003.

[71] K. Rajeshwar, R. McConnell, and S. Licht, Solar hydrogen generation: Toward a renewable energy future. 2008.

[72] S. A. Grigoriev, V. I. Porembsky, and V. N. Fateev, “Pure hydrogen production by PEM electrolysis for hydrogen energy,” *Int. J. Hydrogen Energy*, vol. 31, no. 2, pp. 171–175, 2006, doi: 10.1016/j.ijhydene.2005.04.038.

[73] M. Landgraf, “Power to Gas: Storing the Wind and Sun in Natural Gas,” *Press Release - Karlsruhe Inst. Technol.*, no. 044, pp. 1–2, 2014.

[74] J. Lefebvre, “Coupling of a 3 Phase Methanation Reactor and a High Temperature Electrolyser using Matlab Simulink,” no. July, pp. 1–11, 2014, [Online]. Available: https://www.researchgate.net/publication/271073614.

[75] M. Ni, M. K. H. Leung, and D. Y. C. Leung, “Technological development of hydrogen production by solid oxide electrolyzer cell (SOEC),” *Int. J. Hydrogen Energy*, vol. 33, no. 9, pp. 2337–2354, 2008, doi: 10.1016/j.ijhydene.2008.02.048.

[76] M. Zahid, J. Schefold, and A. Brisse, “High-temperature water electrolysis using planar solid oxide fuel cell technology: a review.,” *Hydrog. Fuel Cells*, vol. 78, pp. 227–242, 2010.

[77] “Statista,” Energy & Environmental Services›Electricity, 2019.

https://www.statista.com/statistics/1046605/industry-electricity-prices-european-union-country/ (accessed Oct. 01, 2020)."

[78] H. Sarptaş, "Assessment of Landfill Gas (Lfg) Energy Potential Based on Estimates of Lfg Models," *Deu Muhendis. Fak. Fen ve Muhendis.*, vol. 18, no. 54, pp. 491–491, 2016, doi: 10.21205/deufmd.2016185416.

[79] R. Seyfioglu, "Models for the Prediction of Landfill Gas Potential – A Comparison Models for the Prediction of Landfill Gas Potential. June, 2012.

[80] H. Kamalan, M. Sabour, and N. Shariatmadari, "A review on available landfill gas models," *J. Environ. Sci. Technol.*, vol. 4, no. 2, pp. 79–92, 2011, doi: 10.3923/jest.2011.79.92.

[81] H. Oonk, et al., "Oonk 1994 (EN) Validation of landfill gas formation models." 1994.

[82] H. Scharff and J. Jacobs, "Applying guidance for methane emission estimation for landfills," *Waste Manag.*, vol. 26, no. 4, pp. 417–429, 2006, doi: 10.1016/j.wasman.2005.11.015.

[83] "International Best Practices Guide for Landfill Gas Energy Projects- U.S. Environmental Protection Agency 2012," 2012.

[84] United States Environmental Protection Agency (EPA), "LFG Energy Project Development Handbook," *Energy*, no. June, p. 94, 2017,.

[85] E. C. Rada, M. Ragazzi, P. Stefani, M. Schiavon, and V. Torretta, "Modelling the potential biogas productivity range from a MSW landfill for its sustainable exploitation," *Sustain.*, vol. 7, no. 1, pp. 482–495, 2015, doi: 10.3390/su7010482.

[86] C. Fischer, "Gas Emission from Landfills: An overview of issues and research needs Survey October 1999," *Swedish Environ. Prot. Agency*, pp. 1–57, 1999.

[87] S. L. Machado, M. F. Carvalho, J. P. Gourc, O. M. Vilar, and J. C. F. do Nascimento, "Methane generation in tropical landfills: Simplified methods and field results," *Waste Manag.*, vol. 29, no. 1, pp. 153–161, 2009, doi: 10.1016/j.wasman.2008.02.017.

[88] M. A. Barlaz, R. K. Ham, D. M. Schaefer, and R. Isaacson, "Methane production from municipal refuse: A review of enhancement techniques and microbial dynamics," *Crit. Rev. Environ. Control*, vol. 19, no. 6, pp. 557–584, Jan. 1990, doi: 10.1080/10643389009388384.

[89] S. Tchobanoglous, G., Theisen, H., Vigil, "Integrated Solid Waste Management," in *McGraw-Hill*, New York, USA, 1993.

[90] M. A. Barlaz, D. M. Schaefer, and R. K. Ham, “Bacterial population development and chemical characteristics of refuse decomposition in a simulated sanitary landfill,” *Appl. Environ. Microbiol.*, vol. 55, no. 1, pp. 55–65, 1989, doi: 10.1128/aem.55.1.55-65.1989.

[91] R. Harries et al., “Development of a biochemical methane potential (BMP) test and application to testing of municipal solid waste samples.,” 2001.

[92] IPCC, “CH4 Emissions from Solid Waste Disposal,” *IPCC Good Pract. Guid. Uncertain. Manag. Natl. Greenh. Gas Invent.*, pp. 419–439, 2006, [Online]. Available: http://www.ipcc-nggip.iges.or.jp/public/gp/bgp/5_1_CH4_Solid_Waste.pdf.

[93] IPCC, “2006 IPCC Guidelines for National Greenhouse Gas Inventories: Vol 5 Chapter 3 Solid Waste Disposal,” *2006 IPCC Guidel. Natl. Greenh. Gas Invent.*, vol. 4, pp. 6.1-6.49, 2006, [Online]. Available: http://www.ncbi.nlm.nih.gov/pubmed/20604432.

[94] Conestoga-Rovers & Associates, “Landfill Gas Generation Assessment Procedure Guidelines,” p. 28pp, 2009, [Online]. Available: http://www.env.gov.bc.ca/epd/codes/landfill_gas/.

[95] Erşan Olcay IŞIN, “DETERMINATION OF LANDFILL GAS BY USING METHEMATICAL MODELS”, DOKUZ EYLÜL UNIVERSITY, Graduate School of Natural and Applied Sciences,2012.

[96] USEPA, “Landfill Air Emissions Estimation Model,” 1998.

[97] D. Muller, “User’s Manual Mexico Landfill Gas Model. Program”, (2003).

[98] G. GÖK, “NİĞDEDüzenli Depolama Alaninin MetaÜretimi VeEnerjPotansiyeliniBirinci DerecedenMatematiksel Modelleme YaklaşimlariİlTahminlenmesi,” *Mühendislik Bilim. ve Tasarım Derg.*, vol. 7, no. 1, pp. 126–135, 2019, doi: 10.21923/jesd.405047.

[99] EPA, “An overview of renewable natural gas from biogas”, July, 2020.

[100] “Guild Landfill Gas Purification Technology,” *Nitrogen Rejection and C02 Removal Made Easy _Landfill Gas Purification*. http://www.moleculargate.com/landfill-gas-purification.html (accessed Jun. 02, 2021).

[101] P. Smyth, “Oxygen Removal at High-Btu Plants Typical Pipeline Quality Gas Specifications,” 2011.

[102] S. Sahota *et al.*, “Review of trends in biogas upgradation technologies and future perspectives,” *Bioresour. Technol. Reports*, vol. 1, pp. 79–88, Mar. 2018, doi: 10.1016/j.biteb.2018.01.002.

[103] E. Barbera, S. Menegon, D. Banzato, C. D'Alpaos, and A. Bertucco, "From biogas to biomethane: A process simulation-based techno-economic comparison of different upgrading technologies in the Italian context," *Renew. Energy*, vol. 135, pp. 663–673, 2019, doi: 10.1016/j.renene.2018.12.052.

[104] Statista, *Energy & Environmental Services›Electricity*, 2019. https://www.statista.com/statistics/1046605/industry-electricity-prices-european-union-country/ (accessed Oct. 01, 2020).

[105] P. A. R. Des, H. D. E. Taxes, E. T. Des, and P. D. E. Gros, "Commissariat général au développement durable Prix du gaz naturel en France et dans l ' Union européenne en 2018," 2019.

[106] "le prix de l'eau." https://www.eaufrance.fr/le-prix-de-leau (accessed Jul. 05, 2021).

[107] "Davis, M., Coony, R., Gould, S., & Daly, A. (2005). Guidelines for Life Cycle Cost Analysis. California: Stanford University."

[108] "ISO. (2008). 15686-5:2008 Buildings and constructed assets -- Service-life planning -- Part 5: Life-cycle costing. Geneva: International Organization for Standardization."

[109] "Lifecycle Cost-Effectiveness: The Commercial, Design and Human Factors of Systems Engineering," , MM Pica, 2014.

[110] P. Rotunno, A. Lanzini, and P. Leone, "Energy and economic analysis of a water scrubbing based biogas upgrading process for biomethane injection into the gas grid or use as transportation fuel," *Renew. Energy*, vol. 102, pp. 417–432, 2017, doi: 10.1016/j.renene.2016.10.062.

[111] A. A. Trendewicz and R. J. Braun, "Techno-economic analysis of solid oxide fuel cell-based combined heat and power systems for biogas utilization at wastewater treatment facilities," *J. Power Sources*, vol. 233, pp. 380–393, 2013, doi: 10.1016/j.jpowsour.2013.01.017.

[112] D., Thrän, E., Billig, T., Persson, M., Svensson, J., Daniel- Gromke, J., Po- nitka, M., Seiffert, J." Baldwin, Biomethane status and factors affecting market development and trade". IEA Task 40 and Task 37 Joint Study. IEA Bioenergy (2 014)

[113] "NRCS, An Analysis of Energy Production Costs from Anaerobic Digestion Systems on U.S, Livestock Production Facilities, 2007."

[114] "W.M. Budzianowski, D.A. Budzianowska, Economic Analysis of Biomethane and Bioelectricity

Generation from Biogas Using Different Support Schemes and Plant Configurations, 2015."

[115] "Valorgas, Seventh Framework Programme Theme -Biowaste as feedstock for 2nd generation", 2009.

[116] "S.A. Gebrezgabher, M.P. Meuwissen, A.G. Oude Lansink, Costs of producing biogas at dairy farms in The Netherlands, Int. J. Food Syst. Dyn. 1 (2010) 26e35."

[117] "K. Krich, D. Augenstein, J.P. Batmale, J. Benemann, B. Rutledge, D. Salour, Chapter 8: financial analysis of biomethane production, in: Biomethane from Dairy Waste: a Sourcebook for the Production and Use of Renewable Natural Gas in California, 2005."

[118] enea, "Overview of the biomethane sector in France," no. October, 2017, [Online]. Available: http://www.enea-consulting.com/wp-content/uploads/2018/04/ENEA-2017-10-biomethane-france-2017-en.pdf.

[119] J. Gao, Q. Liu, F. Gu, B. Liu, Z. Zhong, and F. Su, "Recent advances in methanation catalysts for the production of synthetic natural gas," *RSC Adv.*, vol. 5, no. 29, pp. 22759–22776, 2015, doi: 10.1039/c4ra16114a.

[120] C. V. Miguel, A. Mendes, and L. M. Madeira, "Intrinsic kinetics of CO2 methanation over an industrial nickel-based catalyst," *J. CO2 Util.*, vol. 25, no. January, pp. 128–136, 2018, doi: 10.1016/j.jcou.2018.03.011.

[121] L. Guerra, S. Rossi, J. Rodrigues, J. Gomes, J. Puna, and M. T. Santos, "Methane production by a combined Sabatier reaction/water electrolysis process," *J. Environ. Chem. Eng.*, vol. 6, no. 1, pp. 671–676, 2018, doi: 10.1016/j.jece.2017.12.066.

[122] M. V. Navarro, J. Plou, J. M. López, G. Grasa, and R. Murillo, "Effect of oxidation-reduction cycles on steam-methane reforming kinetics over a nickel-based catalyst," *Int. J. Hydrogen Energy*, vol. 44, no. 25, pp. 12617–12627, 2019, doi: 10.1016/j.ijhydene.2018.12.056.

[123] E. L. G. Oliveira, C. A. Grande, and A. E. Rodrigues, "Effect of catalyst activity in SMR-SERP for hydrogen production: Commercial vs. large-pore catalyst," *Chem. Eng. Sci.*, vol. 66, no. 3, pp. 342–354, 2011, doi: 10.1016/j.ces.2010.10.030.

[124] E. L. G. Oliveira, C. A. Grande, and A. E. Rodrigues, "Methane steam reforming in large pore catalyst," *Chem. Eng. Sci.*, vol. 65, no. 5, pp. 1539–1550, 2010, doi: 10.1016/j.ces.2009.10.018.

[125] D. Schlereth and O. Hinrichsen, "A fixed-bed reactor modeling study on the methanation of CO2," *Chem. Eng. Res. Des.*, vol. 92, no. 4, pp. 702–712, 2014, doi:

10.1016/j.cherd.2013.11.014.

[126] F. Koschany, D. Schlereth, and O. Hinrichsen, “On the kinetics of the methanation of carbon dioxide on coprecipitated NiAl(O)x,” *Appl. Catal. B Environ.*, vol. 181, pp. 504–516, 2016, doi: 10.1016/j.apcatb.2015.07.026.

[127] A. FREUD, “Heinz Hartmann: a Tribute,” *J. Am. Psychoanal. Assoc.*, vol. 13, no. 1, pp. 195–196, 1965, doi: 10.1177/000306516501300201.

[128] J. Zhang, N. Fatah, S. Capela, Y. Kara, O. Guerrini, and A. Y. Khodakov, “Kinetic investigation of carbon monoxide hydrogenation under realistic conditions of methanation of biomass derived syngas,” *Fuel*, vol. 111, pp. 845–854, 2013, doi: 10.1016/j.fuel.2013.04.057.

[129] S. Z. Abbas, V. Dupont, and T. Mahmud, “Kinetics study and modelling of steam methane reforming process over a NiO/Al2O3 catalyst in an adiabatic packed bed reactor,” *Int. J. Hydrogen Energy*, vol. 42, no. 5, pp. 2889–2903, 2017, doi: 10.1016/j.ijhydene.2016.11.093.

[130] G. D. Weatherbee and C. H. Bartholomew, “Hydrogenation of CO2 on group VIII metals,” *J. Catal.*, vol. 77, no. 2, pp. 460–472, 1982, doi: http://dx.doi.org/10.1016/0021-9517(82)90186-5.

[131] T. Kai, T. Takahashi, and S. Furusaki, “Kinetics of the methanation of carbon dioxide over a supported Ni-La2O3 catalyst,” *Can. J. Chem. Eng.*, vol. 66, no. 2, pp. 343–347, 1988, doi: 10.1002/cjce.5450660226.

[132] S. Z. Abbas, V. Dupont, and T. Mahmud, “Kinetics study and modelling of steam methane reforming process over a NiO/Al2O3 catalyst in an adiabatic packed bed reactor,” *Int. J. Hydrogen Energy*, vol. 42, no. 5, pp. 2889–2903, 2017, doi: 10.1016/j.ijhydene.2016.11.093.

[133] S. S. E. H. Elnashaie, A. M. Adris, A. S. Al-Ubaid, and M. A. Soliman, “On the non-monotonic behaviour of methane-steam reforming kinetics,” *Chem. Eng. Sci.*, vol. 45, no. 2, pp. 491–501, 1990, doi: 10.1016/0009-2509(90)87036-R.

[134] D. Schlereth, “Kinetic and reactor modeling for the methanation of carbon dioxide,” *PhD Thesis*, 2015, [Online]. Available: https://mediatum.ub.tum.de/doc/1241448/file.pdf.

[135] J. DUCAMP, “Conception et optimisation d’un réacteur-échangeur structuré pour l’hydrogénation du dioxyde de carbone en méthane de synthèse dédié à la filière de stockage d’énergie électrique renouvelable.,” *Inst. Chim. procédés pour l’énergie, l’environnement la santé*, vol. Docteur, p. p.2, 2015.

[136] M. T. Mazandarani and H. Ebrahim, “Modeling and simulation of industrial adiabatic fixed-bed reactor for the catalytic reforming of methane to syngas,” *Eur. Congr. Chem. Eng.*, no. September, pp. 16–20, 2007.

[137] H. Er-rbib and C. Bouallou, “Modelling and simulation of methanation catalytic reactor for renewable electricity storage,” *Chem. Eng. Trans.*, vol. 35, pp. 541–546, 2013, doi: 10.3303/CET1335090.

[138] N. R. Parlikkad *et al.*, “Modeling of fixed bed methanation reactor for syngas production: Operating window and performance characteristics,” *Fuel*, vol. 107, pp. 254–260, 2013, doi: 10.1016/j.fuel.2013.01.024.

[139] K. Khorsand, M. A. Marvast, N. Pooladian, and M. Kakavand, “Modeling and Simulation of Methanation Catalytic Reactor in Ammonia Unit,” *Pet. Coal*, vol. 49, no. 1, pp. 46–53, 2007.

[140] J. Gao *et al.*, “A thermodynamic analysis of methanation reactions of carbon oxides for the production of synthetic natural gas,” *RSC Adv.*, vol. 2, no. 6, pp. 2358–2368, 2012, doi: 10.1039/c2ra00632d.

[141] “European Parliament. Energy roadmap 2050; 2011.”

[142] “ADEME. Vers un mix électrique 100% renouvelable en 2050; 2015. p. 1–119.”

[143] J. Gorre, F. Ruoss, H. Karjunen, J. Schaffert, and T. Tynjälä, “Cost benefits of optimizing hydrogen storage and methanation capacities for Power-to-Gas plants in dynamic operation,” *Appl. Energy*, vol. 257, no. October 2019, 2020, doi: 10.1016/j.apenergy.2019.113967.

[144] D. I. D. Avenir, “Optimisation d’une Unité de Power-to-Gas nominale pilote,” pp. 2–3.

[145] J. Gorre, C. van Leeuwen, and F. Ortloff, “Innovative large-scale energy storage tech- nologies and Power-to-Gas concepts after optimisation Report on the optimal time profile and operation of the conversion technology during a repre- sentative year, in the perspective of the available storage cap,” no. 691797, p. 52, 2020.

[146] J. Gorre, F. Ortloff, and C. van Leeuwen, “Production costs for synthetic methane in 2030 and 2050 of an optimized Power-to-Gas plant with intermediate hydrogen storage,” *Appl. Energy*, vol. 253, no. June, p. 113594, 2019, doi: 10.1016/j.apenergy.2019.113594.

[147] “Ulleberg Ø, Nakken T, Eté A. The wind/hydrogen demonstration system at Utsira in Norway: evaluation of system performance using operational data and updated hydrogen energy system modeling tools. Int J Hydrogen Energy 2010;35. Nr. 5, S. 1841–1852.”

[148] “Gazey R, Salman SK, Aklil-D’halluin DD. A field application experience of in- tegrating hydrogen technology with wind power in a remote island location. J Power Sources 2006;157. Nr. 2, S. 841–847.”

[149] “Ursúa A, San Martín I, Barrios EL, Sanchis P. Stand-alone operation of an alkaline water electrolyser fed by wind and photovoltaic systems. Int J Hydrogen Energy 2013;38. Nr. 35, S. 14952–14967.”

[150] B. Guinot, F. Montignac, B. Champel, and D. Vannucci, “Profitability of an electrolysis based hydrogen production plant providing grid balancing services,” *Int. J. Hydrogen Energy*, vol. 40, no. 29, pp. 8778–8787, 2015, doi: 10.1016/j.ijhydene.2015.05.033.

[151] “Gas Networks Ireland. Code of Operations; 2015.”

[152] B. Bensmann, R. Hanke-Rauschenbach, G. Müller-Syring, M. Henel, and K. Sundmacher, “Optimal configuration and pressure levels of electrolyzer plants in context of power-to-gas applications,” *Appl. Energy*, vol. 167, pp. 107–124, 2016, doi: 10.1016/j.apenergy.2016.01.038.

[153] G. Leonzio, “Design and feasibility analysis of a Power-to-Gas plant in Germany,” *J. Clean. Prod.*, vol. 162, pp. 609–623, 2017, doi: 10.1016/j.jclepro.2017.05.168.

[154] E. Tsupari, J. Kärki, and E. Vakkilainen, “Economic feasibility of power-to-gas integrated with biomass fired CHP plant,” *J. Energy Storage*, vol. 5, pp. 62–69, 2016, doi: 10.1016/j.est.2015.11.010.

[155] C. Schnuelle, J. Thoeming, T. Wassermann, P. Thier, A. von Gleich, and S. Goessling-Reisemann, “Socio-technical-economic assessment of power-to-X: Potentials and limitations for an integration into the German energy system,” *Energy Res. Soc. Sci.*, vol. 51, no. February, pp. 187–197, 2019, doi: 10.1016/j.erss.2019.01.017.

[156] A. Smallbone, V. Jülch, R. Wardle, and A. P. Roskilly, “Levelised Cost of Storage for Pumped Heat Energy Storage in comparison with other energy storage technologies,” *Energy Convers. Manag.*, vol. 152, no. May, pp. 221–228, 2017, doi: 10.1016/j.enconman.2017.09.047.

[157] Gorre Jachin, Lydement Justin, Felix Ortloff, Jens Hüttenrauch, Ettore Bompard, Andrea Mazza, “Interim report of benchmarks and analysis description and load profile definitions. EU Horizon 2020 Project STORE&GO. Brussels.”

[158] Van Leeuwen Charlotte, Zauner Andreas. D8.3 – Report on the costs involved with PtG technologies and their potentials across the EU. EU Horizon 2020 Project STORE&GO.

Brussels; 04/2018.

[159] “European commission,” *EU Reference Scenario 2016: Energy, transport and GHG emissions Trends to 2050*. https://ec.europa.eu/energy/data-analysis/energy-modelling/eu-reference-scenario-2016_en (accessed May 19, 2021).

[160] C. van Leeuwen and M. Mulder, “Power-to-gas in electricity markets dominated by renewables,” *Appl. Energy*, vol. 232, no. July, pp. 258–272, 2018, doi: 10.1016/j.apenergy.2018.09.217.

Appendices

Appendix A: Sensitivity analysis

1- Sensitivity analysis for electricity cost, with heat recovery

Electricity cost	Water Scrubbing	Amine Scrubber	Membrane	PSA	Cryogenic
(€/KWh)	**M€**	**M€**	**M€**	**M€**	**M€**
0,06	1,54	2,60	1,87	2,00	3,83
0,07	1,57	2,69	1,89	2,04	3,80
0,08	1,60	2,78	1,92	2,08	3,76
0,09	1,63	2,87	1,95	2,12	3,73
0,1	1,66	2,96	1,97	2,16	3,70
0,11	1,70	3,05	2,00	2,19	3,67
0,12	1,73	3,14	2,02	2,23	3,64
0,13	1,76	3,23	2,05	2,27	3,61

2- Sensitivity analysis for electricity cost, without heat recovery

Electricity cost	Water Scrubbing	Amine Scrubber	Membrane	PSA	Cryogenic
(€/KWh)	**M€**	**M€**	**M€**	**M€**	**M€**
0,06	1,60	2,91	2,01	2,00	4,63
0,07	1,64	3,05	2,06	2,04	4,74
0,08	1,69	3,19	2,10	2,08	4,84
0,09	1,73	3,33	2,15	2,12	4,94
0,1	1,77	3,47	2,20	2,16	5,05
0,11	1,82	3,62	2,25	2,19	5,15
0,12	1,86	3,76	2,30	2,23	5,26
0,13	1,90	3,90	2,35	2,27	5,36

3- Sensitivity analysis for discount rate, with heat recovery

Discount rate	2%	4%	6%	8%	10%
	M€	M€	M€	M€	M€
Water Scrubbing	1,68	1,75	1,66	1,60	1,54
Amine Scrubber	3,51	3,21	2,96	2,76	2,59
Membrane	2,28	2,09	1,97	1,88	1,80
PSA	2,40	2,27	2,16	2,06	1,99
Cryogenic	4,16	3,91	3,70	3,54	3,40
Membrane +PSA	4,11	3,88	3,69	3,54	3,41
PSA+PSA	3,66	3,44	3,27	3,12	3,00

4- Sensitivity analysis for discount rate, without heat recovery

Discount rate in %	2%	4%	6%	8%	10%
	M€	M€	M€	M€	M€
Water Scrubbing	1,99	1,87	1,77	1,69	1,63
Amine Scrubber	4,19	3,80	3,47	3,21	2,99
Membrane	2,53	2,35	2,20	2,08	1,98
PSA	2,40	2,27	2,16	2,06	1,99
Cryogenic	5,94	5,45	5,05	4,72	4,45
Membrane +PSA	4,27	4,02	3,81	3,65	3,51
PSA+PSA	3,66	3,44	3,27	3,12	3,00

Appendix B: Total annual costs

1- Total annual costs: landfill biogas upgrading scenarios for different plant size (biogas flow rate)

Flow Rate	Cryogenic with heat recovery	Cryogenic without heat recovery	Membrane+PSA
Nm^3/h	**€/year**	**€/year**	**€/year**
200	381 220	519 800	424 891
300	366 447	574 317	463 035
400	351 675	628 835	501 179
500	336 903	683 353	539 322
600	322 131	737 871	577 466
700	307 358	792 388	615 610

2- Total sales of revenue and net income for landfill biogas upgrading scenarios at different raw biogas flow rates

Flow Rate	Earning - Total sales of revenue (€/year)		Net income = Total Sales of revenue – Total annual costs (€/year)		
Nm^3/h	Cryogenic	Membrane+ PSA	Cryogenic with heat recovery	Cryogenic Without heat recovery	Membrane +PSA
200	592 040	511 024	210 820	72 240	86 133
300	777 053	670 719	410 605	202 735	207 684
400	962 065	830 414	610 390	333 230	329 235
500	1 110 075	958 170	773 172	426 722	418 848
600	1 221 083	1 053 987	898 952	483 212	476 521
700	1 295 088	1 117 865	987 729	502 699	502 255

Appendix C: Cumulative cash flows

1- Cumulative cash flows for landfill biogas upgrading scenarios at biogas flow rate (200 Nm^3/h)

200 Nm^3/h $_{raw\ biogas}$	Cryogenic with heat recovery		Cryogenic without heat recovery		Membrane+PSA	
Year	NPV	Cumulative cash flow	NPV	Cumulative cash flow	NPV	Cumulative cash flow
0	-2 300 000	-2 300 000	-2 300 000	-2 300 000	-2 563 897	-2 563 897
1	210 820	-2 089 180	72 240	-2 227 760	86 133	-2 477 764
2	210 820	-1 878 360	72 240	-2 155 520	86 133	-2 391 631
3	210 820	-1 667 539	72 240	-2 083 279	86 133	-2 305 499
4	210 820	-1 456 719	72 240	-2 011 039	86 133	-2 219 366
5	210 820	-1 245 899	72 240	-1 938 799	86 133	-2 133 234
6	210 820	-1 035 079	72 240	-1 866 559	86 133	-2 047 101
7	210 820	-824 258	72 240	-1 794 318	86 133	-1 960 968
8	210 820	-613 438	72 240	-1 722 078	86 133	-1 874 836
9	210 820	-402 618	72 240	-1 649 838	86 133	-1 788 703
10	210 820	-191 798	72 240	-1 577 598	86 133	-1 702 571
11	210 820	19 023	72 240	-1 505 357	86 133	-1 616 438
12	210 820	229 843	72 240	-1 433 117	86 133	-1 530 305
13	210 820	440 663	72 240	-1 360 877	86 133	-1 444 173
14	210 820	651 483	72 240	-1 288 637	86 133	-1 358 040
15	210 820	862 304	72 240	-1 216 396	86 133	-1 271 907

2- Cumulative cash flows for landfill biogas upgrading scenarios at biogas flow rate (300 Nm^3/h)

300 Nm^3/h raw biogas	Cryogenic with heat recovery		Cryogenic without heat recovery		Membrane+PSA	
Year	NPV	Cumulative cash flow	NPV	Cumulative cash flow	NPV	Cumulative cash flow
0	-2 300 000	-2 300 000	-2 300 000	-2 300 000	-2 563 897	-2 563 897
1	410 605	-1 889 395	202 735	-2 097 265	207 684	-2 356 213
2	410 605	-1 478 790	202 735	-1 894 530	207 684	-2 148 529
3	410 605	-1 068 185	202 735	-1 691 795	207 684	-1 940 845
4	410 605	-657 580	202 735	-1 489 060	207 684	-1 733 161
5	410 605	-246 975	202 735	-1 286 325	207 684	-1 525 477
6	410 605	163 630	202 735	-1 083 590	207 684	-1 317 793
7	410 605	574 235	202 735	-880 855	207 684	-1 110 109
8	410 605	984 840	202 735	-678 120	207 684	-902 425
9	410 605	1 395 445	202 735	-475 385	207 684	-694 741
10	410 605	1 806 050	202 735	-272 650	207 684	-487 057
11	410 605	2 216 655	202 735	-69 915	207 684	-279 373
12	410 605	2 627 261	202 735	132 821	207 684	-71 689
13	410 605	3 037 866	202 735	335 556	207 684	135 995
14	410 605	3 448 471	202 735	538 291	207 684	343 679
15	410 605	3 859 076	202 735	741 026	207 684	551 363

3- Cumulative cash flows for landfill biogas upgrading scenarios at biogas flow rate (400 Nm^3/h)

400 Nm^3/h raw biogas	Cryogenic with heat recovery		Cryogenic without heat recovery		Membrane+PSA	
Year	NPV	Cumulative cash flow	NPV	Cumulative cash flow	NPV	Cumulative cash flow
0	-2 300 000	-2 300 000	-2 300 000	-2 300 000	-2 563 897	-2 563 897
1	610 390	-1 689 610	333 230	-1 966 770	329 235	-2 234 661
2	610 390	-1 079 220	333 230	-1 633 540	329 235	-1 905 426
3	610 390	-468 830	333 230	-1 300 310	329 235	-1 576 191
4	610 390	141 559	333 230	-967 081	329 235	-1 246 956
5	610 390	751 949	333 230	-633 851	329 235	-917 720
6	610 390	1 362 339	333 230	-300 621	329 235	-588 485
7	610 390	1 972 729	333 230	32 609	329 235	-259 250
8	610 390	2 583 119	333 230	365 839	329 235	69 986
9	610 390	3 193 509	333 230	699 069	329 235	399 221
10	610 390	3 803 898	333 230	1 032 298	329 235	728 456
11	610 390	4 414 288	333 230	1 365 528	329 235	1 057 691
12	610 390	5 024 678	333 230	1 698 758	329 235	1 386 927
13	610 390	5 635 068	333 230	2 031 988	329 235	1 716 162
14	610 390	6 245 458	333 230	2 365 218	329 235	2 045 397
15	610 390	6 855 848	333 230	2 698 448	329 235	2 374 633

4- Cumulative cash flows for landfill biogas upgrading scenarios at biogas flow rate (500 Nm^3/h)

500 Nm^3/h raw biogas	Cryogenic with heat recovery		Cryogenic without heat recovery		Membrane+PSA	
Year	NPV	Cumulative cash flow	NPV	Cumulative cash flow	NPV	Cumulative cash flow
0	-2 300 000	-2 300 000	-2 300 000	-2 300 000	-2 563 897	-2 563 897
1	773 172	-1 526 828	426 722	-1 873 278	418 848	-2 145 049
2	773 172	-753 656	426 722	-1 446 556	418 848	-1 726 201
3	773 172	19 516	426 722	-1 019 834	418 848	-1 307 354
4	773 172	792 689	426 722	-593 111	418 848	-888 506
5	773 172	1 565 861	426 722	-166 389	418 848	-469 659
6	773 172	2 339 033	426 722	260 333	418 848	-50 811
7	773 172	3 112 205	426 722	687 055	418 848	368 037
8	773 172	3 885 377	426 722	1 113 777	418 848	786 884
9	773 172	4 658 549	426 722	1 540 499	418 848	1 205 732
10	773 172	5 431 721	426 722	1 967 221	418 848	1 624 579
11	773 172	6 204 894	426 722	2 393 944	418 848	2 043 427
12	773 172	6 978 066	426 722	2 820 666	418 848	2 462 275
13	773 172	7 751 238	426 722	3 247 388	418 848	2 881 122
14	773 172	8 524 410	426 722	3 674 110	418 848	3 299 970
15	773 172	9 297 582	426 722	4 100 832	418 848	3 718 818

DOCTORAT BRETAGNE SCIENCES LOIRE POUR L'INGENIEUR

IMT Atlantique
Bretagne-Pays de la Loire
École Mines-Télécom

Titre : Recherche et étude d'une solution innovante pour l'optimisation de la conversion en bioGNV des effluents gazeux de l'Installation de stockage de déchets non dangereux (ISDND)

Mots clés : Analyse technico-économique, analyse de sensibilité, analyse des coûts de cycle de vie, Power-to-Gas, valorisation du CO_2, coûts de production du biométhane

Résumé : L'utilisation d'énergies fossiles a de nombreux problèmes associés tels que les émissions de gaz à effet de serre et la dépendance à l'égard des importations. Dans cette perspective, la décomposition des déchets biodégradables dans des conditions anaérobies telles que dans les ISDND est un processus bien établi pour la production de biogaz et la génération conséquente de biométhane. Dans ce contexte, cette thèse a porté sur la recherche et l'étude d'une solution innovante pour la transformation du biogaz de (ISDND) en biométhane. Pour le site d'enfouissement étudié, une modélisation mathématique a été réalisée pour prédire la production de biogaz pour les 30 prochaines années. Une analyse de l'état de l'art a été réalisée pour identifier les technologies de traitement du biogaz capables de valoriser le biogaz de l'ISDND en biométhane. Une analyse des coûts du cycle de vie a été réalisée pour cinq technologies afin d'identifier les paramètres les plus influents. Le coût spécifique de la production de biométhane a été estimé dans deux scénarios : Membrane+PSA et distillation cryogénique. Pour remédier au faible débit de biogaz, la valorisation de la fraction de dioxyde de carbone a été étudiée via le procédé Power-to-Gas. Dans le processus Power-to-Gas en deux étapes, la source du carbone dans l'unité de méthanisation a été considérée à partir de la capture du dioxyde de carbone et séparée à la sortie d'une technologie de traitement. La production d'hydrogène dans le processus a été étudiée en utilisant l'électricité renouvelable excédentaire intermittente via la technologie d'électrolyse. Deux modes opératoires ont été étudiés pour le procédé Power-to-Gas avec et sans stockage intermédiaire d'hydrogène : continu et flexible. Le coût spécifique de la production de gaz naturel de synthèse (GNS) a été estimé en €/MWh dans deux stratégies opératoires. Une analyse de sensibilité a été réalisée pour présenter l'effet du prix d'achat de l'électricité ainsi que des heures de fonctionnement à pleine charge sur le coût de production de GNS.

Title : Research and study of an innovative solution for the optimization of the conversion into biomethane of the gaseous effluents of the non-hazardous waste storage facility (Landfill Site)

Keywords : Techno-economic analysis, sensitivity analysis, life cycle cost analysis, power-to-gas, CO_2 valorization, , biomethane production costs

Abstract: Use of fossil fuel energy has many associated problems such as decreasing reserves, greenhouse gas emissions and dependency on importation. In this perspective, the decomposition of biodegradable waste in anaerobic conditions such as in landfills is a well-established process for the biogas production and consequent biomethane generation. In this context, this thesis focused on research and study of an innovative solution for the transformation of landfill biogas into biomethane. For the case study landfill site, a landfill gas mathematical modeling was carried out to predict the production of gas for the next 30 years. A state of the art study has been carried out to identify the different biogas upgrading technologies able to upgrade landfill biogas into biomethane. A life cycle cost analysis has been carried out for five different upgrading technologies to identify the most influencing parameters. Specific cost of biomethane production was estimated in two scenarios: Membrane+PSA and cryogenic distillation. To overcome the low biogas flow rate, the valorization of carbon dioxide content of the raw biogas was studied via power-to-gas process. In the two-step power-to-gas process, source of the carbon in the methanation unit has been considered from the carbon dioxide captured and separated in the outlet of an upgrading technology. Hydrogen production in the process was studied using intermittent surplus renewable electricity via electrolysis technology. Two operating strategies were studied for the power-to-gas process with and without intermediate hydrogen storage facility: continuous and flexible. Specific cost of synthetic natural gas (SNG) production was estimated in €/MWh in two operating strategies. A sensitivity analysis was carried out to present the effect of electricity purchase price as well as full load operating hours on the production cost of SNG.